

For Reference

NOT TO BE TAKEN FROM THIS ROOM

For Reference

NOT TO BE TAKEN FROM THIS ROOM

Ex LIBRIS
UNIVERSITATIS
ALBERTAENSIS





Digitized by the Internet Archive
in 2020 with funding from
University of Alberta Libraries

<https://archive.org/details/Chan1969>

THE UNIVERSITY OF ALBERTA

DEHYDROGENATION OF 3-PENTANOL ON AN ALUNDUM CATALYST

BY

(C) ANTHONY Y.H. CHAN

A THESIS

SUBMITTED TO THE FACULTY OF GRADUATE STUDIES
IN PARTIAL FULFILMENT OF THE REQUIREMENTS FOR THE DEGREE
OF MASTER OF SCIENCE

DEPARTMENT OF CHEMICAL AND PETROLEUM ENGINEERING

EDMONTON, ALBERTA

SPRING, 1969

UNIVERSITY OF ALBERTA
FACULTY OF GRADUATE STUDIES

The undersigned certify that they have read, and recommend to the Faculty of Graduate Studies for acceptance a thesis entitled DEHYDROGENATION OF 3-PENTANOL ON AN ALUNDUM CATALYST submitted by Anthony Y.H. Chan in partial fulfilment of the requirements for the degree of Master of Science in Chemical Engineering.

ACKNOWLEDGEMENTS

The author is indebted to Dr. I.G. Dalla Lana of the Department of Chemical and Petroleum Engineering, University of Alberta, for his guidance and supervision during the course of this investigation.

The financial support received from the National Research Council of Canada and the University of Alberta is gratefully acknowledged.

REPORT

The purpose of this report is to provide a detailed analysis of the data collected during the experiment. The results show that the system is capable of performing the required tasks with a high degree of accuracy and efficiency. The data indicates that the system is able to handle a wide range of inputs and outputs, and that it is able to adapt to changing conditions. The results also show that the system is able to maintain a high level of performance over a long period of time. The data suggests that the system is capable of handling a large number of tasks simultaneously, and that it is able to maintain a high level of accuracy and efficiency even when the workload is high. The results also show that the system is able to adapt to changing conditions, and that it is able to maintain a high level of performance over a long period of time. The data suggests that the system is capable of handling a large number of tasks simultaneously, and that it is able to maintain a high level of accuracy and efficiency even when the workload is high.

ABSTRACT

The vapor phase catalytic reactions of 3-pentanol on a sodium hydroxide-treated Alundum catalyst were investigated in a Vycor glass fixed-bed flow reactor. The effects of temperature and contact time on the product distribution were determined at an average pressure of 700 mm Hg over the following ranges of operating conditions:

Temperature: 350°C to 452°C at a constant space velocity of 1.578×10^{-2} (gm-mole of 3-pentanol)/(hr-gm of catalyst)

Space Velocity: 1.103×10^{-2} to 3.862×10^{-1} (gm-mole of 3-pentanol)/(hr-gm of catalyst) at a constant temperature of 370°C .

Two parallel reaction steps were observed, dehydrogenation and dehydration of 3-pentanol. The extent of other side-reactions was found to be negligible. Thermal decomposition of the 3-pentanol was not observed at temperatures up to 474°C , the maximum temperature employed. The rates of dehydrogenation and dehydration at 370°C obtained from a numerical differentiation of the experimental integral kinetic data were correlated using Langmuir-Hinshelwood mechanistic rate equations derived from plausible mechanisms based upon two types of sites without interaction. Analysis of the results of these correlations for various rate-

controlling steps indicated that dehydrogenation and dehydration occurred separately at two different types of active sites, and each reaction involved a single site mechanism with adsorption of 3-pentanol being the rate-controlling step. This finding was in agreement with the results of an independent study of the adsorption characteristics and surface chemistry of 3-pentanol on the Alundum catalyst.

TABLE OF CONTENTS

	<u>Page</u>
LIST OF FIGURES	i
LIST OF TABLES	ii
1. INTRODUCTION	1
2. LITERATURE SURVEY	3
2.1. Alundum as a Catalyst	4
2.2. Chemical Reactions	4
2.2.1. Dehydrogenation and Dehydration of Secondary Alcohols	5
2.2.2. Thermal Decomposition	7
2.2.3. Other Reaction	8
2.3. Correlation of Data	8
2.3.1. Rate Data from Numerical Differen- tiation Methods	9
2.3.2. Correlation of Rate Data with Empirical Equations	10
2.3.3. Correlation of Rate Data with Mechanistic Equations	11
3. EQUIPMENT AND OPERATION	13
3.1. Equipment	13
3.1.1. Feed System	13
3.1.2. Vaporization System	14
3.1.3. Reactor	14
3.1.4. Temperature Recording System	18
3.1.5. Product Collection System	18
3.2. Operation of Equipment	20
3.2.1. Preparation of Equipment	20

1
2
3
4
5
6
7
8
9
10
11
12
13
14
15
16
17
18
19
20
21
22
23
24
25
26
27
28
29
30

	<u>Page</u>
3.2.2. Start-up	21
3.2.3. Steady State Operation	21
3.2.4. Sampling	22
3.2.5. Shutdown	23
3.3. Raw Material	23
3.3.1. Alundum Catalyst	23
3.3.2. 3-Pentanol	23
3.3.3. Pyrex Glass Packing	25
3.4. Analysis of Products	26
3.4.1. Liquid Product	26
3.4.2. Gas Product	28
3.4.3. Accuracy of Analysis	29
4. EXPERIMENTAL PROGRAM AND RESULTS	31
4.1. Definition of Terms	31
4.1.1. Reaction Temperature	31
4.1.2. Space Velocity	31
4.1.3. Conversion of 3-Pentanol	32
4.1.4. Material Balance	32
4.1.5. Material Accountability	32
4.2. Thermal Decomposition of 3-Pentanol	33
4.3. Effect of Temperature on Product Distribution	34
4.4. Effect of Time on Catalytic Activity	34
4.5. Effect of Space Velocity on Product Distribution	35

	<u>Page</u>
4.6. Effect of Film Diffusion	36
4.7. Effect of Pore Diffusion	37
4.8. Reproducibility of Experiments	38
5. INTERPRETATION AND DISCUSSION OF RESULTS	55
5.1. Chemical Reactions	55
5.2. Effects of Vycor and Pyrex Glass Surfaces	56
5.3. Effect of Temperature on Product Distribution	57
5.4. Effect of Time on Catalytic Activity	57
5.5. Effects of Space Velocity and Film Diffusion	59
5.6. Effect of Pore Diffusion	63
5.7. Reproducibility of Experiments	64
6. CORRELATION OF DATA	66
6.1. Reaction Rates	66
6.2. Correlation of Rate Data	69
6.2.1. Empirical Method	69
6.2.2. Mechanistic Approach	71
7. CONCLUSIONS	81
8. RECOMMENDATIONS	83
BIBLIOGRAPHY	85
APPENDIX I CALIBRATION OF MICRO-FEEDER	I-1
APPENDIX II METHODS OF ANALYSIS	II-1
APPENDIX III EXPERIMENTAL CONDITIONS	III-1
APPENDIX IV PRODUCTS ANALYSES	IV-1
APPENDIX V DERIVATION OF RATE EQUATIONS	V-1

APPENDIX VI	PRESSURE DROPS ACROSS CATALYST SURFACE AND AMBIENT GAS STREAM	VI-1
APPENDIX VII	GAS FEEDING SYSTEM	VII-1
APPENDIX VIII	NUMERICAL DIFFERENTIATION	VIII-1

1. The first part of the document is a list of the names of the persons who have been appointed to the various offices of the corporation. The names are listed in alphabetical order, and each name is followed by the office to which he or she has been appointed. The list is as follows:

Name	Office
John A. Smith	President
James B. Jones	Vice President
William C. Brown	Secretary
Robert D. White	Treasurer
Charles E. Black	Director
Thomas F. Green	Director
Richard H. Gray	Director
Joseph K. Blue	Director
Samuel L. Red	Director
David M. Yellow	Director

2. The second part of the document is a list of the names of the persons who have been appointed to the various offices of the corporation. The names are listed in alphabetical order, and each name is followed by the office to which he or she has been appointed. The list is as follows:

Name	Office
John A. Smith	President
James B. Jones	Vice President
William C. Brown	Secretary
Robert D. White	Treasurer
Charles E. Black	Director
Thomas F. Green	Director
Richard H. Gray	Director
Joseph K. Blue	Director
Samuel L. Red	Director
David M. Yellow	Director

3. The third part of the document is a list of the names of the persons who have been appointed to the various offices of the corporation. The names are listed in alphabetical order, and each name is followed by the office to which he or she has been appointed. The list is as follows:

Name	Office
John A. Smith	President
James B. Jones	Vice President
William C. Brown	Secretary
Robert D. White	Treasurer
Charles E. Black	Director
Thomas F. Green	Director
Richard H. Gray	Director
Joseph K. Blue	Director
Samuel L. Red	Director
David M. Yellow	Director

4. The fourth part of the document is a list of the names of the persons who have been appointed to the various offices of the corporation. The names are listed in alphabetical order, and each name is followed by the office to which he or she has been appointed. The list is as follows:

Name	Office
John A. Smith	President
James B. Jones	Vice President
William C. Brown	Secretary
Robert D. White	Treasurer
Charles E. Black	Director
Thomas F. Green	Director
Richard H. Gray	Director
Joseph K. Blue	Director
Samuel L. Red	Director
David M. Yellow	Director

5. The fifth part of the document is a list of the names of the persons who have been appointed to the various offices of the corporation. The names are listed in alphabetical order, and each name is followed by the office to which he or she has been appointed. The list is as follows:

Name	Office
John A. Smith	President
James B. Jones	Vice President
William C. Brown	Secretary
Robert D. White	Treasurer
Charles E. Black	Director
Thomas F. Green	Director
Richard H. Gray	Director
Joseph K. Blue	Director
Samuel L. Red	Director
David M. Yellow	Director

6. The sixth part of the document is a list of the names of the persons who have been appointed to the various offices of the corporation. The names are listed in alphabetical order, and each name is followed by the office to which he or she has been appointed. The list is as follows:

Name	Office
John A. Smith	President
James B. Jones	Vice President
William C. Brown	Secretary
Robert D. White	Treasurer
Charles E. Black	Director
Thomas F. Green	Director
Richard H. Gray	Director
Joseph K. Blue	Director
Samuel L. Red	Director
David M. Yellow	Director

LIST OF FIGURES

<u>Figure</u>		<u>Page</u>
3.1.	Schematic Layout of Equipment	15
3.2.	Sketch of Cross-Section of Reactor	16
4.1.	Effect of Temperature on Product Distribution	51
4.2.	Effect of Time on Catalytic Activity	52
4.3.	Effect of Space Velocity on Product Distribution	53
4.4.	Effect of Space Velocity on Product Distribution (Lower Conversion Range)	54
6.1.	Rates of Formation	73
6.2.	Rates of Formation as Function of Conversion	74

TABLE 1

No.	Description	Value
1	Interest on bonds of \$100,000	1.25
2	Interest on Government bonds of \$100,000	1.25
3	Interest on bonds of \$100,000	1.25
4	Interest on bonds of \$100,000	1.25
5	Interest on bonds of \$100,000	1.25
6	Interest on bonds of \$100,000	1.25
7	Interest on bonds of \$100,000	1.25
8	Interest on bonds of \$100,000	1.25
9	Interest on bonds of \$100,000	1.25

LIST OF TABLES

<u>Table</u>		<u>Page</u>
3.1.	Properties of Catalyst	24
4.1.	Effect of Temperature on Product Distribution	40
4.2.	Effect of Time on Catalytic Activity	41
4.3.	Effect of Space Velocity on Product Distribution	42
4.4.	Effect of Space Velocity on Product Distribution	43
4.5.	Effect of Space Velocity on Product Distribution	44
4.6.	Effect of Space Velocity on Product Distribution	45
4.7.	Effect of Space Velocity on Product Distribution	46
4.8.	Effect of Space Velocity on Product Distribution	47
4.9.	Reproducibility of Experiments in Terms of Product Distribution	48
4.10.	Effect of Space Velocity on Product Distribution	49
4.11.	Effect of Pore Diffusion on Product Distribution	50
5.1.	Comparison of Product Distribution	58
5.2.	Effect of Average Catalyst Bed Temperature on 3-Pentanol Conversion	62
5.3.	Effect of Particle Size of Catalyst on Conversion	62
6.1.	Reaction Rates and Partial Pressures	72
6.2.	Postulated Mechanisms and Rate Equations for Dehydrogenation	78

Table 1

No.	Description	Value
1
2
3
4
5
6
7
8
9
10
11
12
13
14
15
16
17
18
19
20
21
22
23
24
25
26
27
28
29
30
31
32
33
34
35
36
37
38
39
40
41
42
43
44
45
46
47
48
49
50
51
52
53
54
55
56
57
58
59
60
61
62
63
64
65
66
67
68
69
70
71
72
73
74
75
76
77
78
79
80
81
82
83
84
85
86
87
88
89
90
91
92
93
94
95
96
97
98
99
100

<u>Table</u>		<u>Page</u>
6.3.	Postulated Mechanisms and Rate Equations for Dehydration	79
6.4.	Summary of Kinetic Constants	80

1980

1980

1981

1981

1982

1. INTRODUCTION

In studies of dehydrogenation of n-propanol over solid catalysts, Vasudeva (1, 2) found that a silica-alumina when treated with sodium hydroxide enhanced its capability for dehydrogenating n-propanol to diethyl ketone and suppressed the dehydrating tendency. His work concentrated on clarifying the chemistry and reaction sequence of the n-propanol system. Wanke (3) continued this work and studied the kinetics of n-propanol on the same base-exchanged silica-alumina catalyst. Because of the visible thermal reactions and catalytic activity of stainless steel, subsequent work on n-propanol was carried out by Imai (4) who investigated the extent of thermal decomposition and the catalytic effects of both stainless steel and pyrex glass.

Due to the complexity of the chemistry and multiple chemical reactions steps involved, the kinetic rate data obtained by Wanke (3) were not sufficiently accurate for a quantitative analysis of the n-propanol system kinetics (5). To improve the experimental techniques, it was considered that a simpler kinetic study of one of the intermediate products would be useful and would help to throw light on the multiple reactions steps of n-propanol system (5). One such intermediate product found in the dehydrogenation of n-propanol was 3-pentanol, a very stable secondary alcohol. The 3-pentanol was chosen for the present investigation

THE JOURNAL OF THE ROYAL ANTHROPOLOGICAL INSTITUTE

THE JOURNAL OF THE ROYAL ANTHROPOLOGICAL INSTITUTE

THE JOURNAL OF THE ROYAL ANTHROPOLOGICAL INSTITUTE

THE JOURNAL OF THE ROYAL ANTHROPOLOGICAL INSTITUTE

THE JOURNAL OF THE ROYAL ANTHROPOLOGICAL INSTITUTE

THE JOURNAL OF THE ROYAL ANTHROPOLOGICAL INSTITUTE

THE JOURNAL OF THE ROYAL ANTHROPOLOGICAL INSTITUTE

THE JOURNAL OF THE ROYAL ANTHROPOLOGICAL INSTITUTE

THE JOURNAL OF THE ROYAL ANTHROPOLOGICAL INSTITUTE

THE JOURNAL OF THE ROYAL ANTHROPOLOGICAL INSTITUTE

THE JOURNAL OF THE ROYAL ANTHROPOLOGICAL INSTITUTE

THE JOURNAL OF THE ROYAL ANTHROPOLOGICAL INSTITUTE

THE JOURNAL OF THE ROYAL ANTHROPOLOGICAL INSTITUTE

THE JOURNAL OF THE ROYAL ANTHROPOLOGICAL INSTITUTE

THE JOURNAL OF THE ROYAL ANTHROPOLOGICAL INSTITUTE

THE JOURNAL OF THE ROYAL ANTHROPOLOGICAL INSTITUTE

THE JOURNAL OF THE ROYAL ANTHROPOLOGICAL INSTITUTE

THE JOURNAL OF THE ROYAL ANTHROPOLOGICAL INSTITUTE

THE JOURNAL OF THE ROYAL ANTHROPOLOGICAL INSTITUTE

THE JOURNAL OF THE ROYAL ANTHROPOLOGICAL INSTITUTE

because the information obtained from the dehydrogenation of this secondary alcohol on the base-treated silica-alumina catalyst, could provide more understanding of the ketone synthesis process.

This investigation involved the measurement of more reliable chemical kinetic data and the correlation of these data by a simple kinetic expression. Attempts were made to improve the material balance and product analysis as well as to conduct the experiments under such conditions that the undesirable side-reactions could be eliminated or minimized.

2. LITERATURE SURVEY

The catalytic dehydrogenation of primary alcohols to aldehydes and secondary alcohols to ketones are well known industrial processes. The preparation of ketones by dehydrogenation of secondary alcohols over metals and metal oxides catalysts have been adequately covered by standard references on catalysis. The books of Sabatier (6), Bond (9), Goldstein (10) and Berkman (11) present excellent reviews of this subject. Extensive works have been done on the dehydrogenation of isopropanol on various catalysts to produce acetone (12 - 15) and the dehydrogenation of sec-butyl alcohol to methyl ethyl ketone (16 - 18).

However, very few studies of catalytic reactions of 3-pentanol on silica-alumina have been reported in the literature (3, 19). During the investigation of n-propanol dehydrogenation on alundum catalyst, Wanke (3) made a special run using pure 3-pentanol as feed in a glass reactor operated at 462°C and space velocity of 0.72 gm of feed per gm-hr of catalyst. The products obtained were 2-pentene, methyl ethyl ketone, diethyl ketone, ethyl isopropyl ketone, water, 3-pentanol, hydrogen, carbon monoxide and carbon dioxide. The diethyl ketone yield of this run was 75.3% which indicated that this catalyst was suitable for dehydrogenation of 3-pentanol to produce diethyl ketone. From the products obtained, it seemed that the reactions involved dehydrogenation, dehydration and decomposition.

2.1. Alundum as a Catalyst

Alundum is the commercial name of one type of impure alumina which contains approximately 21% SiO_2 and 2% other metal oxides (see Table 3.1.). Alumina can exist in seven different crystalline structures and its catalytic activity, to a certain extent, depends on which structure is present (3). In general, alumina catalyzes reactions such as polymerization, isomerization, cracking and alkylation of hydrocarbons, and dehydration of alcohols (2). The catalytic activity of alumina is usually attributed to "acid sites" on the surface (20).

In investigating the dehydrogenation of n-propanol, Vasudeva (1, 2) found that alumina was dehydrating, converting n-propanol to n-propyl ether and water at low temperatures and to propylene and water at higher temperatures. However, when the alumina was treated with 2N NaOH solutions, the acid sites on the surface were largely destroyed and the dehydrating activity was suppressed. The base-treated alumina then became a dehydrogenation catalyst.

2.2. Chemical Reactions

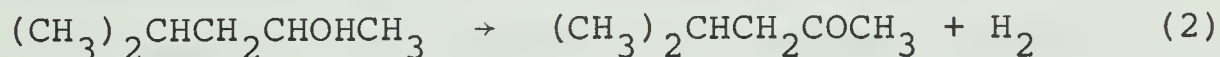
The catalytic dehydrogenation of primary alcohols to aldehydes and secondary alcohols to ketones are well known reactions. Vasudeva (2) and Wanke (3) present a good review of the dehydrogenation of primary alcohols. The dehydrogenation of secondary alcohols to ketones is more

readily accomplished than primary alcohols (7). Since the ketones formed are more stable than the aldehydes formed from the primary alcohols, a higher temperature can be employed to give a higher ketone yield.

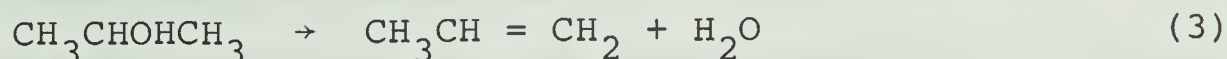
The chemical reactions involved in the catalytic decomposition of alcohols on mostly non-reducible metallic oxides are mainly dehydrogenation and dehydration in parallel (8). These parallel reactions did occur in the n-propanol alundum system (2, 3).

2.2.1. Dehydrogenation and Dehydration of Secondary Alcohols

Ipatieff (21) was one of the first to study the catalytic decomposition of alcohol. He passed isopropyl alcohol and methyl isobutyl carbinol respectively through an iron tube at 600°C, and the alcohols decomposed chiefly into ketones and hydrogen.



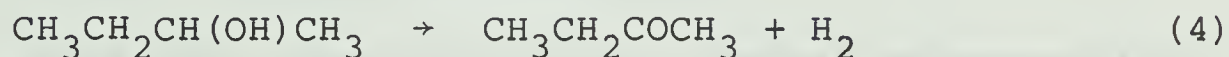
In addition, isopropyl alcohol was converted into propylene and water by passing over alumina at 500°C in a copper tube.



Hence, he concluded that catalytic decomposition of secondary

alcohols would proceed in either or both directions depending on the selectivity of the catalyst used. Dehydrogenation converted secondary alcohols to the corresponding ketones and hydrogen, while dehydration produced olefins and water.

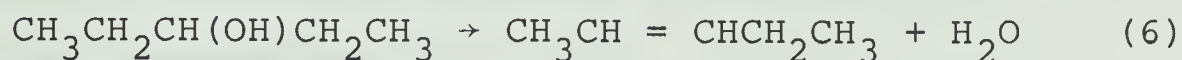
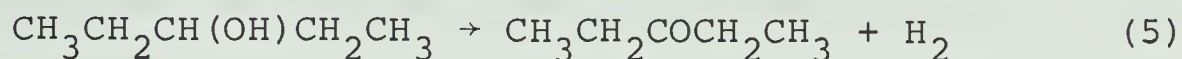
Extensive investigations (6, 10, 19, 22, 23) of the catalytic decomposition of alcohols have been reported since Ipatieff's (21) pioneering work was published. Because of their industrial importance, the dehydrogenations of isopropanol and sec-butyl alcohol to produce acetone and methyl ethyl ketone respectively have been studied by many workers (12-16, 18). Rubinshtein (50) reported, on the study of the



decomposition of isopropyl alcohol on alumina-chromia catalyst, that the catalytic selectivity toward dehydrogenation and dehydration of isopropanol depended on the concentration of Cr_2O_3 , increasing dehydrogenation with an increase in Cr_2O_3 concentration in the catalyst. Garcia De La Banda (13) studied the kinetics and mechanism of isopropyl alcohol dehydrogenation to acetone on Cr_2O_3 and $\text{ZnO-Cr}_2\text{O}_3$ catalysts and concluded that the reaction involved dual-site mechanism, with isopropyl alcohol, acetone and hydrogen being adsorbed and surface reaction being the rate controlling step. Various catalysts were employed for the dehydrogenation of isopropyl alcohol to acetone and hydrogen by many investigators, such as nickel catalysts reduced with sodium borohydride by Mears

(12), reduced copper by Kazuaki Kawamoto (14), erbium oxide by Tolstopyatova (15) and germanium powders by Frolov (51), and others.

More recently, Wanke (3) reported that the catalytic decomposition of 3-pentanol over NaOH-treated alundum catalyst involved mainly dehydrogenation and dehydration.

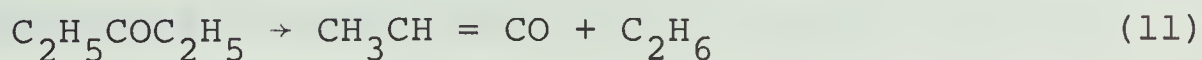
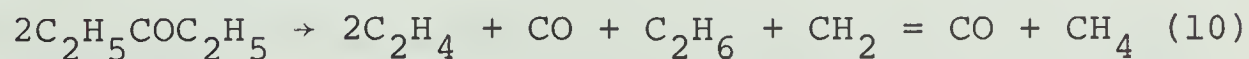


2.2.2. Thermal Decomposition

Rice (24) reported that the thermal decomposition of lower aliphatic alcohols consisted chiefly of the direct separation of molecular hydrogen and the formation of the corresponding aldehydes or ketones.



The ketones formed from dehydrogenation could undergo further decomposition to ketenes, methane, ethane and ethylene (25).



The 2-pentene obtained from dehydration could also decompose to methane and butadiene (26),



Reactions (9), (10), (11) and (12) are overall reactions which consist of series of chain reactions involving free radical mechanisms.

In investigating the decomposition of n-propanol, Imai (4) reported that the conversion of homogeneous thermal reaction was 0.865 mole % at a residence time of 78.0 sec. and a temperature of 463°C. He also reported that pyrex glass exhibited negligible catalytic effect while 316 stainless steel had catalytic effect on the decomposition of n-propanol at temperature up to 463°C. From his results, it is expected that the extent of thermal decomposition of 3-pentanol, a more stable secondary alcohol, would be negligible when operating at temperature under 400°C in a glass reactor.

2.2.3. Other Reaction

Vasudeva (2) indicated that the diethyl ketone from dehydrogenation would react further to yield methyl ethyl ketone and ethyl isopropyl ketone. The mechanism of this reaction



probably involved an aldol type condensation of the ketone followed by an alkyl rearrangement and a bond cleavage.

2.3. Correlation of Data

The fitting of experimental kinetic data to suitable rate expressions is described in most standard reaction

kinetics references (27, 29, 32). Two approaches, empirical or theoretical, are generally employed in correlating the kinetic rate data. In most cases, the rate data cannot be obtained directly by experimental measurement. Normally, this would require differentiation of the integral experimental data such as the composition-time curve. The method of numerically differentiating the rate data has often had a direct bearing upon the success obtained with the correlation.

2.3.1. Rate Data from Numerical Differentiation Methods

Nevers (34) reported a detailed study on rate data and derivatives obtained by using different methods. The most commonly used methods described by Nevers (34) are as follows:

(a) Plot the data, draw a smooth curve through it, and read the slopes directly from the curve. This method is the least accurate and rarely reproducible.

(b) Fit the entire set of data to some suitable function, such as a power series, and then differentiate this function. This method is widely used because of the convenient availability of computer programs for fitting such power series by least squares fit.

(c) Fit small segments of the data to a fitting function and then obtain local derivatives by differentiating the

segmented functions. An example of this latter method is given by Whitaker and Pigford (35). This method determines the derivative at a point by fitting a parabola to five consecutive data points by least squares, with the point in question as the midpoint. The calculated derivative at any one point has up to five different values, one for the fit where it is the midpoint, one for the fit where it is one point lower, etc. The five values of derivative at each individual point are then averaged using equal weighting of each derivative. The standard error of the first derivative can be calculated when the experimental data points are equally spaced.

(d) Differentiate numerically via a difference table, plot and smooth the differences, either graphically or numerically.

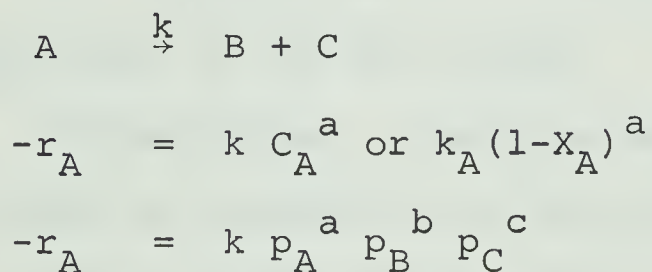
Nevers (34) concluded that the first derivatives obtained by all of the above methods, except (a), were approximately equal, with method (c) giving the best result. He stated that no method could yield the correct derivative in a mathematical sense. The method of Whitaker and Pigford (Method c) will be employed to calculate the reaction rates in this work.

2.3.2. Correlation of Rate Data with Empirical Equations

The use of an empirical equation provides the easiest

way to correlate the rate data. The rate of reaction normally is expressed in terms of a simple function, such as a power function, of the concentration or conversion of the reactant (3, 27). This kind of correlation applies very well to noncatalytic reactions. However, in the case of heterogeneous catalytic reactions, the validity of this sort of correlation is very doubtful. As an alternative, the rate of catalytic reaction can be expressed in terms of simple power form of the partial pressures of reactant and products as described by Walas (30). The former method will be used in this investigation because of its simplicity and easy handling of the data.

The forms of the equations mentioned above will be shown in the following:



The empirical approach has limited applications because it is not usually safe to extrapolate beyond the range of experimental data. The other disadvantage is that no insight into the mechanism involved in the reaction steps is gained.

2.3.3. Correlation of Rate Data with Mechanistic Equations

This approach is widely used in correlating catalytic

reaction rate data. In this approach, the rate data are fitted to a model describing a rational mechanism by which the reactions occur. The most commonly used approach to describe the mechanism was developed by Hinshelwood using Langmuir's adsorption theory (29). In the absence of rate controlling diffusional or physical steps, the mechanism to be considered consists of three chemical steps.

(a) Adsorption of reactants on the active sites on the surface of catalyst.

(b) Surface reaction on the active sites. The adsorbed reactants react, either by themselves, with other adsorbed species on the neighbouring sites or with molecules in the gas phase adjacent to the active sites.

(c) Desorption of the products from the surface of the catalyst to the gas stream.

In describing a reaction model based upon such chemical steps, an assumption is made that one of the above three steps is rate-controlling and the diffusion of reactants to the catalyst surface and diffusion of products from the catalyst surface to the bulk gas phase are not rate-controlling. A systematic application of this approach to catalytic reaction has been made by Hougen (32, 36).

3. EQUIPMENT AND OPERATION

3.1. Equipment

The equipment used in the study of dehydrogenation of 3-pentanol consists of a 3-pentanol feed system, vaporization system, the reactor, product-collection system, and temperature control and recording system. Figure 3.1. is a schematic layout of the equipment and instrumentation used. Figure 3.2. shows the detail of the reactor. Each system will be discussed in detail.

3.1.1. Feed System

The feed system employed a syringe-type micro-feeder. Liquid 3-pentanol was fed by a 50 c.c. leak-proof brass syringe which had Teflon O-ring seals and a uniform diameter chrome plated piston. The piston was driven by a synchronous motor through a system of gears. By changing the transmission gears, seven piston velocities could be obtained

Piston Velocities (cm/hr)	1.06	1.59	2.12	3.18	4.24	6.36	8.47
3-pentanol Feed Rates (gm/hr) @ 26.0°C	4.2842	6.4234	8.5626	12.8234	17.0843	25.5995	34.1147

Very precise and constant feed rates with average variations of less than 0.5% (see Appendix I) could be obtained. The calibration of the micro-feeder is given in Appendix I.

3.1.2. Vaporization System

The vaporizer was made from a 2 cm O.D. 22 cm long pyrex glass tubing. At the inlet was a 1/8 in. glass-metal joint which was connected to the syringe by 3/32 in. O.D. stainless steel tubing. The outlet of the vaporizer was a 12/5 female ball joint socket which was coupled to the inlet of the reactor. A 3/32 in. O.D. iron-constantan thermocouple which measured the temperature of the vapor, was placed inside a 2 mm I.D. glass thermocouple well located near the outlet of the vaporizer. The 17 ohms vaporizer heater was controlled by a powerstat power supply. The outside of the vaporizer was covered by 1½ cm. thickness of asbestos insulation.

3.1.3. The Reactor

The reactor was fabricated from vycor glass which could stand thermal shock and temperatures up to 800°C. Details of its construction and dimensions are shown in Figure 3.2. The reactor consisted of an outer jacket and an inner tube, the upper part of which served as a container for the catalyst. The incoming vapor flowed up through the outer annulus, which acted as a heat exchanger, and down through the catalyst bed. The volume of the outlet tube of the reactor was markedly reduced to minimize the extent of homogeneous reactions. The outer jacket was heated by a

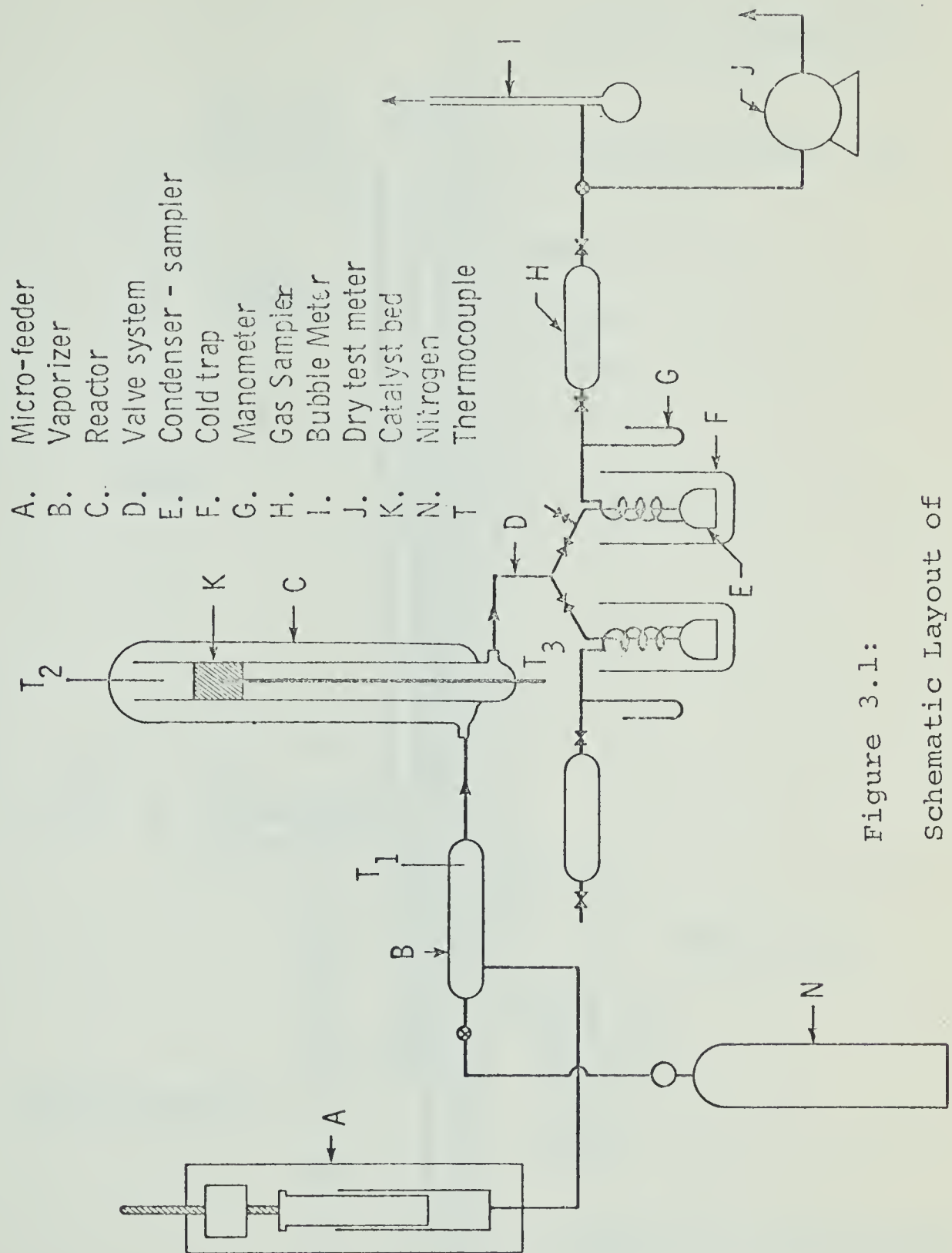


Figure 3.1:
Schematic Layout of
Equipment

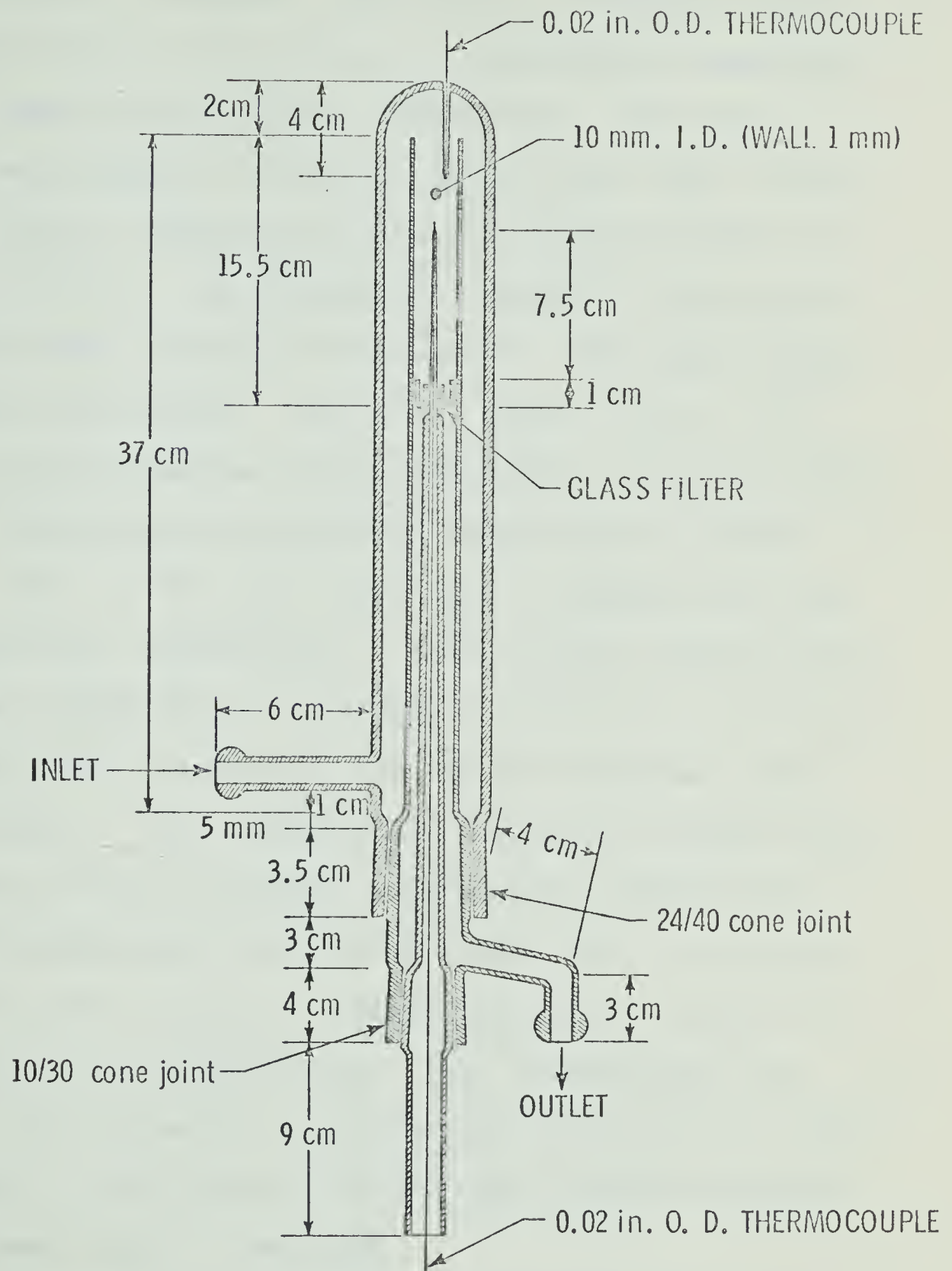


Figure 3.2:

Sketch of Cross-Section of
Reactor

45 ohms heating coil whose outside surface was covered by 1 cm thickness of asbestos insulation. The power supply was controlled by a 115 volts A.C., 1500 watts Thermolyne Stepless Input Control (Model CN-A8005 M). To reduce further heat losses, a 4 cm I.D. pyrex glass shell coated with reflecting aluminium foil on the outside surface and insulated with 1.5 cm thickness of asbestos, was placed around the outer jacket of the reactor. The whole system was mounted vertically. Two 20 in. long, 0.02 in. O.D., stainless steel-sheathed ceramic-insulated iron-constantan Xactpack thermocouples (purchased from Claud S. Gordon Company, Cat. No. 402-1101) were used to measure the gas and catalyst bed temperatures. One of these thermocouples was placed inside the 4.5 cm long, 0.8 mm I.D., 1.5 mm O.D., thermocouple well located at the top of the outer jacket of the reactor. This thermocouple was used to measure the temperature of the gas before entering the catalyst bed. The other thermocouple was placed inside the 7.5 cm long, 0.8 mm I.D. and 1.5 mm O.D. thermocouple well located at the center of the catalyst bed. This thermocouple was inserted from the bottom of the reactor and could be moved up and down in the catalyst bed so that the axial temperature gradient could be measured.

Once the reactor reached steady-state conditions (temperature and flow), the temperature of the catalyst bed

would remain constant provided that the room temperature did not change. However, when the room temperature dropped more than 3°C , the temperature of the reactor would also drop slightly requiring adjustment of the setting on the Thermolyne Stepless Input Control.

3.1.4. Temperature Recording System

The two thermocouples from the reactor and the one from the vaporizer were connected to Honeywell Electronik 16 24-point variable-range variable-zero multipoint recorder. The zero and range of the recorder were calibrated and occasionally checked by feeding a known voltage into the recorder from a potentiometer. The output of the thermocouple in the catalyst bed was also connected to a Leeds and Northrup Millivolt Potentiometer so that the reaction temperatures could be measured precisely during experimental runs. Three separate cold junctions were placed in an ice-water bath for the three thermocouples.

3.1.5. Product Collection System

The vapor products leaving the reactor passed through an inverted Y-shaped pyrex glass valve system to the condenser-sampler immersed in an ice-water bath. The valve system had one Teflon stopcock in each branch of the Y so that they could be either opened or closed simultaneously without having to disturb the steady state condition when

the sample was taken. Each branch was connected to an identical condenser-sampler and identical gas sampling tube. This enabled the system to maintain equal pressure drops before or during sampling.

To prevent condensation of the vapor product in the line of valve system, a 6 ft. 12 ohm heating tape was wrapped around the valve system. A power supply of approximately 30 volts was required to maintain a temperature of 170°C.

For better liquid sample collection, thereby improving the material balance, an integral condenser-sampler was used to collect the liquid sample. This condenser-sampler was constructed of pyrex glass as a single unit so that it could easily be removed from the rest of the equipment and weighed without having to transfer the liquid sample.

The noncondensable gases from the cold trap passed through a manometer which measured the pressure of the gas in the reaction and sample collection systems (the manometer was disconnected because the pressure drops across the reaction and sample collection systems were later found out to be negligible during some trial runs at extreme flow rates and reaction temperatures). Then the gas products passed to a 75 c.c. gas sampling tube and then to a bubble meter or to a dry test meter of 0.1 cu.ft. capacity per revolution. To improve gas analyses, the air inside the gas sampling tube and cold trap was displaced by passing through helium before sampling.

3.2. Operation of Equipment

A detailed discussion of the preparation of equipment, start-up, sampling, and shut-down phases of operation is given below.

3.2.1. Preparation of Equipment

The inner concentric tube of the reactor was removed downward vertically from the outer shell by releasing the springs which held the inner tube to the outer shell. A new charge of catalyst was placed inside this tube in such a way that a 3 cm height of pyrex glass chips of the same range of mesh sizes as the catalyst was on top and a variable height of glass chips was placed at the bottom of the catalyst bed. The inert pyrex glass chips were used to minimize the end effects arising from the flow pattern and temperature gradients. The top of the upper glass bed was positioned in line with the top of the thermocouple well so that the top of the catalyst bed remained at the same position and the void volume ahead of the catalyst bed remained constant for all runs irrespective of the depth of catalyst employed. This set-up enabled more consistent experimental results to be obtained if the extent of homogeneous reactions occurring proved to be significant. Then the inner tube was re-assembled in the outer shell of the reactor. After all joints were sealed with silicone grease and secured, the equipment was ready for an experimental run.

3.2.2. Start-up

Both reactor heater and vaporizer heater were turned on at the desired temperatures, the settings depending on the feed rate. The temperature recorder was switched on roughly 15 minutes later. The desired reactor temperature was set by adjustment of the stepless input control. After the vaporizer and reactor temperatures reached approximately 150°C and 200°C respectively, the micro-feeder was turned on. Liquid 3-pentanol feed was introduced to the vaporizer at the slowest flow rate. This method of start-up was used to reduce the time required to reach the desired reaction temperature. During this time, the heating tape at the exit of the reactor was switched on and the cold traps were installed. The reaction products were diverted to one side of the sample collection system by opening and closing the stopcocks between reactor exit and cold traps. Approximately $1\frac{1}{2}$ to 3 hours were required to achieve a steady temperature at the set reaction level.

3.2.3. Steady State Operation

Any new charge of catalyst required steady-state conditioning for a certain period of time to stabilize its activity. The required duration for stabilization was determined by experiments as given in Section 4.4. Once the catalyst had been stabilized, the desired feed

rate was set by changing the setting of transmission gears of the micro-feeder. The reaction temperature was reset if necessary. A steady-state condition was regained in approximately 20 minutes. The steady-state operation was defined by the constancy of feed-rate, vaporizer and reaction temperatures, and flow-rate of the gas product. During this period, the temperatures of the vaporizer, reactor top and catalyst bed were continuously recorded. The temperature of the catalyst bed was periodically checked by using the potentiometer. The flow rate of the gas product was measured with a stop-watch and a bubble meter, in which the soap solution had been saturated with the gas product. In the meantime, helium was being introduced to the sampling device for about 10 minutes to purge the air inside. When all of the above variables were constant, sampling began.

3.2.4. Sampling

The flow of reaction products was diverted to the other branch of the sampling system by switching the two valves simultaneously and the time was recorded by a stop-watch. The gaseous product rate was measured by another stop-watch and a bubble meter. The duration of sampling varied from 10 to 20 minutes depending on the rate of product generation. After sampling, the condenser-sampler was sealed with stoppers and weighed immediately.

3.2.5. Shutdown

The liquid feeder, the heaters and temperature recorder were shut off in this sequence. Nitrogen gas was passed through the vaporizer, reactor and sampling system to purge the equipment.

3.3. Raw Material

3.3.1. Alundum Catalyst

An alundum catalyst support, as supplied by Norton Company of Canada Ltd., was used in preparing the catalyst. The physical and chemical properties of this catalyst are given in Table 3.1. The 1/8" x 1/8" cylinders of alundum were crushed and the -10 + 20 mesh fraction was immersed in 2N sodium hydroxide solution for 6 hours. The excess solution was filtered off and the solids were dried at 150°C for 5 hours. Of these treated solids, only -16 + 20 mesh portion was used in the present study (except runs 44 and 45 which used -20 + 30 mesh). All charges of catalyst used in this work were taken from this single batch of treated catalyst. Each charge of catalyst was subjected to some conditioning which will be described in Section 4.4.

3.3.2. 3-Pentanol

Pure 3-pentanol was supplied by Aldrich Chemical Co. Inc., Milwaukee, Wisconsin (Cat. No. P802-5). The purity

Table 3.1

Properties of Catalyst

Manufacturer: Norton Company of Canada, Limited

Manufacturer's Designation: LA-617

Properties as specified by manufacturer:

1. Chemical (Typical) Analysis:

Al_2O_3	=	77.0%	K_2O	=	0.2%
SiO_2	=	21.2%	MgO	=	0.2%
* Fe_2O_3	=	0.2%	CaO	=	0.2%
Ti_2O	=	0.5%	ZrO_2	=	-
Na_2O	=	0.5%			

*Note: All elements are reported as metal oxides. The actual presence of the metals is in the form of complex silicates and/or aluminates.

2. Physical Properties:

Porosity	=	60-65%
Water Absorption	=	51-56%
Bulk Density	=	1.1-1.2 gm/cc
App. Sp. Gravity	=	3.0-3.2 gm/cc
Packing Density	=	46 lbs/cu.ft.
Surface Area	=	60-70 sq. meters/gm
**After treated with NaOH	=	26 sq. meters/gm
Max. Service Temperature	=	700°C
X-Ray Analysis	=	predominantly γ -alumina some γ -alumina and quartz

**Note: Measured by SORPTOMAT

was indicated to be higher than 99.99% by gas phase chromatography analysis based on peak area percentage using a Di-n-decyl phthalate-celite column. Only trace amounts of unknown compounds were detected by the gas-phase chromatography analysis.

The physical properties of 3-pentanol (37) are given as follows:

Molecular weight	88.15
Boiling point	115.5°C
Density @ 25°C	0.8154 gm/cc

3.3.3. Pyrex Glass Packing

Pyrex glass packing was provided by crushing pyrex glass tubing. The packing was washed with acetone, aqueous HCl, NaOH solutions and water and then dried before it was used. The properties of Pyrex glass packing are given below:

Particle size range	-16 + 20 mesh
Density (38)	2.23 gm/cc
Thermal conductivity (38) @ 25°C	0.0023 cal/(sec) (sq.cm) (°C/cm)
Mean specific heat (38) 25°C-175°C	0.20 cal/(gm) (°C)
Composition (38)	
Silica	80%
Boric oxide	14%
Soda	4%
Alumina	2%

3.4. Analysis of Products

The components of liquid and gas products were separated by gas-liquid chromatography using a Beckman Model G.C.4. The chromatogram peak areas of the components were integrated by using an Aerograph Model 471 Digital Integrator manufactured by Infotronics Corporation. The following is a description of the type of column used and the operating conditions under which the product analysis was carried out.

3.4.1. Liquid Product

Two separate columns, one for separation of hydrocarbon components and the other for separation of water, were used to analyze the liquid product sample.

- (a) Column: 3/16 inch diameter, 12 feet, stainless steel tubing packed with 30% Di-n-decyl phthalate on celite (-30 + 60 mesh). The Di-n-decyl phthalate was supplied by Eastman Chemical Co. (Cat. No. P6447). The celite was obtained from Burrell Company.

Column temperature: 100°C

Detector temperature: 170°C

Detector current: 200 ma
Sample size: 3 microliters
Carrier and reference
gas: Helium
Gas flow rate: Carrier side 50 c.c./min
Reference side 50 c.c./min

The components separated and identified by retention times under the above conditions were 2-pentene, methyl ethyl ketone, n-propanol, diethyl ketone and 3-pentanol. All components except methyl ethyl ketone and n-propanol were also identified by mass spectroscopy. The 2-pentene in the product consisted of both cis and trans isomers. The retention times of the components separated under the above conditions are given in Appendix IV.

(b) Column: 1/8 inch diameter, 6 feet, stainless steel tubing packed with Porapak Q(-100 + 120 mesh). The Porapak Q was purchased from Waters Assoc., Inc., Framingham, Mass.

Column temperature: 150°C
Detector temperature: 170°C
Detector current: 350 ma
Sample size: 2 microliters
Carrier and reference
gas: Helium

Gas flow rate: Carrier side 50 c.c./min
Reference side 50 c.c./min

This column was mainly used for analysis of water. The components separated under above conditions were 2-pentene, water, methyl ethyl ketone, n-propanol, diethyl ketone and 3-pentanol. The separation of diethyl ketone from 3-pentanol in this column was very poor.

3.4.2. Gas Product

Since no single column could separate all gaseous products, two separate columns were used.

(a) Column: 30% Di-n-decyl phthalate on celite
(same as for liquid product)

Column temperature: 55°C

Detector temperature: 160°C

Detector current: 200 mA

Carrier and reference
gas: Helium

Gas flow rate: Carrier side 50 c.c./min
Reference side 50 c.c./min

Components separated were ethylene and 2-pentene.

(b) Column: 1/8 inch diameter, 30 feet, copper tubing packed with high activity charcoal. The charcoal was supplied by Burrell Corporation (Catalogue No. 341-10).

Column temperature:	90°C
Detector temperature:	150°C
Detector current:	200 mA
Carrier and reference gas:	Helium
Gas flow rate: Carrier side	30 c.c./min.
Reference side	30 c.c./min.

The products separated under above conditions were air, hydrogen and methane. The products were identified by comparing their respective retention times with those of pure gas samples passing through the same column.

3.4.3. Accuracy of Analysis

In this work, an "Internal Reference Method" (see Appendix II) was used to improve the accuracy of product analysis. The essence of this method was to account for the variation of sample size and G.C. operating conditions. Synthetic mixtures of liquid components were used to calibrate the columns on a relative basis. By using this method, the error of the major liquid components analysis was reduced to the order of $\pm 0.5\%$ (see Appendix II).

For gas analysis, no synthetic mixture was used to calibrate the columns because it was difficult to blend a gas mixture with less than 2% error. Only relative thermal response (39) was employed. The error of the major gas component analysis was estimated to be $\pm 2.0\%$. This relative-

ly higher error as compared with that of liquid analysis was partly due to the small amount of gas sample collected, which was insufficient to purge the gas sampling loop in the G.C.

Since over 99% by weight of the product was in liquid form, the relatively higher error in the gas analysis had very little effect on the overall accuracy of analysis, it being largely determined by the accuracy of liquid analysis.

4. EXPERIMENTAL PROGRAM AND RESULTS

4.1. Definition of Terms

4.1.1. Reaction Temperature

The reaction temperatures reported in the present study (shown in the tables) were the temperatures recorded by the thermocouple located at the center of the catalyst bed. These temperatures corresponded to approximately the mean temperatures measured at the top and the bottom of the catalyst bed. The thermocouple was fixed at the center of the bed during sampling, but could be moved up and down to measure the temperature gradient across the catalyst bed before and after sampling.

4.1.2. Space Velocity

The term space velocity as used in this work is defined as

$$\text{Space Velocity} = \frac{\text{gm-mole of 3-pentanol feed}}{(\text{gm of catalyst})(\text{hour})}$$

The reciprocal of the above defined space velocity (1/S.V.) is the form of space time which was frequently used in this work.

4.1.3. Conversion of 3-Pentanol

Conversion of 3-Pentanol =

$$\left(1 - \frac{\text{moles of 3-pentanol in product}}{\text{moles of 3-pentanol in feed}}\right)$$

4.1.4. Material Balance

The material balance provided a measure of the accuracy of product collection and thus of the reliability of the experimental data.

(a) Overall Material Balance (%) =

$$\frac{(\text{Wt. of Liq. Product}) + (\text{Wt. of Gas Product})}{(\text{Wt. of Liquid Feed})} \times 100$$

(b) Balance Based on 3-Pentanol Conversion (%) =

$$\frac{\text{Wt. of all products except 3-pentanol}}{\text{Wt. of 3-pentanol converted}} \times 100$$

The balance based on 3-pentanol conversion is a more sensitive measure of the reliability of the data at low 3-pentanol conversion.

4.1.5. Material Accountability

Material Accountability was used as a measure of the completeness and reliability of product analysis. These are gram-atom balances of carbon, hydrogen and oxygen.

Carbon Accountability (%) =

$$\frac{\text{gm-atoms of carbon in analyzed products per mole of 3-pentanol feed}}{\text{gm-atoms of carbon in 1 mole of 3-pentanol feed}} \times 100$$

Similar definitions applied to hydrogen and oxygen accountabilities. Material accountability which took into account of the accuracy of product analysis was a secondary material balance. When both material balance and material accountability were satisfactory, the experimental data were assumed to be correct and were accepted.

4.2. Thermal Decomposition of 3-Pentanol

Three experimental runs, runs 1 to 3, were performed to investigate the effects of temperature and pyrex glass surface on the thermal decomposition of 3-pentanol. A slow feed rate of 8.5626 gm of 3-pentanol per hour and 6.8832 gm pyrex glass packing were used for all three runs. The reaction was studied at temperatures of 377°C, 414°C and 474°C.

Gas product was not obtained in any of the three runs. Analysis of the liquid samples revealed that all the liquid samples contained pure 3-pentanol only (see Appendix IV). These results indicated that pyrex glass had no measurable catalytic effect on 3-pentanol and furthermore that homogeneous thermal decomposition of 3-pentanol did not occur under the experimental conditions.

4.3. Effect of Temperature on Product Distribution

A set of 5 runs, runs 4 to 8, was carried out at constant space velocity to study the effect of temperature on the product distribution. These 5 runs used the first charge catalyst of 3.0805 gm. The water content of the liquid samples was not analyzed because the column for analyzing water was not available at that time. The experimental results are shown in Table 4.1. and Figure 4.1. It is noted that the reactions at 370°C consist of dehydrogenation and dehydration at 3-pentanol conversion of 0.47, the extent of side-reactions being negligible. Therefore, it was decided to carry out the subsequent experimental runs at 370°C.

4.4. Effect of Time on Catalytic Activity

Runs 9 to 12 using a second charge of catalyst weighing 0.9254 gm were designed to study the effect of time on catalytic activity at a constant temperature of 370°C and constant feed rate of 4.2842 gm 3-pentanol per hour (the lowest flow rate). Table 4.2. and Figure 4.2. show the results obtained in terms of product distribution. The catalytic activity remained fairly constant between the seventh and the thirteenth hours of use. Sample was not taken before the seventh hour of operation because the reaction system required two to three hours to reach the steady

state and the catalyst required another two to three hours of pre-treatment under steady reaction conditions. The experiment was terminated after the thirteenth hour of operation because the catalytic activity appeared to start declining (see Figure 4.2.). Approximately 4 to 6 runs could be done during this period of 6 hours. Hence, the following experimental runs will be performed as close as possible within this period of catalyst life.

4.5. Effect of Space Velocity on Product Distribution

Four sets of experimental runs, runs 13 to 31, totalling 19 runs, were performed to investigate the effect of space velocity on product distribution at a constant temperature of 370°C. A total of 4 charges of catalyst were used in these 19 runs. They are summarized in the following table.

Catalyst		Runs
<u>Charge No.</u>	<u>Weight (gm)</u>	
3	4.4077	13-19
4	2.2045	20-23
5	1.4977	24-27
6	1.0022	28-31

The results of the four sets of experimental runs are shown in Tables 4.3. to 4.6. Figures 4.3. and 4.4. show the major product distributions.

The reaction pressures of all runs were measured to be approximately equal to atmospheric pressure, about

700 mm Hg (see Appendix III).

4.6. Effect of Film Diffusion

It is important that film diffusion be minimized or accounted for before any meaningful analysis or interpretation of the kinetic data can be attempted. For this purpose, runs 13 to 31, described in the previous section, were also designed to study the effect of film diffusion. Some of the conditions of the 19 runs overlapped with one another so that, at a certain space velocity, there were two or three experiments using different feed rates (28). In other words, two or three experiments used the same ratio of catalyst weight to feed but different feed rates and different weights of catalyst. If film diffusion played a significant role or was the controlling factor of the reaction rate, the experimental run involving higher fluid velocities through the bed, i.e. the higher feed-rates, should exhibit less film resistance to diffusion and consequently, higher conversions. The reverse was also to be expected. When film diffusion was not a rate-controlling factor, the conversions would be expected to remain unaffected regardless of flow rates providing that the "isothermal plug flow" behavior existed.

The results are shown in Figures 4.3. and 4.4.

4.7. Effect of Pore Diffusion

In chemical reactions catalyzed by solid surfaces, the reaction rate exhibited per unit mass of catalyst is influenced by the area associated with the catalyst particles. In general, an increase in gross external surface area per unit mass (or decrease in particle size) for given reaction conditions increases the rate (32). For a completely impervious (nonporous) catalyst, the reaction is confined to the external surface, and the rate is hence directly proportional to the external surface area. In permeable (porous) catalysts the reaction extends by pore diffusion to the interior surfaces, and the gross external area is generally a negligible fraction of the total effective interfacial area. Most of the catalysts have characteristics falling between the above two extreme cases. Therefore, the effect of pore diffusion must be determined in order to permit meaningful analysis and interpretation of the rate data.

To investigate the effect of pore diffusion, experimental runs using charges of catalyst of equal weight but different particle sizes are performed under the same conditions. The charge of smaller particle size is usually obtained by crushing a portion of the batch of catalyst. If pore diffusion is not the rate-determining step, the conversions of all runs will be expected to be the same. However,

if pore diffusion is rate controlling, the run using smaller particles of catalyst will exhibit higher conversion due to shorter pores for diffusion and more pores created by crushing in the preparation of the catalyst.

Runs 44 and 45 using a charge of 1.0023 gm, -20 + 30 mesh catalyst were carried out at the same experimental conditions as runs 36 and 38 which used a charge of 1.0022 gm, -16 + 20 mesh catalyst. Results are given in Tables 4.11. and 5.3.

4.8. Reproducibility of Experiments

To estimate the overall errors of the primary experimental data, 8 runs, runs 32 to 39, were made at two different space velocities but at the same temperature. The 8 runs were divided into two groups, each of 4 runs. Each group used a different but equal weight of catalyst. Each group of 4 runs was performed at lower and higher space velocities alternatively to simulate the changes in conditions under which most of the experimental runs were carried out. The results obtained at the same space velocity from two groups of experiments are summarized in Table 4.9. Tables 4.7. and 4.8. show the detailed product distributions.

Further tests of reproducibility of the experiments were made by using a catalyst bed mixed with inert pyrex glass chips. Runs 40 to 43, using a charge of 1.0023 gm

catalyst mixed with glass in 1 to 1 volume ratio, were performed under the same conditions as runs 28 to 31 which used 1.0022 gm of catalyst only. Results are given in Table 4.10. and Figure 4.4.

The values for product distributions, conversions, and rate constants which are reported in the following pages, especially in Tables 4.1. to 4.11, 6.1. and 6.4, represent computed values. In most cases, the statistically significant number of figures do not exceed three figures.

Table 4.1.

Effect of Temperature on Product Distribution at 1/S.V. = 63.383

Run No.	4	5	6	7	8
Reaction temp. (C°)	350	374	401	427	452
Wt. of catalyst (gm)	3.0805	3.0805	3.0805	3.0805	3.0805
Product Distribution: (Mole of Product/Mole of 3-Pentanol Feed)					
Hydrogen	0.14811	0.49961	0.74206	0.85667	0.94110
Methane	0.00007	0.00012	0.00121	0.00311	0.00826
Ethylene	0.00003	0.00005	0.00035	0.00096	0.00267
2-Pentene	0.00317	0.02652	0.04724	0.06327	0.07688
Water		not analyzed			
M.E.K.	0.00005	0.00137	0.00243	0.00369	0.00636
n-Propanol	0.0	0.00098	0.00180	0.00193	0.00265
D.E.K.	0.17832	0.51643	0.75115	0.85231	0.91722
3-Pentanol	0.81660	0.47486	0.20187	0.07210	0.00217
3-Pentanol Conversion	0.18340	0.52514	0.79813	0.92790	0.99783
Material Balance (%)	99.68	100.74	99.07	99.01	99.14

Table 4.2.

Effect of Time on Catalytic Activity at 370°C and 1/S.V. = 19.041

Run No.	9	10	11	12
Wt. of catalyst (gm)	0.9254	0.9254	0.9254	0.9254
Duration of run (hr)	7	9	11	13
Product Distribution: (Mole of Product/Mole of 3-Pentanol Feed)				
Hydrogen	0.23499	0.23819	0.23020	0.23101
Methane	0.00024	0.00023	0.00021	0.00019
Ethylene	0.0	0.0	0.0	0.0
2-Pentene	0.00719	0.00672	0.00677	0.00650
Water	0.002254	0.02555	0.02459	0.02543
M.E.K.	0.00065	0.00073	0.00095	0.00070
n-Propanol	0.0	0.0	0.0	0.0
D.E.K.	0.25276	0.25199	0.24881	0.24804
3-Pentanol	0.73673	0.73710	0.74037	0.74136
3-Pentanol Conversion	0.26327	0.26290	0.25963	0.25864
Material Balance (%)				
Overall	99.98	99.98	99.99	99.96
Based on 3-Pentanol converted	99.97	99.93	99.98	99.94
Accountability (%)				
Carbon	99.72	99.64	99.68	99.65
Hydrogen	99.68	99.72	99.65	99.67
Oxygen	101.27	101.54	101.47	101.55

Table 4.3.

Effect of Space Velocity on Product Distribution at 370°C

Run No.	13	14	15	16	17	18	19
Wt. of Catalyst (gm)	4.4077	4.4077	4.4077	4.4077	4.4077	4.4077	4.4077
Feed Rate (gm/hr)	4.2842	6.4234	8.5626	12.8234	17.0843	25.5995	34.1147
l/S.V.	90.691	60.488	45.376	30.299	22.742	15.178	11.389
Product Distribution: (Mole of Product/Mole of 3-pentanol Feed)							
Hydrogen	0.46627	0.40982	0.36753	0.30504	0.26229	0.19056	0.17633
Methane	0.00038	0.00037	0.00029	0.00033	0.00033	0.00050	0.00050
Ethylene	0.00011	0.00010	0.00007	0.00006	0.00006	0.00005	0.00005
2-Pentene	0.01276	0.1042	0.00866	0.00679	0.00625	0.00451	0.00420
Water	0.01452	0.01347	0.01222	0.01193	0.01186	0.00801	0.00748
M.E.K.	0.00109	0.00065	0.00061	0.00047	0.00045	0.00039	0.00026
n-Propanol	0.00085	0.00048	0.00044	0.00034	0.00032	0.00027	0.00017
D.E.K.	0.48160	0.41848	0.38319	0.32187	0.27671	0.19903	0.18474
3-Pentanol	0.48522	0.54985	0.59258	0.66083	0.70989	0.79282	0.80800
3-Pentanol Conversion	0.51478	0.45015	0.40742	0.33917	0.29011	0.20718	0.19200
Material Balance (%)							
Overall	98.12	98.02	98.57	99.09	99.44	99.75	99.79
Based on 3-pentanol converted	96.35	95.59	96.49	97.31	98.05	98.79	98.89
Accountability (%)							
Carbon	99.81	97.97	98.53	99.02	99.35	99.70	99.74
Hydrogen	97.88	97.87	98.32	98.82	99.20	99.62	99.66
Oxygen	98.33	98.29	98.90	99.54	99.92	100.05	100.07

Table 4.4.

Effect of Space Velocity on Product Distribution at 370°C

Run No.	20	21	22	23
Wt. of Catalyst (gm)	2.2045	2.2045	2.2045	2.2045
Feed Rate (gm/hr)	4.2842	8.5626	17.0843	34.1147
l/S.V.	45.359	22.695	11.375	5.696
Product Distribution: (Mole of Product/Mole of 3-Pentanol Feed)				
Hydrogen	0.38379	0.28352	0.16325	0.10294
Methane	0.00030	0.00024	0.00028	0.00055
Ethylene	0.00006	0.00005	0.00003	0.00003
2-Pentene	0.00968	0.00605	0.00389	0.00297
Water	0.01219	0.01028	0.00818	0.00405
M.E.K.	0.00061	0.00050	0.00031	0.00027
n-Propanol	0.00045	0.00036	0.00036	0.00018
D.E.K.	0.40070	0.29524	0.16619	0.10199
3-Pentanol	0.56657	0.68673	0.81827	0.89207
3-Pentanol Conversion	0.43343	0.31328	0.18173	0.10794
Material Balance (%)				
Overall	97.80	98.93	98.95	99.77
Based on 3-pentanol converted	94.92	96.60	94.25	97.89
Accountability (%)				
Carbon	97.78	98.87	98.87	99.75
Hydrogen	97.54	98.74	98.89	99.79
Oxygen	98.05	99.31	99.30	99.85

Table 4.5.

Effect of Space Velocity on Product Distribution at 370°C

Run No.	24	25	26	27
Wt. of Catalyst (gm)	1.4977	1.4977	1.4977	1.4977
Feed Rate (gm/hr)	12.8234	17.0843	25.5995	34.1147
l/S.V.	10.295	7.728	5.157	3.870
Product Distribution: (Mole of Product/Mole of 3-Pentanol Feed)				
Hydrogen	0.15094	0.11937	0.09046	0.07090
Methane	0.00027	0.00037	0.00025	0.00046
Ethylene	0.0	0.0	0.0	0.0
2-Pentene	0.00519	0.00449	0.00346	0.00283
Water	0.00600	0.00508	0.00435	0.00374
M.E.K.	0.00051	0.00050	0.00048	0.00044
n-Propanol	0.0	0.0	0.0	0.0
D.E.K.	0.14978	0.12267	0.09023	0.07049
3-Pentanol	0.84358	0.87115	0.90490	0.92574
3-Pentanol Conversion	0.15642	0.12885	0.09510	0.07426
Material Balance (%)				
Overall	99.92	99.88	99.92	99.97
Based on 3-pentanol converted	99.50	99.09	99.18	99.61
Accountability (%)				
Carbon	99.90	99.88	99.90	99.95
Hydrogen	99.93	99.83	99.92	99.97
Oxygen	99.99	99.94	100.00	100.04

Table 4.6.

Effect of Space Velocity on Product Distribution at 370°C

Run No.	28	29	30	31
Wt. of Catalyst (gm)	1.0022	1.0022	1.0022	1.0022
Feed Rate (gm/hr)	12.8234	17.0843	25.5995	34.1147
l/S.V.	6.889	5.171	3.451	2.590
Product Distribution: (Mole of Product/Mole of 3-Pentanol Feed)				
Hydrogen	0.11156	0.08949	0.06795	0.05328
Methane	0.00019	0.00022	0.00021	0.00014
Ethylene	0.0	0.0	0.0	0.0
2-Pentene	0.00416	0.00347	0.00263	0.00201
Water	0.00533	0.00442	0.00386	0.00328
M.E.K.	0.00049	0.00048	0.00046	0.00043
n-Propanol	0.0	0.0	0.0	0.0
D.E.K.	0.11551	0.08923	0.06462	0.04922
3-Pentanol	0.87896	0.90549	0.93162	0.94775
3-Pentanol Conversion	0.12104	0.09451	0.06838	0.05225
Material Balance (%)				
Overall	99.92	99.88	99.96	99.97
Based on 3-pentanol converted	99.36	98.76	99.43	99.44
Accountability (%)				
Carbon	99.91	99.86	99.93	99.93
Hydrogen	99.86	99.88	100.00	100.02
Oxygen	100.03	99.96	100.06	100.07

Table 4.7.

Effect of Space Velocity on Product Distribution at 370°C

Run No.	32	33	34	35
Wt. of Catalyst (gm)	1.0020	1.0020	1.0020	1.0020
Feed Rate (gm/hr)	12.8234	25.5995	12.8234	25.5995
l/S.V.	6.888	3.450	6.888	3.450
Product Distribution: (Mole of Product/Mole of 3-Pentanol Feed)				
Hydrogen	0.11296	0.06904	0.11069	0.06836
Methane	0.00020	0.00023	0.00020	0.00021
Ethylene	0.0	0.0	0.0	0.0
2-Pentene	0.00412	0.00258	0.00425	0.00269
Water	0.00502	0.00380	0.00484	0.00401
M.E.K.	0.00048	0.00045	0.00050	0.00045
n-Propanol	0.0	0.0	0.0	0.0
D.E.K.	0.11443	0.06512	0.11632	0.06554
3-Pentanol	0.87680	0.93030	0.87664	0.93005
3-Pentanol Conversion	0.12320	0.06971	0.12336	0.06995
Material Balance (%)				
Overall	99.59	99.88	99.77	99.90
Based on 3-pentanol converted	99.69	98.21	98.10	98.61
Accountability (%)				
Carbon	99.58	99.84	99.77	99.87
Hydrogen	99.56	99.93	99.68	99.93
Oxygen	99.67	99.97	99.83	100.00

Table 4.8.

Effect of Space Velocity on Product Distribution at 370°C

Run No.	36	37	38	39
Wt. of Catalyst (gm)	1.0022	1.0022	1.0022	1.0022
Feed Rate (gm/hr)	12.8234	25.5995	12.8234	25.5995
1/S.V.	6.889	3.451	6.889	3.451
Product Distribution: (Mole of Product/Mole of 3-Pentanol Feed)				
Hydrogen	0.11148	0.06808	0.10955	0.06771
Methane	0.00018	0.00022	0.00017	0.00021
Ethylene	0.0	0.0	0.0	0.0
2-Pentene	0.00412	0.00259	0.00403	0.00254
Water	0.00540	0.00394	0.00493	0.00358
M.E.K.	0.00049	0.00045	0.00048	0.00046
n-Propanol	0.0	0.0	0.0	0.0
D.E.K.	0.11449	0.06412	0.11377	0.06374
3-Pentanol	0.87911	0.93189	0.87921	0.93193
3-Pentanol Conversion	0.12089	0.06811	0.12079	0.06807
Material Balance (%)				
Overall	99.84	99.94	99.75	99.89
Based on 3-pentanol converted	98.64	99.09	97.95	98.43
Accountability (%)				
Carbon	99.82	99.90	99.74	99.86
Hydrogen	99.78	99.99	99.68	99.94
Oxygen	99.95	101.04	99.84	99.97

Table 4.9.

Reproducibility of Experiments in Terms of Product Distribution
(Mole of Product/Mole of 3-Pentanol Feed)

Reaction temperature = 370°C

Run No.	Hydrogen	2-Pentene	Water	D.E.K.	3-Pentanol Conversion
32	0.11296	0.00412	0.00502	0.11443	0.12320
34	0.11069	0.00425	0.00484	0.11632	0.12336
36	0.11148	0.00412	0.00540	0.11449	0.12089
38	0.10955	0.00403	0.00493	0.11377	0.12079
Ave.	0.11117	0.00413	0.00505	0.11475	0.12206
Devia- tion	±0.00228	±0.00015	±0.00039	±0.00174	±0.00225
	±2.05%	±3.52%	±7.80%	±1.52%	±1.84%
33	0.06904	0.00258	0.00380	0.06512	0.06971
35	0.06836	0.00269	0.00401	0.06554	0.06995
37	0.06808	0.00259	0.00394	0.06412	0.06811
39	0.06771	0.00254	0.00358	0.06374	0.06807
Ave.	0.06830	0.00260	0.00383	0.06463	0.06896
Devia- tion	±0.00090	±0.00010	±0.00030	±0.00134	±0.00160
	±1.31%	±3.74%	±7.86%	±2.08%	±2.32%

Note: Deviations were estimated at 95% confidence limit.

Runs 32, 34, 36 and 38 at 1/S.V. = 6.888

Runs 33, 35, 37 and 39 at 1/S.V. = 3.450

Table 4.10.

Effect of Space Velocity on Product Distribution at 370°C

Run No.	40	41	42	43
Wt. of Catalyst (gm)	1.0023	1.0023	1.0023	1.0023
Feed Rate (gm/hr)	12.8234	17.0843	25.5995	34.1147
l/S.V.	6.890	5.172	3.451	2.590
Product Distribution: (Mole of Product/Mole of 3-Pentanol Feed)				
Hydrogen	0.11147	0.08945	0.06795	0.05320
Methane	0.00019	0.00022	0.00021	0.00014
Ethylene	0.0	0.0	0.0	0.0
2-Pentene	0.00416	0.00345	0.00264	0.00201
Water	0.00511	0.00449	0.00393	0.00325
M.E.K.	0.00049	0.00048	0.00045	0.00043
n-Propanol	0.0	0.0	0.0	0.0
D.E.K.	0.11469	0.08939	0.06460	0.04928
3-Pentanol	0.87896	0.90486	0.93118	0.94759
3-Pentanol Conversion	0.12104	0.09515	0.06882	0.05241
Material Balance(%)				
Overall	99.84	99.83	99.92	99.96
Based on 3-pentanol converted	98.65	98.26	98.80	99.24
Accountability (%)				
Carbon	99.83	99.81	99.88	99.93
Hydrogen	99.78	99.83	99.96	100.01
Oxygen	99.92	99.92	100.02	100.05

Table 4.11.

Effect of Pore Diffusion on Product Distribution at 370°C

(Mole of Product/Mole of 3-Pentanol Feed)

Run No.	44	45
Wt. of Catalyst (gm)	1.0023	1.0023
Particle size (mesh)	-20 + 30	-20 + 30
Feed Rate (gm/hr)	12.8234	12.8234
1/S.V.	6.8900	6.8900
Product		
Hydrogen	0.11251	0.11264
Methane	0.00019	0.00019
Ethylene	0.0	0.0
2-Pentene	0.00422	0.00420
Water	0.00474	0.00459
M.E.K.	0.00050	0.00050
n-Propanol	0.0	0.0
D.E.K.	0.11690	0.11632
3-Pentanol	0.87762	0.87834
3-Pentanol Conversion	0.12238	0.12166
Material Balance (%)		
Overall	99.91	99.93
Based on 3-pentanol converted	99.34	99.43
Accountability (%)		
Carbon	99.92	99.93
Hydrogen	99.85	99.87
Oxygen	99.98	99.98

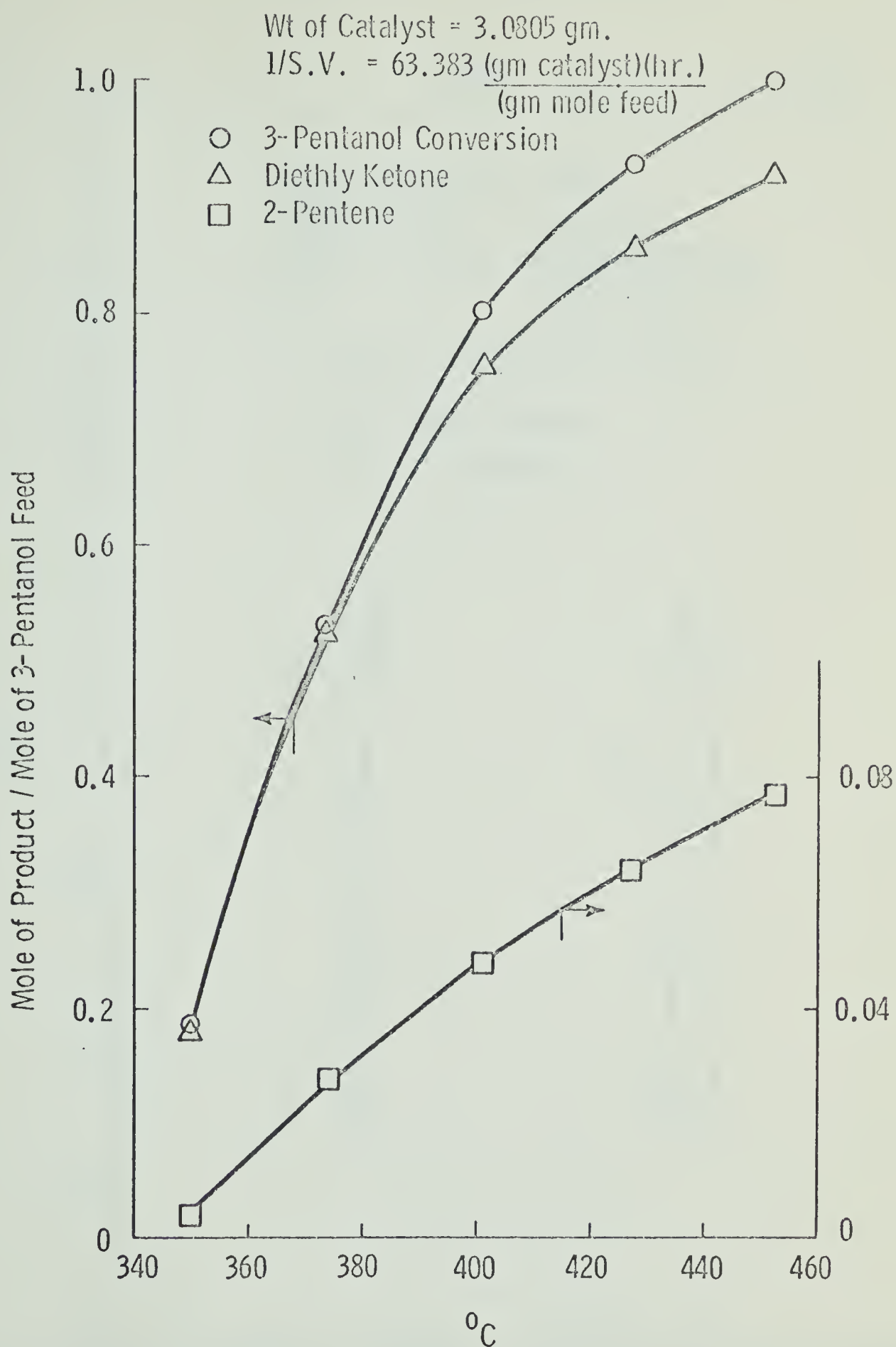


Figure 4.1:
Effect of Temperature on
Product Distribution

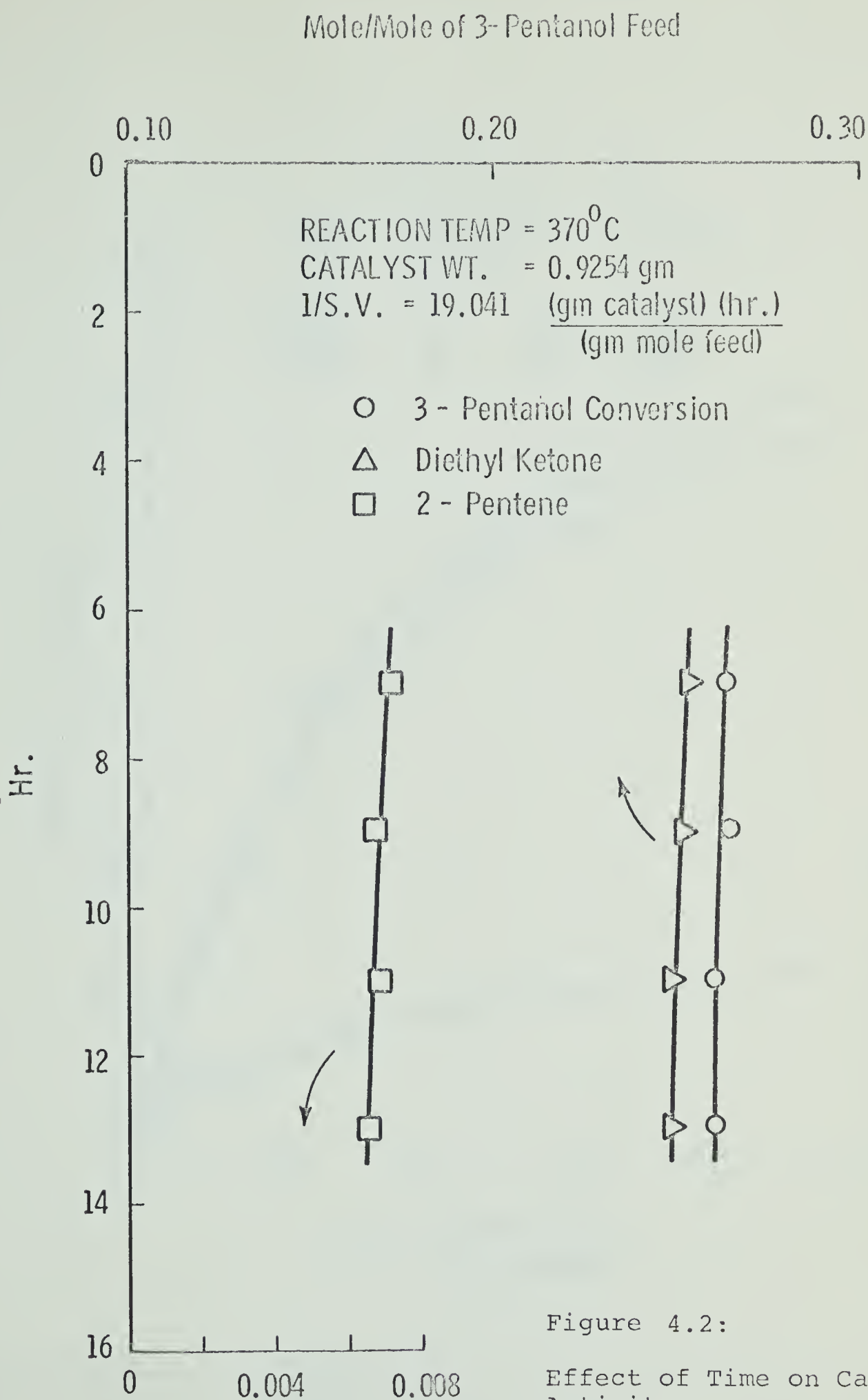


Figure 4.2:

Effect of Time on Catalytic Activity

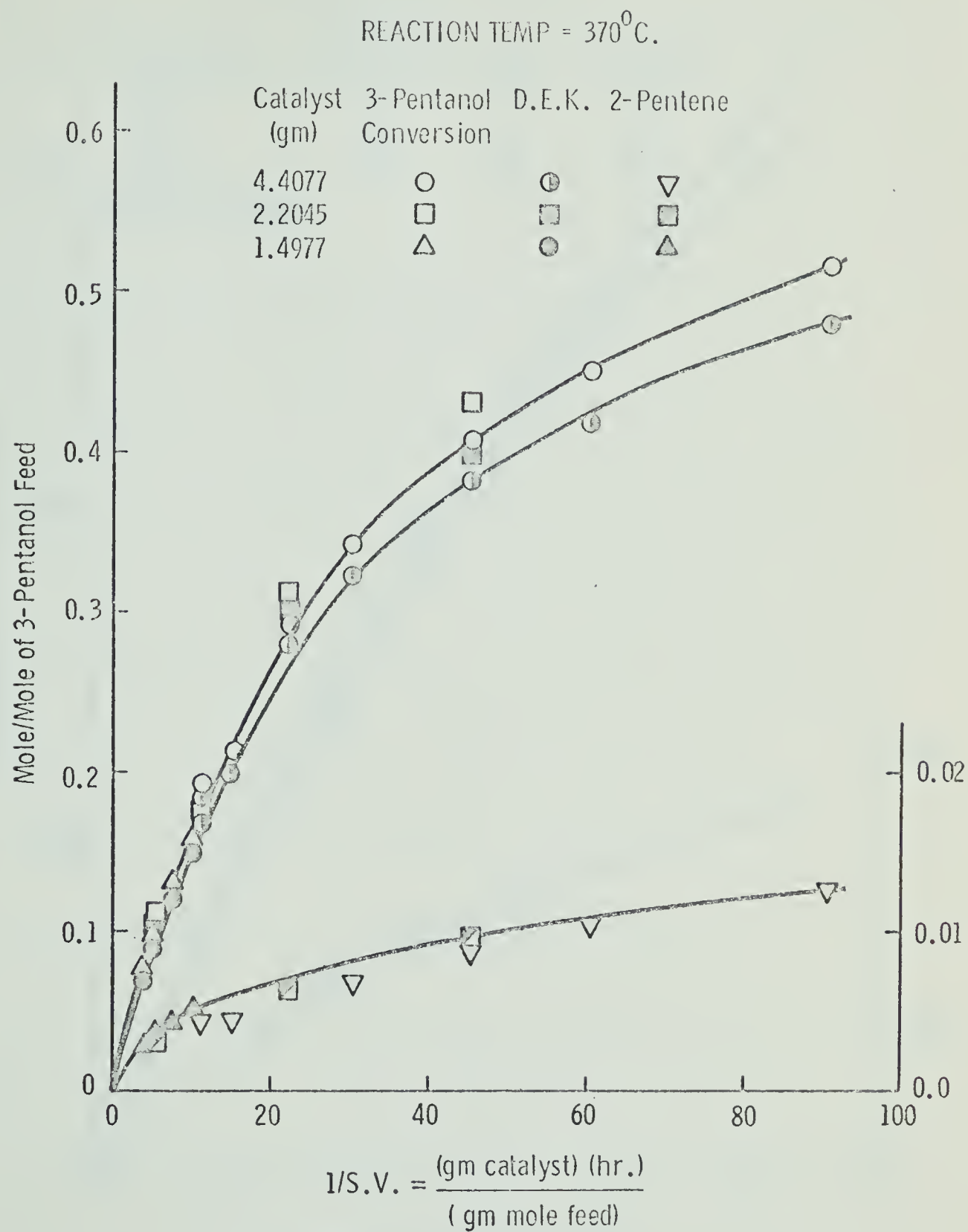


Figure 4.3:

Effect of Space Velocity
upon Product Distribution

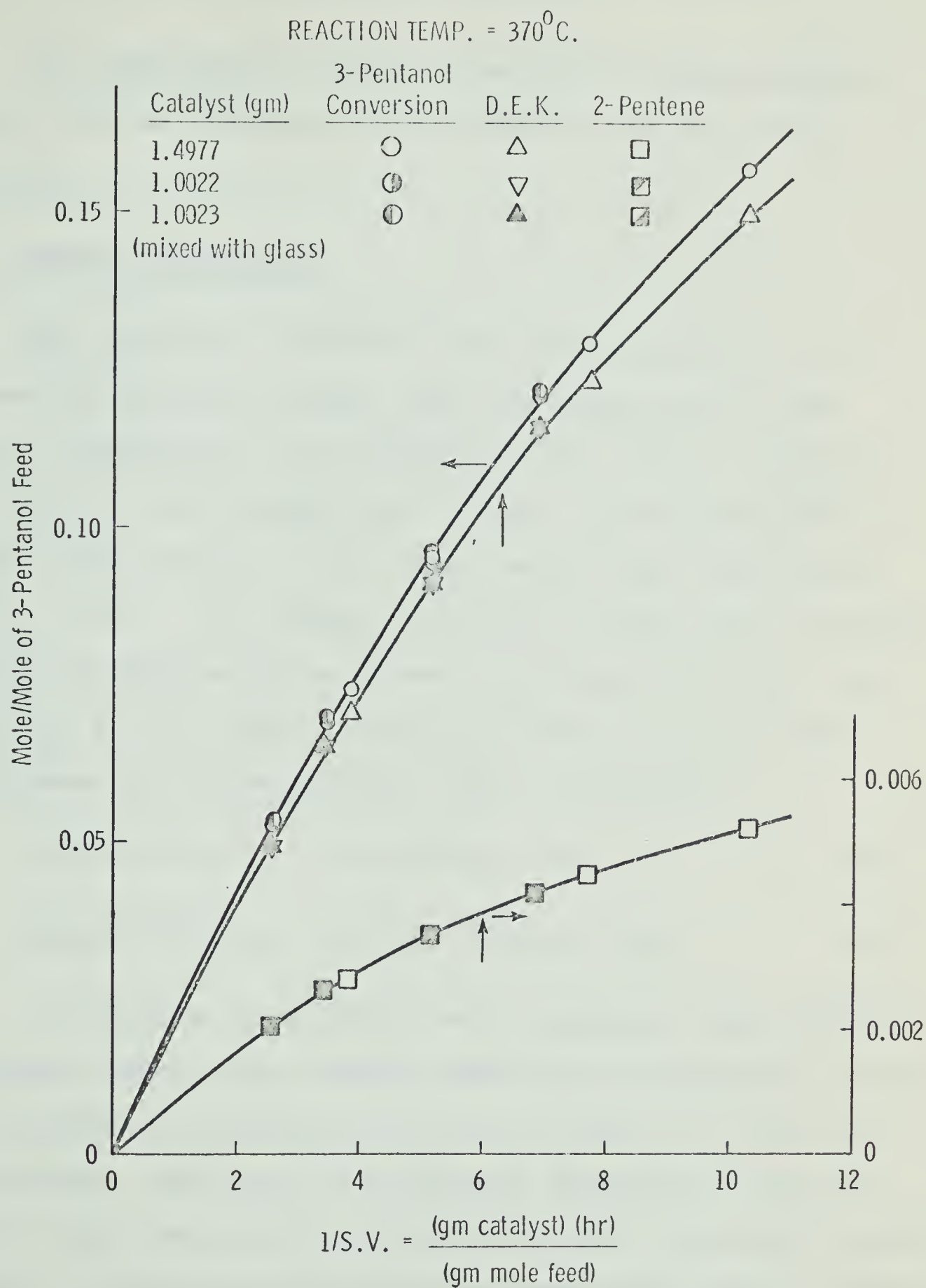


Figure 4.4:

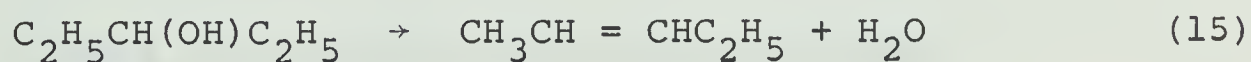
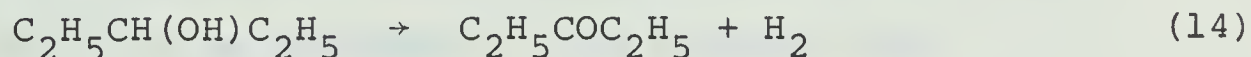
Effect of Space Velocity on
Product Distribution (Lower
Conversion Range)

5. INTERPRETATION AND DISCUSSION OF RESULTS

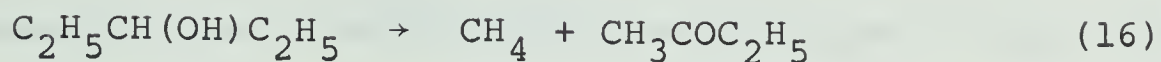
The experimental results presented in the preceding chapter will be discussed and analyzed in the following sections.

5.1. Chemical Reactions

The reactions involved in the dehydrogenation of 3-pentanol on alundum catalyst under the conditions of the present investigation are dehydrogenation (major), dehydration (minor), and decomposition (trace), as seen from the product distributions of all experimental runs (see Tables 4.1. to 4.11.). The amounts of diethyl ketone and 2-pentene are approximately equal to those of hydrogen and water, respectively, for all runs. This relationship suggests that dehydrogenation and dehydration occur in parallel,



In addition to the above major products, trace amounts of methane, methyl ethyl ketone, ethylene and n-propanol were also detected at temperature and l/S.V. above 370°C and 10.0 respectively. Ethylene and n-propanol disappeared from the products when the reactions occurred at 370°C and higher space velocity. The decomposition may be speculated to occur according to the following reactions:



Since the main objective of this work is to obtain kinetic data for the main reactions, the chemistry of these side-reactions was not emphasized and verification was not attempted.

Table 5.1. is a comparison of the result of run number 8 with that obtained by Wanke (3) who used a pyrex glass reactor. The difference is that ethyl isopropyl ketone, carbon monoxide and carbon dioxide were not encountered in the present investigation, while methane, ethylene and n-propanol were not present in Wanke's run. The reason is probably that different side reactions occurred at conditions of lower temperature and higher space velocity as employed in the present work.

5.2. Effects of Vycor and Pyrex Glass Surfaces

As mentioned in Section 4.2., 3-pentanol remained unchanged when passing through pyrex glass bed in the vycor glass reactor at temperatures up to 474°C. This indicated that homogeneous thermal decomposition did not occur and the pyrex and vycor glass surfaces were inert to 3-pentanol decomposition under the experimental conditions in the present investigation. Because of the

inertness and resistance to high temperatures, Vycor glass was used for the construction of the reactor used in this work.

5.3. Effect of Temperature on Product Distribution

As a rule, dehydrogenation and dehydration of alcohol are endothermic reactions (40) and when the reactions are reversible higher temperatures would be expected to increase the conversion. From the high yield and nearly complete conversion such as in Run 8, the dehydrogenation of 3-pentanol on this catalyst appeared to be irreversible. This is shown in the case of 3-pentanol in Figure 4.1. and Table 4.1. At 452°C and $1/\text{S.V.} = 63.383$, 3-pentanol was almost completely converted. The 3-pentanol conversion of 0.998 with the diethyl ketone yield of 92% and 2-pentene yield of 7.7% were obtained under the above conditions. The total yield of the products from the side reactions was only 0.3%. It is apparent that the sodium hydroxide-treated alundum is a good catalyst for production of diethyl ketone from 3-pentanol as far as yield is concerned.

5.4. Effect of Time on Catalytic Activity

The catalytic activity of the alundum catalyst on both dehydrogenation and dehydration decreased with time of use due to the deposition of elemental carbon on the catalyst surface (3) and probably the deactivation by water absorption

Table 5.1.

Comparison of Product Distribution

(Mole of Product/Mole of 3-Pentanol Feed)

Run	No. 8	Wanke's No. 18
Reaction temp. ($^{\circ}\text{C}$)	452	462
3-Pentanol feed rate (gm/hr)	4.2842	not reported
Wt. of catalyst (gm)	3.0805	not reported
1/S.V.	63.383	122.43
Product		
Hydrogen	0.94110	0.982
Methane	0.00826	-
Ethylene	0.00267	-
2-Pentene	0.07688	0.181
Water	not analyzed	0.060
Methyl Ethyl Ketone	0.00636	0.0292
n-Propanol	0.00265	0.0
Diethyl Ketone	0.91722	0.753
3-Pentanol	0.00217	0.008
Ethyl Isopropyl Ketone	-	0.0134
Carbon Monoxide	-	0.0234
Carbon Dioxide	-	0.0500

in the catalyst (41). The colour of the catalyst changed from an initial near-white to light grey after 14 hours of use. To determine the effect of time on catalyst activity, a sample was taken every two hours at constant conditions, after the initial seven hours of stabilization of the catalyst. Four samples were taken. The results obtained as shown in Table 4.2. and Figure 4.2. indicated that there was a slight decrease in activity between 7 and 13 hours of use. The difference in activity was about 0.4% in terms of 3-pentanol conversion. Since the decrease was small, subsequent runs were performed within this range of catalyst life. The life of any charge of catalyst used in the various runs never exceeded 14 hours.

5.5. Effects of Space Velocity and Film Diffusion

For the effect of varying space velocity on the product distributions, the results obtained at low conversion are very good, but those obtained at high conversion are not satisfactory. The reasons will now be discussed.

Referring to Figure 4.3. at equal space velocities, the 3-pentanol conversions and amounts of diethyl ketone of the runs using 2.2045 gm catalyst are consistently higher than those using 4.4077 gm. If the runs were truly

isothermal and film resistance were significant, the reverse trend would be expected. The effect of higher gas velocities would be to promote diffusion and thus increase conversion. If film diffusion alone constituted the parameter being varied and it was found to be unimportant, the conversions for both sets of runs should be on the same curve (28). The erratic behavior which was encountered might be caused by one or a combination of the following factors:

- (1) The activities of the two charges of catalyst were different (unlikely);
- (2) The number of active centers of the catalyst was not directly proportional to its weight (also unlikely);
- (3) The two sets of runs occurred at different temperatures within the catalyst beds (very likely);
- (4) Channelling or other dispersion effects at the two flow rates (likelihood uncertain).

The first cause was unlikely because the two charges of catalyst were taken from the same batch and subjected to the same conditions of stabilization before used. Moreover, the runs were performed within the range of catalyst life where the activity was shown to be nearly constant. The second cause also seemed unlikely because the catalyst

used was of a narrow range of particle sizes (-16 + 20 mesh) such that the surface area would probably be proportional to the weight. The third cause appears to be the more plausible reason. The explanation may lie in that the average catalyst bed temperatures of two sets of runs are different as illustrated in Table 5.2. (also see Appendix III). The difference of 2.7°C in average catalyst bed temperatures caused 0.02601 difference in 3-pentanol conversion. To confirm this, a difference of 0.04 in conversion is estimated for a difference of 2.7°C around 370°C from Figure 4.1. This difference of 0.04 in conversion is approximately equal to the difference in conversion between the lines drawn through the two sets of runs at $1/\text{S.V.}$ of 63.383 in Figure 4.3.

Large axial temperature gradients were encountered at high conversion for those runs using a large amount of catalyst (see Appendix III). A maximum of 17°C difference was recorded in this work. The endothermic effect of the reactions and the 'heat exchange' nature of the reactor are believed to play a major role. The lower portion of a long catalyst bed was always at much lower temperature because it extended too close to the incoming cold reactant (see Figure 3.2.), as in runs 13 to 19. As a result, the average catalyst bed temperature was lower than the center temperature which was defined as the reaction temperature in this work. It seems more

Table 5.2.

Effect of Average Catalyst Bed Temperature on 3-Pentanol Conversion

Run No.	Catalyst wt. (gm)	l/S.V.	Reaction Temperature (°C)	Average Bed Temperature (°C)	Temperature Gradient (°C)	3-Pentanol Conversion
15	4.4077	45.376	369.9	368.0	12.1	0.40742
20	2.2045	45.359	370.0	370.7	3.8	0.43343
				2.7		0.02601
17	4.4077	22.742	370.0	368.5	10.6	0.29011
21	2.2045	22.695	370.0	370.6*	3.4*	0.31328
				2.1		0.02317

*Interpolated between runs 20 and 23 in Appendix III

Table 5.3.

Effect of Particle Size of Catalyst on Conversion

Run No.	Particle size (mesh)	Catalyst wt. (gm)	l/S.V.	Reaction Temperature (°C)	3-Pentanol Conversion
36	-16 + 20	1.0022	6.889	369.6	0.1209
38	-16 + 20	1.0022	6.889	370.0	0.1208
			Ave.	369.8	0.1209
44	-20 + 30	1.0023	6.890	370.3	0.1224
45	-20 + 30	1.0023	6.890	370.0	0.1217
			Ave.	370.2	0.1221

realistic to use average bed temperature as reaction temperature instead of center temperature. In the present work, to measure the temperature at the top and bottom of the catalyst bed simultaneously presented certain difficulty because only one thermocouple could be inserted in the small diameter thermocouple well. Consequently, only one temperature could be monitored continuously. The temperature gradient was measured only once just before sampling.

The results obtained at lower conversion were good (see Figure 4.4.) because of more uniform temperature in a shorter catalyst bed (see Appendix III). The effects of film diffusion and non-isothermal behavior were apparently negligible at the range of conversion below 0.16 (1/S.V. below 11).

5.6. Effect of Pore Diffusion

As shown in Table 5.3., under the same experimental conditions, runs 44 and 45 which used smaller particles of catalyst (-20 + 30 mesh) and runs 36 and 38 which used larger particles of catalyst (-16 + 20 mesh) had approximately equal 3-pentanol conversions, hence equal reaction rates. These results indicated that the effect of pore diffusion appeared to be negligible within the range of particle sizes investigated. If the effect of pore diffusion were significant, the two sets of runs would have

exhibited significantly different conversions at the same experimental conditions. If this were the case, the runs using smaller catalyst particles would have yielded higher 3-pentanol conversions because of less diffusional resistance due to shorter pores and possibly more pores created during reduction of the particle size by crushing.

The average conversion of runs 44 and 45 appeared to be 0.0012 higher than that of runs 36 and 38 (see Table 5.3). This difference in conversions was believed to be caused by an average of 0.4°C higher reaction temperature under which runs 44 and 45 were performed (see Figure 4.1.). However, the difference, being only 1% of 0.120 in conversion, was considered to be negligible, and the 3-pentanol conversions of runs 36, 38, 44 and 45 were considered to be equal and thus to demonstrate that pore diffusion effects were negligible.

5.7. Reproducibility of Experiments

The experiments at 3-pentanol conversion lower than 0.16 were reproducible within the range of experimental errors as shown in Table 4.9. The runs with either catalyst alone or catalyst mixed with pyrex glass exhibited very little difference in conversion as indicated in Figure 4.4. These results indicated that the experimental results were independent of the flow and reactor characteristics. This is an important criterion of a well-

designed reactor operating at the proper experimental conditions within the chemical regime, under which conditions the true chemical kinetic data can be obtained.

The experimental results obtained at the lower range of conversions (below 0.16) will be correlated in the next chapter. Because the data were reproducible and the effects of film and pore diffusion were shown to be negligible, mechanistic rate equations based upon chemical steps alone may be applied.

6. CORRELATION OF DATA

The reaction rates will be derived from the experimental data presented in Chapter 4 and then the rate data will be correlated empirically and by a mechanistic approach. The procedure will be described in detail in the following sections.

6.1. Reaction Rates

For a catalytic reaction in a flow reactor, the rate of reaction can be defined from the material balance equation for a tubular reactor:

$$r_A = F \frac{dN_A}{dW} = \frac{dN_A}{d(1/S.V.)} \quad (18)$$

where r_A = rate of disappearance or formation of A
(moles/hr-gm of catalyst)

F = feed rate (moles/hr)

W = weight of catalyst in reactor (gm)

N_A = moles of A per mole of feed

$S.V.$ = space velocity (moles of feed/hr-gm of catalyst)

When the experimental data are plotted as N_A versus $1/(S.V.)$, the slope of such a curve, according to equation (18), gives the rate of reaction of A. The slope may be obtained by direct measurement from the curve or by

numerical differentiation of the experimental data. The latter method is used in this work because of its better precision.

The data in the higher range of space velocity, as shown in Figure 4.4., are first interpolated at equal spacing of $1/(S.V.)$ by Newton's interpolation formula (44), which passes a polynomial of degree, $(n-1)$, through the data points. The choice of the degree of the polynomial generally depends on the shape of the curve representing the data points to be interpolated. If a higher degree polynomial is used to interpolate a set of data points which form a relatively flat curve, oscillation of the resulting polynomial will generally occur. When this polynomial is differentiated, the oscillation is magnified by numerical errors to yield an incorrect derivative. As a remedy, the original curve can be divided into several segments, each of which consists of a few data points, such that a lower degree interpolation polynomial can be used in each segment to give a smooth curve. In the present work, the experimental data form relatively flat curves (see Figure 4.4.). To obtain more smooth interpolations, a second degree polynomial was employed to interpolate each segment of three data points using a 3-point marching technique in which the adjacent data points overlapped in the next segment. This procedure was a result of trials which employed

polynomials of different degrees, and was found most satisfactory to obtain a smooth interpolation (see Appendix VIII).

The interpolated equally spaced data were differentiated by the method of Whitaker and Pigford (35). This method calculated the derivative at a point by fitting a parabola to five consecutive data points by least squares, with the point in question as the midpoint. The calculated derivative at any one point had up to five different values, one for the fit obtained when it was the midpoint, one for the fit when it was one point lower, and so on. Then, the five values of the first derivative at each individual point were averaged with equal weighting. Table 6.1. and Figure 6.1. show the results of such numerical differentiation, giving the reaction rates as defined by equation (18). A computer program of the interpolation and the numerical differentiation employed in this work is given in Appendix VIII.

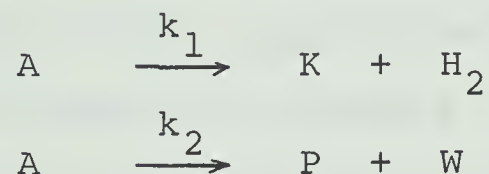
The size of the equal spacing on $1/(S.V.)$ or the increment $\Delta(1/S.V.)$ in the above numerical differentiation had a strong effect on the derivative. The larger the $\Delta(1/S.V.)$ value employed the less accurate the derivative that would be obtained, and vice-versa. Derivatives were also obtained by direct differentiation

of the interpolating polynomial and were found to be, very close in value to those obtained by the method of Whitaker and Pigford. Due to the inherent smoothing characteristics of the latter method, the derivatives from the direct differentiation were not as smooth.

6.2. Correlation of Rate Data

6.2.1. Empirical Method

Consider both catalytic dehydrogenation and dehydration to follow pseudo-homogeneous first order reactions behavior:



where A = 3-pentanol

K = diethyl ketone

P = 2-pentene

W = water

$$r_K = k_1 C_A = k_1 C_{A_0} (1 - X_A)$$

$$r_P = k_2 C_A = k_2 C_{A_0} (1 - X_A)$$

where X_A = 3-pentanol conversion (mole converted/mole in feed).

When the reactions occur at constant temperature and pressure (370°C and 700 mm Hg) and the initial concentration of the reactant C_{A_0} is constant, the terms,

$k_1 C_{A0}$ and $k_2 C_{A0}$, can be replaced by the constants, k_K and k_P , respectively. The rates of formation of diethyl ketone and 2-pentene can be expressed as,

$$r_K = k_K (1 - X_A) \quad (19)$$

$$r_P = k_P (1 - X_A) \quad (20)$$

The overall rate of disappearance of 3-pentanol is then given by,

$$(-r_A) = r_K + r_P = (k_K + k_P)(1 - X_A) \quad (21)$$

If the above correlation is valid, a plotting of rate versus $(1 - X_A)$ should give a straight line. Such a graph is shown in Figure 6.2. It is noted that this correlation is good only within the range of conversion below 0.10 for the reason cited earlier. The constants k_K and k_P thus evaluated from Figure 6.2. are given below.

$$k_K = 0.208 \times 10^{-1} \text{ mole/hr-gm of catalyst}$$

$$k_P = 0.935 \times 10^{-3}$$

The above correlation assumes that the reaction rate is a function of the concentration of the reactant only. This assumption is true in the case of homogeneous reactions. In the case of heterogeneous catalytic reactions, the effects of the surface of catalyst, the adsorption and desorption of reactant and products as well as concentration

of the reactant must be taken into account if the correlation is to be a meaningful one.

6.2.2. Mechanistic Approach

Using this approach, the rate data are fitted to an equation which may be derived on the basis of a plausible reaction mechanism. For parallel reactions of dehydrogenation and dehydration which occur simultaneously on the same catalyst and on the same active sites, a large number of mechanisms can be postulated. The task of determining the best model involves discriminating between a large number of alternative models. If information on the surface chemistry and adsorption characteristics of the catalyst are available, the number of possible mechanisms to be considered may be reduced considerably. Deo and Dalla Lana (46) reported that dehydrogenation and dehydration of n-propanol, respectively, occurred on different types of active sites on the same sodium hydroxide-treated alumina catalyst. Deo (47) also reported that diethyl ketone and water adsorbed much more strongly on that particular catalyst than hydrogen and 2-pentene, respectively. This information, which provides chemical insights, can be used to simplify the derivation of the rate expressions because there is no competition for active sites between the two reactions and only the adsorption of ketone and water need be considered. In effect, each

Table 6.1.

Reaction Rates and Partial Pressures

1/(S.V.)	Overall Rate	T = 370°C							P = 700 mm Hg		
		r_K	r_P	$(1-X_A)$	P_A	P_K	P_H	P_P	P_W		
1	0.020225	0.01940	0.000825	0.9784							
2	0.018935	0.01820	0.000735	0.9584	642.5	25.5	25.5	1.03	1.03		
3	0.017590	0.01695	0.000640	0.9401	619.7	37.2	37.2	1.52	1.52		
4	0.016505	0.01595	0.000555	0.9230	599.8	47.5	47.5	1.90	1.90		
5	0.015230	0.01475	0.000480	0.9069	582.6	56.5	56.5	2.19	2.19		
6	0.013755	0.01335	0.000405	0.8922	566.8	64.5	64.5	2.44	2.44		
7	0.012650	0.01230	0.000350	0.8787	552.4	71.7	71.7	2.65	2.65		
8	0.011460	0.01115	0.000310	0.8667	538.8	78.1	78.1	2.83	2.83		
9	0.010275	0.01000	0.000275	0.8559	526.6	83.8	83.8	2.98	2.98		
10	0.009245	0.00900	0.000245	0.8463	515.0	89.4	89.4	3.12	3.12		

Note: partial pressure in mm Hg

$$\text{Rate} = \frac{\text{moles}}{(\text{gm cat.}) (\text{hr})}$$

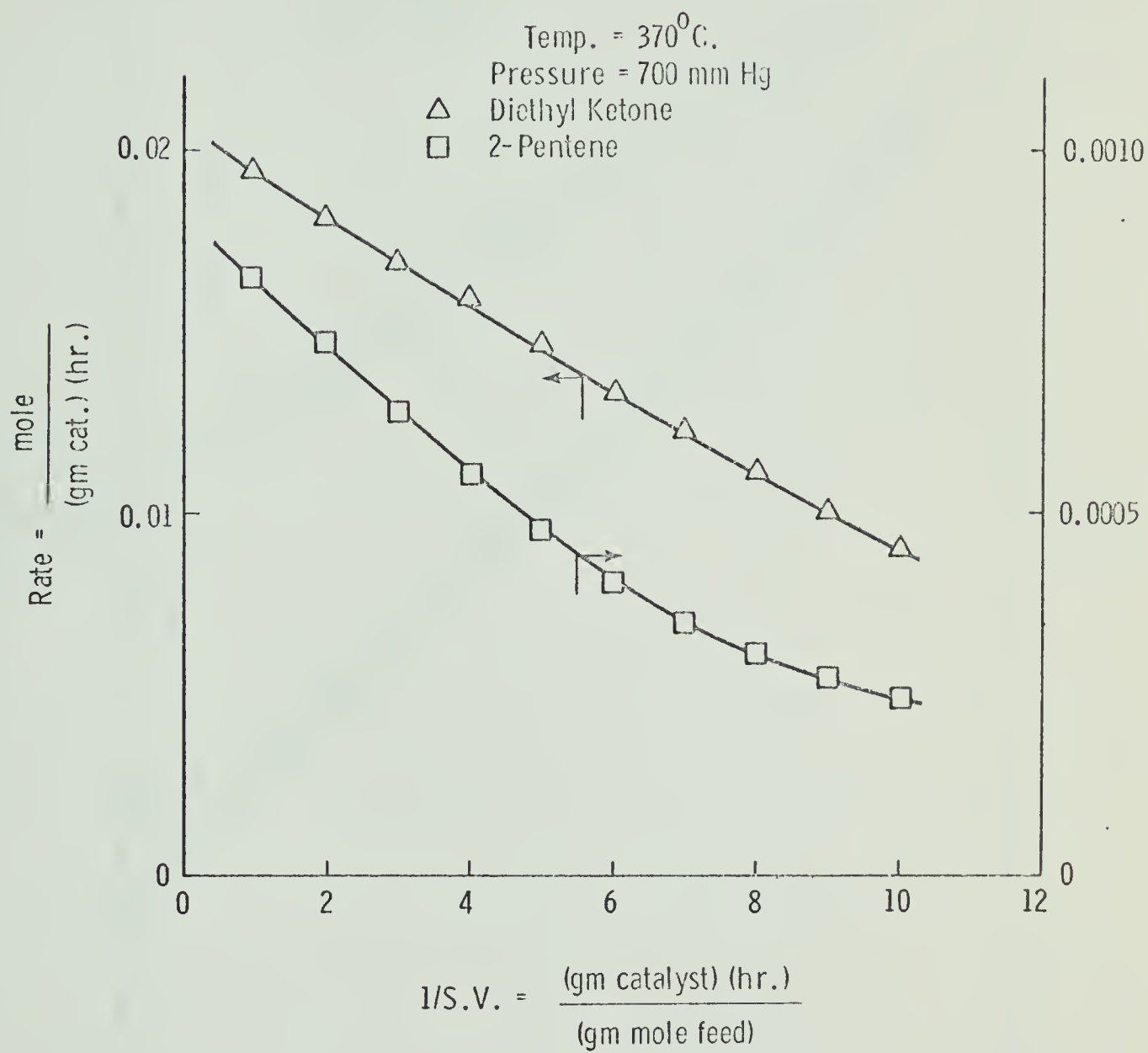


Figure 6.1:

Rate of Formation

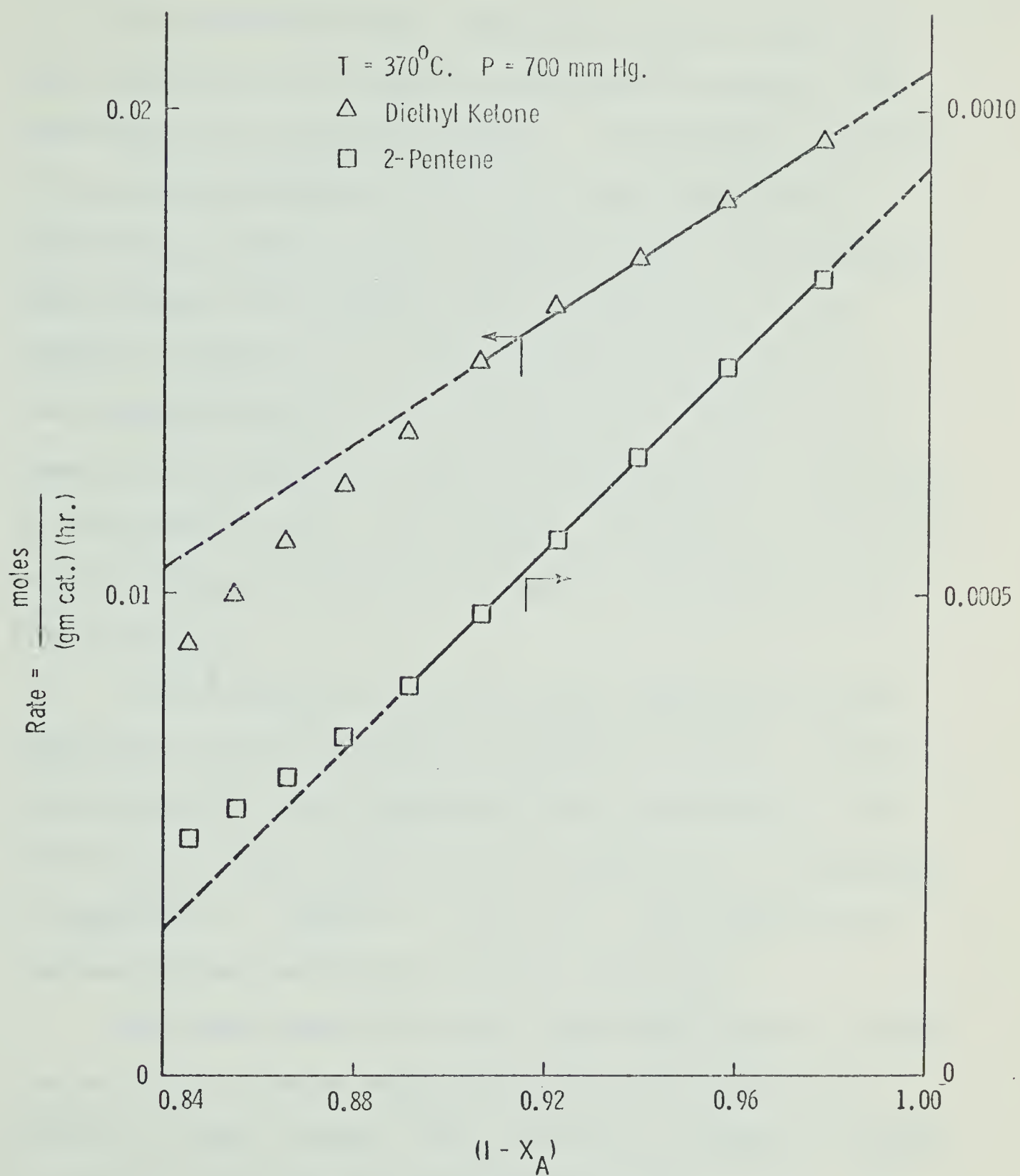


Figure 6.2:

Rate of Formation as Function
of Conversion

reaction can be treated independently in a quantitative manner.

In the mechanistic approach, the rate data are correlated with the partial pressures of reactant and products at the catalyst surface. To determine whether the partial pressures of the bulk gas stream can be replaced by those at the catalyst surface, the pressure drops across the stagnant film are estimated by the method of Hougen et al (48) as given in Appendix VI. The pressure drops of all products and reactant were found to be negligible under the experimental conditions in the present work. As a result, the partial pressures in the bulk gas stream will be used in correlation with the rate data.

In the present work, the rate expressions were developed from the Langmuir-Hinshelwood theory. Both single and dual site mechanisms were postulated. The derivation of the resulting rate equations is presented in Appendix V. Tables 6.2. and 6.3. are summaries of the postulated mechanisms and rate equations.

The rate equations were linearized and the coefficients of the linear equations were estimated by the method of least squares (33), in which systems of linear equations were solved by linear programming (45). The constants obtained are shown in Table 6.4.

Those models which yield negative constants of statistical significance are assumed to be incorrect because negative constants have no physical meaning (31). When more than one of the linearized postulated rate equations have all constants positive (or zero), a choice can be made on the basis of the least squares minimization criterion. The model which exhibits the smallest sum of squares of the deviations is then assumed to represent the system most satisfactorily.

An examination of Table 6.4. shows that, of the postulated mechanisms, only one mechanism for each of the dehydrogenation and dehydration steps (mechanisms (a-1) and (b-1)) yielded no negative constants. The controlling step is adsorption of 3-pentanol while the surface reactions occur by means of single site mechanisms forming adsorbed diethyl ketone and adsorbed water, respectively, in dehydrogenation and dehydration.

$$\text{Dehydrogenation:} \quad r_K = r_H = \frac{k_1 p_A}{(1+K_K p_K)} \quad (22)$$

$$\text{Dehydration:} \quad r_P = r_W = \frac{k_2 p_A}{(1+K_W p_W)} \quad (23)$$

The overall rate of disappearance of 3-pentanol is given by the sum of the two contributing steps,

$$-r_A = r_K + r_P = \frac{k_1 p_A}{(1+K_K p_K)} + \frac{k_2 p_A}{(1+K_W p_W)} \quad (24)$$

where k_1, k_2 are rate constants, (moles)/(gm catalyst)
(hr) (mm Hg)

K_K, K_W are adsorption constants, (mm Hg)⁻¹

p_A, p_K, p_W are partial pressures (mm Hg)

The above mechanisms obtained for dehydrogenation and dehydration are in agreement with the finding by Deo (47) who reported that diethyl ketone and water adsorbed much more strongly on the sodium hydroxide-treated alundum catalyst than hydrogen and 2-pentene, respectively. Since the correlations are based on low conversions and the rate-controlling steps for both reactions appear to be adsorption of the reactant, the interaction of the reactant between two types of sites, at first glance, seems to be insignificant. When one considers the processes at the molecular level, screening of the first type of site by molecules of 3-pentanol adsorbed on the second type of site, or vice-versa, may be present. This type of interaction could result in the adsorption-controlling mechanism.

Table 6.2.

Postulated Mechanisms and Rate Equations for Dehydrogenation

- (a-1) Single site, adsorption of alcohol controlling, ketone adsorbed.

$$r = \frac{k p_A}{(1 + K_K p_K)}$$

- (a-2) Single site, surface reaction controlling, ketone adsorbed.

$$r = \frac{k p_A}{(1 + K_A p_A + K_K p_K)}$$

- (a-3) Single site, desorption of ketone controlling

$$r = \frac{k p_A}{p_H (1 + K_A p_A + K_{AH} p_A / p_H)}$$

- (a-4) Dual site, adsorption of alcohol controlling

$$r = \frac{k p_A}{(1 + K_K p_K + K_H p_H)}$$

- (a-5) Dual site, surface reaction controlling

$$r = \frac{k p_A}{(1 + K_A p_A + K_K p_K + K_H p_H)^2}$$

- (a-6) Dual site, desorption of ketone controlling

$$r = \frac{k p_A}{p_H (1 + K_A p_A + K_{AH} p_A / p_H + K_H p_H)}$$

Table 6.3.

Postulated Mechanisms and Rate Equations for Dehydration

- (b-1) Single site, adsorption of alcohol controlling,
water adsorbed

$$r = \frac{k p_A}{(1 + K_W p_W)}$$

- (b-2) Single site, surface reaction controlling, water
adsorbed

$$r = \frac{k p_A}{(1 + K_A p_A + K_W p_W)}$$

- (b-3) Single site, desorption of water controlling

$$r = \frac{k p_A}{p_P (1 + K_A p_A + K_{AP} p_A / p_P)}$$

- (b-4) Dual site, adsorption of alcohol controlling

$$r = \frac{k p_A}{(1 + K_W p_W + K_P p_P)}$$

- (b-5) Dual site, surface reaction controlling

$$r = \frac{k p_A}{(1 + K_A p_A + K_W p_W + K_P p_P)^2}$$

- (b-6) Dual site, desorption of water controlling

$$r = \frac{k p_A}{p_P (1 + K_A p_A + K_{AP} p_A / p_P + K_P p_P)}$$

Table 6.4.

Summary of Kinetic Constants

(a) Dehydrogenation

Mecha- nism	k	k _A	K _K	K _H	K _{AH}	No. of negative constants	Sum of squared deviations
(a-1)	0.42518x10 ⁻⁴		0.14029x10 ⁻¹			None	0.65834x10 ⁻⁵
(a-2)	0.13071x10 ⁻⁵	-0.13963x10 ⁻²	-0.23481x10 ⁻²			2	0.30355x10 ⁻⁵
(a-3)	0.59237x10 ⁻³	-0.15981x10 ⁻²			0.33773x10 ⁻¹	1	0.21436x10 ⁻⁶
(a-4)	0.42518x10 ⁻⁴		-0.16012	0.17415		1	0.65835x10 ⁻⁵
(a-5)	0.34564x10 ⁻⁶	-0.13047x10 ⁻²	0.21520x10 ⁻³	-0.23516x10 ⁻²		2	0.23230x10 ⁻⁵
(a-6)	0.49659x10 ⁻³	-0.15695x10 ⁻²		-0.47875x10 ⁻³	0.28235x10 ⁻¹	2	0.20435x10 ⁻⁶

(b) Dehydration

	k	k _A	K _W	K _P	K _{AP}		
(b-1)	0.12298x10 ⁻⁴		0.72254x10 ¹			None	0.48117x10 ⁻⁷
(b-2)	0.50154x10 ⁻⁷	-0.13986x10 ⁻²	-0.56137x10 ⁻¹			2	0.21532x10 ⁻⁹
(b-3)	0.42670x10 ⁻⁶	-0.15822x10 ⁻²			0.60902x10 ⁻³	1	0.16314x10 ⁻⁹
(b-4)	0.12299x10 ⁻⁴		-0.56705x10 ⁻¹	0.12896x10 ²		1	0.52000x10 ⁻³
(b-5)	0.18268x10 ⁻⁷	-0.12888x10 ⁻²	0.24165x10 ⁻¹	-0.69202x10 ⁻¹		2	0.26855x10 ⁻⁹
(b-6)	0.43255x10 ⁻⁶	-0.15864x10 ⁻²		0.14043x10 ⁻²	0.61902x10 ⁻³	1	0.16575x10 ⁻⁹

7. CONCLUSIONS

A. Homogeneous thermal decomposition of 3-pentanol was not detected. Both pyrex and vycor glass surfaces exhibited no catalytic effects on 3-pentanol at temperatures up to 474°C , the maximum temperature employed.

B. The sodium hydroxide-treated alundum catalyst catalyzed dehydrogenation and dehydration of 3-pentanol in parallel, with dehydrogenation being the predominant reaction.

C. Dehydrogenation of 3-pentanol increased markedly with increasing temperature. At 452°C and a space velocity of 1.578×10^{-2} , 3-pentanol conversion of 0.998 was obtained with a diethyl ketone yield of 92% and a 7.7.% yield of 2-pentene, the dehydration product. The extent of side-reactions was negligible (0.3% yield).

D. The activity of the sodium hydroxide-treated alundum catalyst decreased slightly with the time of use. At 370°C and a space velocity of 5.252×10^{-2} (0.9254 gm of catalyst), the decrease in activity between the seventh and thirteenth hours of use was 1% in terms of the 3-pentanol conversion at the above conditions. This slight decline in catalytic activity could be attributed to declines in both dehydrogenation and dehydration steps at the above conditions.

E. Film diffusion was shown to be negligible at 370°C and space velocities above 9.713×10^{-2} (conversion below 0.157).

F. The effect of pore diffusion appeared to be insignificant within the range of catalyst particles from -16 to +30 mesh at 370°C and a space velocity of 1.452×10^{-1} (1.0023 gm catalyst).

G. The primary experimental data were reproducible within the experimental error (± 0.002 of 3-pentanol conversion) at 370°C and space velocities above 9.713×10^{-2} (conversion below 0.157).

H. On the basis of the data correlated as well as independent mechanistic studies (47), dehydrogenation and dehydration of 3-pentanol at 370°C appear to involve two different types of active sites on the sodium hydroxide-treated alundum catalyst surface. The mechanisms for each reaction seemed to involve different single sites, with chemisorption of diethyl ketone and water being predominant, the rate-controlling step being the adsorption of 3-pentanol on the catalyst.

8. RECOMMENDATIONS

8.1. Equipment

8.1.1 The liquid feed system provided very constant and precise feed rates with variations of less than 0.5%. This was more than adequate for the experimental system employed.

8.1.2. The vaporization, reactor, and heating systems had quick thermal response which reduced the time required to attain the reaction temperature level when starting-up or changing operating conditions. This feature is desirable in dealing with a catalyst of changing activity.

8.2. Methods

8.2.1. The chromatographic analytical methods used in the present work were very accurate. The 'Internal Reference Method' for liquid product analysis was excellent (with error less than 0.5%).

8.2.2. The numerical differentiation method used in the present investigation provided very precise rate data.

8.3. Experiments

8.3.1. To attain more uniform catalyst bed temperature, a shorter catalyst bed or the use of catalyst diluted

with inert solid such as pyrex glass should be used in future experiments.

8.3.2. If further investigation of the reaction mechanisms is attempted, an initial rate study at different pressures and different temperature level is recommended.

BIBLIOGRAPHY

1. Vasudeva, K., "Reactions of n-Propanol on Alumina Supported Chromia Catalyst", M.Sc. Thesis, U. of Alberta, Edmonton, Alberta, April, 1963.
2. Vasudeva, K., "Vapor Phase Reactions of n-Propanol on Solid Catalysts", Ph.D. Thesis, U. of Alberta, Edmonton, Alberta, September, 1965.
3. Wanke, S.E., "Dehydrogenation of n-Propanol of an Alundum Catalyst", M.Sc. Thesis, U. of Alberta, Edmonton, Alberta, April 1966.
4. Imai, T., "The Influence of Homogeneous Reactions and of Reactor Surface upon n-Propanol Decomposition", M.Sc. Thesis, U. of Alberta, Edmonton, Alberta, September, 1967.
5. Dalla Lana, I.G., Wanke, S.E., and Deo, A.V., "Interpretation of Multiple Catalytic Reaction Steps in n-Propanol Dehydrogenation", Paper presented at the Second Symposium on Catalysis, Hamilton, Ontario, June, 1967.
6. Emmett, P.H., Sabatier, P. and Reid, E.E., "Catalysis Then and Now", Franklin Publishing Co., Inc., N.J., 1965, Chapters 14 and 15, Part II.
7. *ibid.* P. 650, 658
8. *ibid.* P. 674
9. Bond, G.C., "Catalysis by Metals", Chapter 18, Academic Press, London, 1962.
10. Goldstein, R.F., "The Petroleum Chemicals Industry", 2nd Ed., Chapter 17, E. and F.N. Spon, London, 1958.
11. Berkman, S., Morrell, J.C. and Egloff, G., "Catalysis", Chapters 8 and 10, Reinhold Publishing Corporation, N.Y., 1940.
12. Mears, D.E. and Boudart, M., "The Dehydrogenation of Isopropanol on Catalysts Prepared by Sodium Borohydride Reductions", Vol. 12, No. 2, P. 313-320, A.I.Ch.E. Journal, 12, 313 (1966).

13. Garcia De La Banda, J.F., "Semiconductivity and Catalytic Activity. The Dehydrogenation of Isopropyl Alcohol on $\text{ZnO-Cr}_2\text{O}_3$ Catalysts", J. Cat. 1, 136 (1962).
14. Kazuaki Kawamoto (Univ. Hiroshima) Bull. "Dehydrogenation of Secondary Alcohols with Reduced Copper. Catalytic Dehydrogenation of Isopropyl Alcohol", Chem. Soc. Japan 34, 161 (1961).
15. Tolstopyatova, A.A., Balandin, A.A. and Yu Chi-Chuan, "Kinetic Parameters of Dehydrogenation of Ethyl and Isopropyl Alcohols", Kinetics and Catalysis, Academic of Science of the U.S.S.R., Vol. 6, No. 1, p. 89-94.
16. Thaller, L.H. and Thodos, G., "The Dual Nature of the Catalytic Reactions: The Dehydrogenation of Sec-Butyl Alcohol to Methyl Ethyl Ketone at Elevated Pressures", A.I.Ch.E. Journal, 6, No. 3, p. 369-373 (1960).
17. Bashkirov, A.N., Kamzolkin, V.V. and Potarin, M.M., "The Preparation of Higher Ketones by Dehydrogenation of Secondary Alcohols on Copper-Chromium and Nickel-Chromium Catalysts", Neftekhimiya, 4 (2), p. 298-300 (1964).
18. Ford, F.E. and Perlmutter, D.D., "The Kinetics of the Brass-Catalysed Dehydrogenation of Sec-Butyl Alcohol", Chemical Engineering Science, 19, p. 371-378, 1964.
19. Pines, H. and Manassen, J., "Advances in Catalysis and Related Subjects", 16, p. 83-90, 1966.
20. Pines, H. and Haag, W.O., "Alumina: Catalyst and Support. I. Alumina, Its Intrinsic Acidity and Catalytic Activity", J.Am.Chem.Soc., 82, 2471, (1960).
21. Ipatieff, V.N., "Catalytic Reactions at High Pressures and Temperatures", The MacMillan Company, N.Y., 1936, Chapters 1 and 2.
22. Mourgues, L.D., Peyron, F. and Trambouze, Y., "Kinetics of the Catalytic Dehydration of 2-Pentanol", J. Cat. 7, 117, (1967).
23. Winfield, M.E., "Catalysis", (P.H. Emmett Ed)., 7, 1960, Reinhold, N.Y., p. 93, 116, 131, 134, 157, 173.

24. Rice, F.O. and Rice, K.K., "The Aliphatic Free Radicals", The John Hopkins Press, 1935, p. 134.
25. *ibid.* p. 110.
26. *ibid.* p. 130.
27. Levenspiel, O., "Chemical Reaction Engineering", John Wiley and Sons, Inc., N.Y. (1962).
28. *ibid.* p. 455.
29. Walas, S.M., "Reaction Kinetics for Chemical Engineers", Toronto, McGraw-Hill Book Co., Inc., 1959, Chapter 7.
30. *ibid.* p. 166.
31. *ibid.* p. 167.
32. Hougen, O.A. and Watson, K.M., "Chemical Process Principles, Part III, Kinetics and Catalysis", John Wiley and Sons, Inc., London, 1958, Chapter XIX.
33. *ibid.* p. 940.
34. Nevers, N., "Rate Data and Derivatives", A.I.Ch.E. Journal, 12, 6, 1110-1115, (1966).
35. Whitaker, S. and Pigford, R.L., "Numerical Differentiation of Experimental Data", Ind. and Eng. Chem., 52, 2, 185-187 (1960).
36. Hougen, O.A. and Young, K.H., "Determination of Mechanism of Catalyzed Gaseous Reactions", Chem. Eng. Progress, 46, 3, 146-157, (1950).
37. Weast, R.C., "Handbook of Chemistry and Physics", C-457, 47th Ed., The Chemical Rubber Company.
38. Corning Glass Works Catalogue B-83, "Properties of Selected Commercial Glasses", N.Y., Corning Glass Works, (1965).
39. Messner, A.E., Rosie, D.M., and Argabright, P.A., "Correlation of Thermal Conductivity Cell Response with Molecular Weight and Structure", Anal. Chem., 31, 2, 230-233, (1959).

40. Morrison, R.T. and Boyd, R.N., "Organic Chemistry", Allyn and Bacon, Inc., Boston, p. 526 (1967).
41. Deo, A.V., personal communication.
42. Bowker, A.H. and Lieberman, G.J., "Engineering Statistics", Prentice-Hall, Inc., N.J., p. 217-218, 558, 8. (1960).
43. Ibid. p. 245-246.
44. Froburg, C.E., "Introduction to Numerical Analysis", Addison-Wesley Publishing Co., Inc., London, p. 148-150 (1965).
45. Ibid. p. 74.
46. Deo, A.V. and Dalla Lana, I.G. "Infrared Study of the Adsorption and Surface Mechanism of n-propanol on γ -Alumina and γ -Alumina doped with Sodium Hydroxide and Chromium Oxide", read at the C.I.C. Conference, Vancouver, June 2-5, 1968.
47. Deo, A.V., unpublished work, University of Alberta, Edmonton, Alberta.
48. Hougen, O.A., Ramaswami, D. and Yoshida, F., "Temperatures and Partial Pressures at the Surface of Catalyst Particles", A.I.Ch.E. Journal, 8, 1, 5-11, (1962).
49. Johns, T., "Beckman Gas Chromatography Application Manual", Bulletin 756-A, 1961. Applications Engineering, Scientific and Process Instruments Division, Beckman Instruments, Inc., p. 39-47.
50. Rubinshtein, A.M., Sagalovich, A.V. and Pribytkova, N.A. "Decomposition of Isopropyl Alcohol on Alumina-Chromia Catalyst", Izv. Akad. Nauk SSSR, Otd. Klim. Nauk 996 (1961).
51. Frolov, V.M., "The Kinetics of the Catalytic Dehydrogenation of Alcohol on Germanium", Kinetics and Catalysis, 5, 6, 951.

APPENDIX I

CALIBRATION OF MICRO-FEEDER

The micro-feeder was calibrated by feeding 3-pentanol at an average room temperature of 26°C. The 3-pentanol was collected in a 25 ml Erlenmeyer flask after it has passed through the 3/16 in. stainless steel tubing. To prevent the loss of 3-pentanol by evaporation, the Erlenmeyer flask was cooled in an ice-water bath. The duration of each run was 30 minutes. The amount of 3-pentanol was obtained by weighing. Each piston speed (gear) was calibrated in such a way that the whole range of piston travel (11 cm) was covered. The calibration of micro-feeder is shown in Table A-I-1. Only the 1st, 3rd, 5th and 7th gears of the micro-feeder were calibrated. The 2nd, 4th, and 6th gears were interpolated from the calibration because the gear system of the micro-feeder was so constructed that the 2nd gear was exactly half-way between 1st and 3rd gears, and 4th gear between 3rd and 5th gears and so on.

The confidence intervals of the means of 3-pentanol feed rates have been estimated (42) in the following.

The confidence interval for m is given by

$$\bar{x} \pm t_{\alpha/2; n-1} \cdot \frac{s}{\sqrt{n}} \quad (I-1)$$

where, \bar{x} is the sample mean

s is the sample standard deviation

n is the sample size

m is the population mean

$$t \text{ is defined as } \int_{-t_{a/2;n-1}}^{t_{a/2;n-1}} \frac{e^{-y^2/2}}{\sqrt{2\pi}} dy = a/2$$

$$s = \sqrt{\frac{\sum_{i=1}^n (x_i - \bar{x})^2}{n-1}} \quad (I-2)$$

For $n = 5$ and $a = 0.05$, $t_{a/2;n-1} = 2.776$

Table A-I-2 shows the values of $t_{a/2;n-1} \cdot s/\sqrt{n}$ and Table A-I-3 gives the means of feed rates. Figure A-I-1 is the calibration curve of micro-feeder.

Table A-I-1

Calibration of Micro-Feeder

Fluid 3-Pentanol
Feeder 50 cc brass syringe
Temperature 26°C

Speeds of Syringe Piston (gears)

RUN	1st		3rd		5th		7th	
	gm/hr	cm/hr	gm/hr	cm/hr	gm/hr	cm/hr	gm/hr	cm/hr
1	4.2874	1.060	8.5710	2.124	17.2100	4.232	34.0996	8.480
2	4.2822	1.064	8.5850	2.121	17.1416	4.248	34.1744	8.472
3	4.2906	1.060	8.5546	2.120	16.9938	4.240	34.0746	8.476
4	4.2848	1.060	8.5590	2.120	16.9235	4.243	34.1160	8.468
5	4.2760	1.064	8.5432	2.130	17.1528	4.232	34.1090	8.472
AVE.	4.2842	1.062	8.5626	2.123	17.0843	4.239	34.1147	8.474

Table A-I-2

Values of $t_{a/2;n-1} \cdot s/\sqrt{n}$

Piston speeds (gears)	1st	3rd	5th	7th
$t_{a/2;n-1} \cdot s/\sqrt{n}$				
gm 3-Pentanol/hr	0.0069	0.0199	0.1493	0.0458

Table A-I-3

Means of 3-Pentanol Feed Rates at 26°C

Gear	gm/hr*	± %
1	4.2842 ± 0.0069	0.16
2	6.4234 ± 0.0134	
3	8.5626 ± 0.0199	0.23
4	12.8234 ± 0.0846	
5	17.0843 ± 0.1493	0.87
6	25.5995 ± 0.0975	
7	34.1147 ± 0.0458	0.13

* at 95% confidence interval

Note: gears 2, 4 and 6 were interpolated.

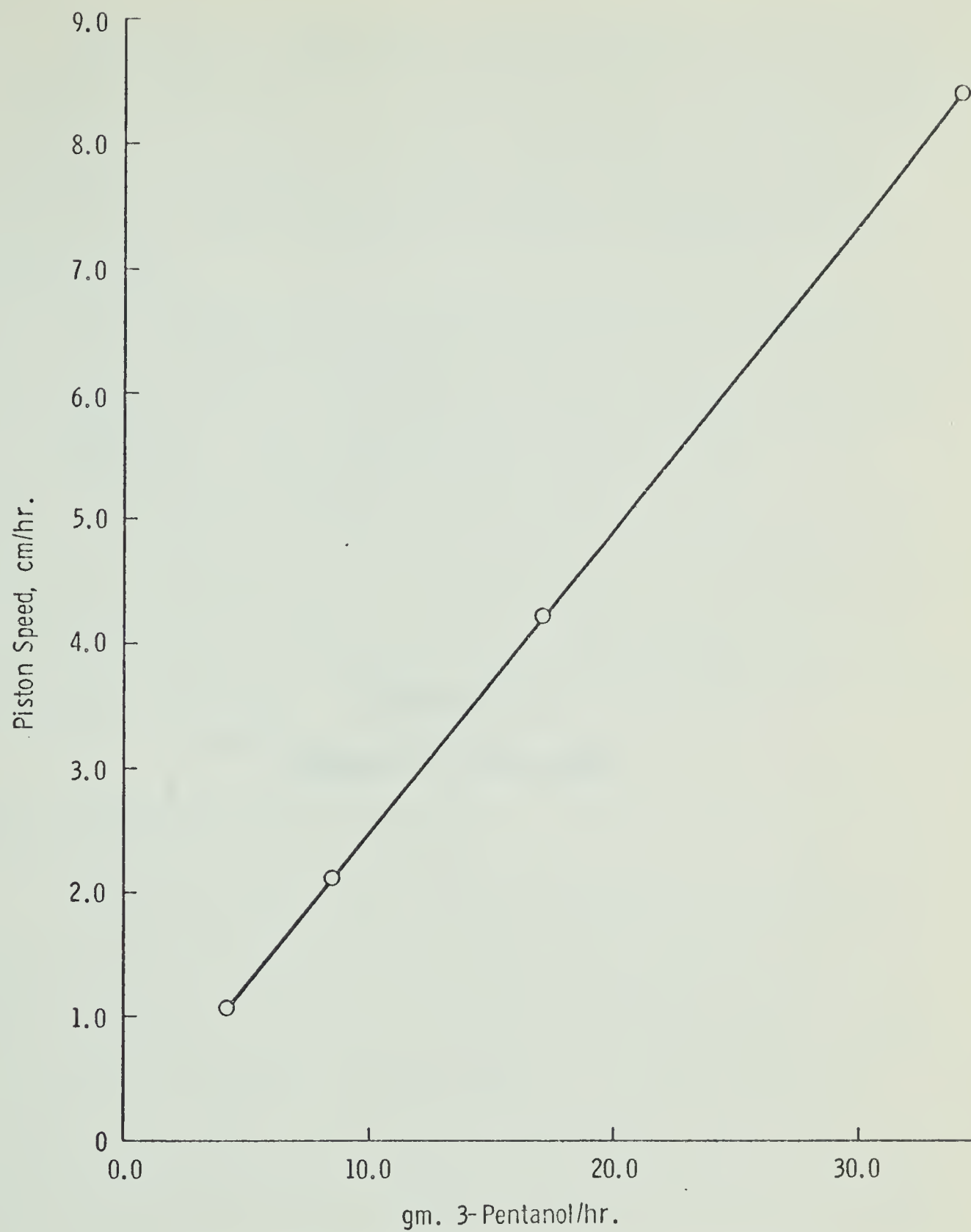


Figure A-1-1 CALIBRATION CURVE FOR MICROFEEDER

APPENDIX II

METHODS OF ANALYSES

The use of liquid-gas chromatography for analysis of organic compounds is a common practice. High accuracy of analyses can usually be obtained if the operating variables are kept constant throughout calibration and analyses (49).

The simplest way of calibration is to correlate the weight percent or mole percent with the thermal response of a component. This requires that the weight or the number of moles of samples must be kept constant during analyses. This procedure is impractical. To account for the variations of sample sizes and other operating variables, the following methods have been developed to improve the product analyses.

II-1 Internal Reference Method

In this method, the relative weight percents are correlated with the relative thermal responses (39. 49). Each component is related to an arbitrarily chosen component which is present in the sample. In this work, 3-pentanol was chosen as internal reference. The following procedure shows how this method is applied to calibration and analyses.

(1) From the analyses of the standard samples of synthetic mixtures, the following equations are obtained.

$$X_r = f_r (A_r) \quad (\text{II-1})$$

$$\frac{X_i}{X_r} = f_i \left(\frac{A_i}{A_r} \right) \quad (\text{II-2})$$

where X_r = wt. % of 3-pentanol (reference component)
in the sample.

X_i = wt. % of component i in the sample.

A_r = peak area of 3-pentanol.

A_i = peak area of component i.

i = 1, 2, ..., r-1, r is also the number of
components in the sample.

f_i = simple function for component i.

f_r = simple function for 3-pentanol.

Equation II-1 is not exact due to sample size variation because the peak area (thermal response) of a component is a function of its weight only. Equation II-2 is exact because the weight ratio and thermal response ratio remain constant in spite of change in sample size. The f_i can usually be represented by simple linear function or power function. In the present studies, a simple power function is used.

$$\frac{X_i}{X_r} = a_i \left(\frac{A_i}{A_r} \right)^{b_i} \quad (\text{II-2A})$$

Where a_i and b_i are constants determined by method of

least square (43). Table A-II-2 shows the values of a and b for each component. The function f_r is approximated by Newton's interpolating formula with divided differences (44). Figures A-II-1, A-II-2 and A-II-3 are graphical presentations of the calibration. As an example, only those of diethyl ketone and 3-pentanol are given.

(2) Analysis of unknown sample

From chromatography analysis, all A_i 's and A_r are obtained and f_i 's and f_r have been established by calibration. The remaining unknowns in Equation II-2 are X_i 's and X_r . Solution of Equation II-2 to find all X_i 's and X_r becomes trial and error. However, Equation II-1, though not exact, can be used as a first approximation. Now, all A_i 's can be calculated by using X_r obtained from Equation II-1. A new value of X_r is then obtained from Equation II-3.

$$X_r = 1.0 - \sum_{i=1}^{r-1} X_i \quad (\text{II-3})$$

Then use this new X_r in Equation II-2 to calculate a new set of X_i 's. This procedure is repeated until the difference between the present and previous values of X_i is very small.

$$|x_i^{(k-1)} - x_i^{(k)}| \leq \epsilon_i, \quad i = 1, 2, \dots, r \quad (\text{II-4})$$

where k is number of iterations and ϵ_i is a very small number arbitrarily chosen. Alternatively, convergence can be achieved by normalization.

$$x_r^{(k)} = \frac{x_r^{(k-1)}}{\sum_{i=1}^r x_i^{(k-1)}} \quad (\text{II-5})$$

To speed up the convergence, the first two iterations used Equation II-3 and the remaining used Equation II-5 in this work. This procedure took about 5 iterations on the average to get $\epsilon_i \leq 0.00005\%$.

Although the derivation of above equations is based on an analysis by a single column, the procedure can be applied to an analysis which requires two columns for complete separation. For example, in this work, water is analysed by a Porapak column while the other components by a Phthalate column.

$$\frac{x_w}{x_p} = g_w \left(\frac{A_w'}{A_p} \right) \quad (\text{II-2B})$$

$$\frac{x_p}{x_r} = f_p \left(\frac{A_p}{A_r} \right) \quad (\text{II-2C})$$

From above two equations, we have

$$\frac{X_w}{X_r} = g_w \left(\frac{A_w'}{A_p'} \right) f_p \left(\frac{A_p}{A_r} \right) \quad (\text{II-2D})$$

where A_w' = thermal response of water in Porapak column

A_p' = thermal response of 2-pentene in Porapak column

A_p = thermal response of 2-pentene in Phthalate column

X_w = wt. % of water in the sample

X_p = wt. % of 2-pentene in the sample

The functions g_w and f_p are calibrated by using synthetic mixtures in Porapak and Phthalate columns respectively.

For analyses, two injections are made in the two columns, so that all terms on the right hand side of Equation II-5D are known. Now Equation II-5D can be handled as Equation II-2.

Very accurate analyses can be obtained by the Internal Reference Method. Table A-II-3 shows the results of the analyses of a sample of known composition.

Table A-II-1

Example of Calibration

(Phthalate Column by Synthetic Mixture)

	Diethyl Ketone		3-Pentanol		Wt % DEK Wt % 3PeOH	A DEK A 3PeOH
	Wt %	Area	Wt %	Area		
1	5.2728	42849	91.8294	807891	0.057420	0.053038
2	8.5459	72283	85.1168	747005	0.100402	0.096764
3	10.5585	85071	78.6881	690293	0.134182	0.123239
4	30.8566	243914	51.9106	469759	0.594418	0.519232
5	50.5238	393599	31.0798	312064	1.62562	1.26128
6	73.4565	583725	25.7009	271702	2.85813	2.14840
7	1.9152	15495	66.7451	583866	0.028694	0.026539
8	18.0422	146114	75.1780	656516	0.239993	0.222560

Table A-II-2

Constants Obtained From Calibration

<u>Component</u>	<u>a</u>	<u>b</u>
2-Pentene	1.1019	1.0313
Methyl Ethyl Ketone	0.85028	0.96120
n-propanol	0.94686	1.0443
Diethyl Ketone	1.2309	1.0521
Water*	16.696	1.0973

* relative to 2-pentene

Table A-II-3

Accuracy of Analysis by Internal Reference Method

(Weight Percent)

Analysis	2-Pentene	Water	M.E.K.	n-Propanol	D.E.K.	3-Pentanol
1	9.7278	1.6452	2.1738	2.1264	32.3340	51.9928
2	9.7725	1.5067	2.3434	2.0346	32.2692	52.0736
3	9.8293	1.4137	2.2502	2.1907	32.1787	52.1374
4	9.7539	1.5124	2.2783	2.1107	32.2754	52.0693
Ave.	9.7709	1.5195	2.2614	2.1156	32.2643	52.0683
True	9.7804	1.5233	2.2620	2.1084	32.2561	52.0698
Max. Deviation*	-0.0526	+0.1219	-0.0882	+0.0823	+0.0779	-0.0770
% Max. Deviation*	-0.53%	+8.00%	-3.89%	+3.90%	+0.24%	-0.15%

* Maximum deviation from true composition

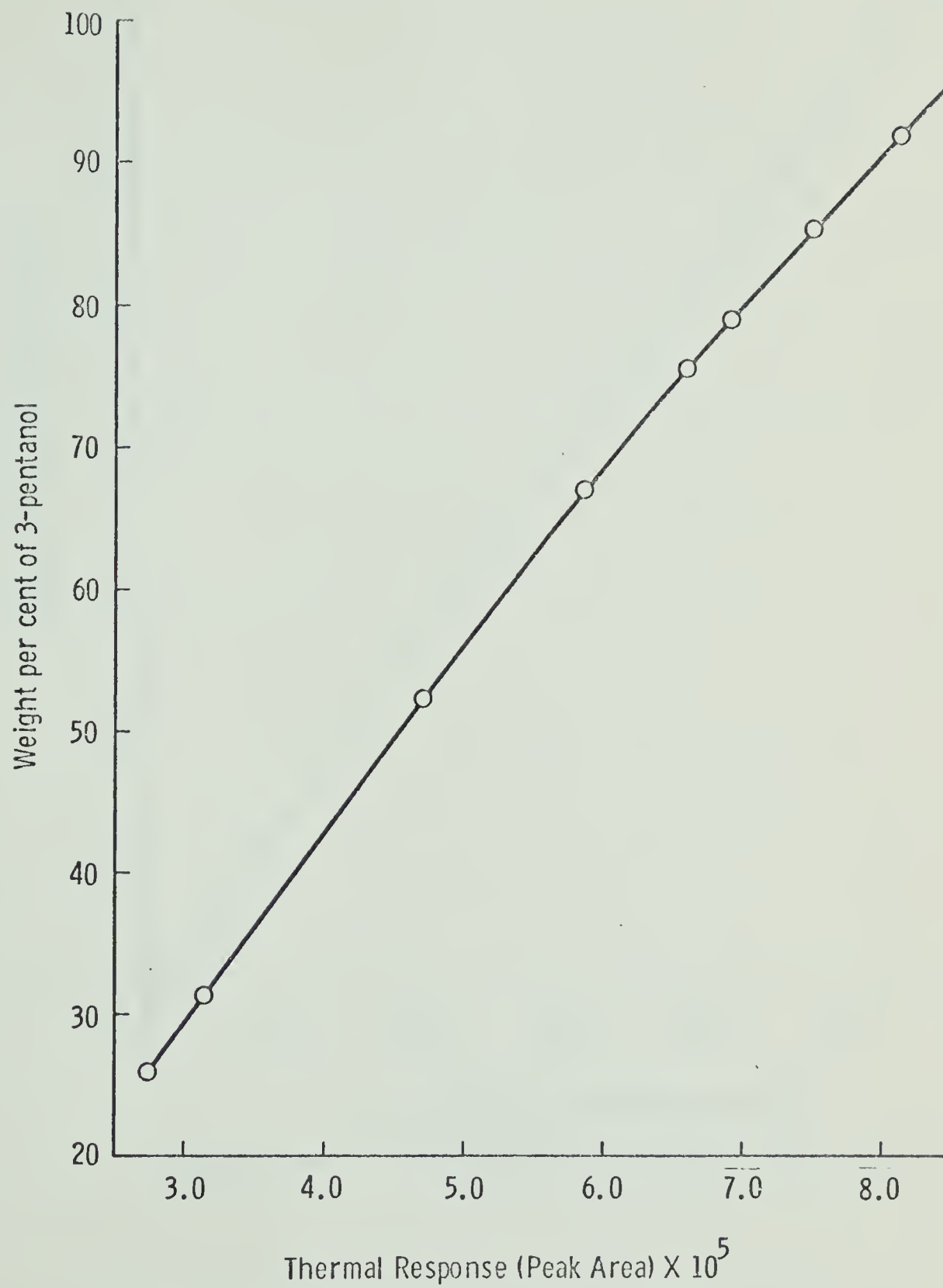


Figure A-II-1 CALIBRATION OF 3-PENTANOL ANALYSIS

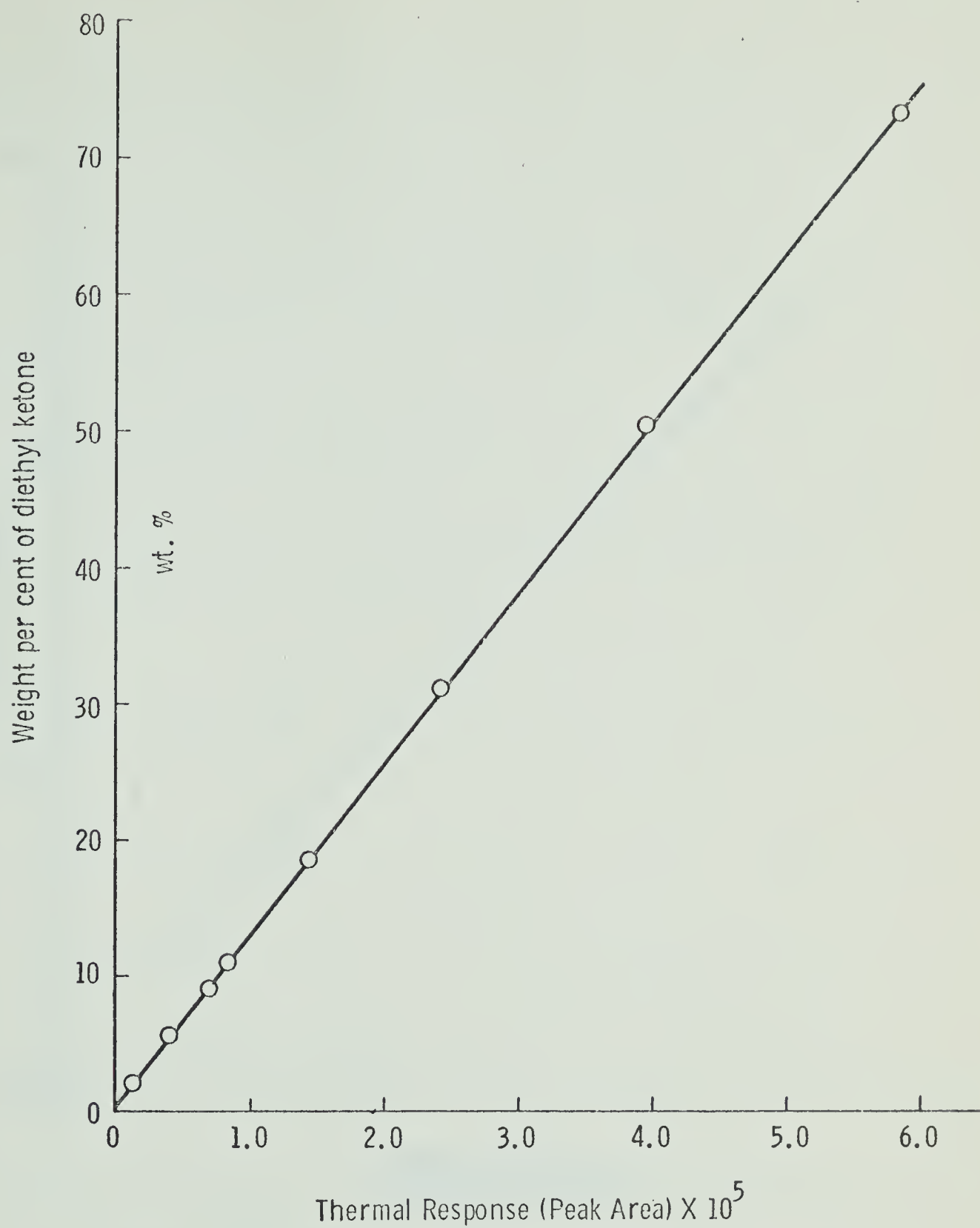


Figure A-II-2

CALIBRATION OF DIETHYL KETONE ANALYSIS

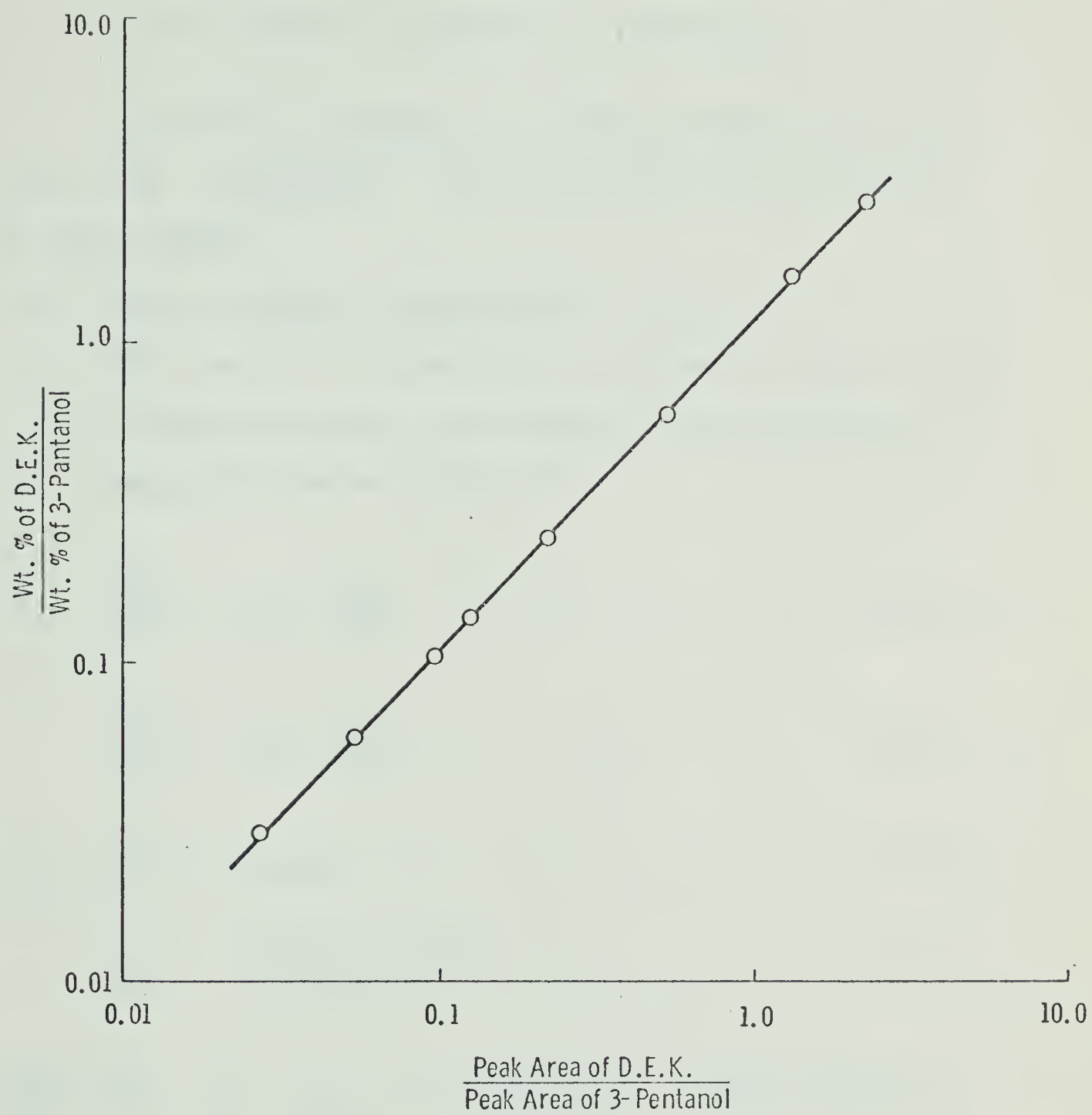


Figure A-II-3 RELATIVE THERMAL RESPONSE OF DIETHYL KETONE

II-2A External Reference Method - Use reference component which is present in the sample.

The major component is usually chosen as reference, e.g. 3-pentanol. The following is the procedure of this method.

- (a) Original sample is analyzed.
- (b) Known weight of 3-pentanol is added to known weight of sample and this new sample is then analyzed.
- (c) Four equations are obtained.

$$\frac{X_i}{X_r} = f_i \left(\frac{A_i}{A_r} \right) \quad (\text{II-6})$$

$$\frac{X_i'}{X_r'} = f_i \left(\frac{A_i'}{A_r'} \right) \quad (\text{II-7})$$

$$X_i' = \frac{P}{P + Q} X_i \quad (\text{II-8})$$

$$X_r' = \frac{P X_r + 100 Q}{P + Q} \quad (\text{II-9})$$

where X_i = wt. % of component i in the original sample

X_r = wt. % of 3-pentanol in the original sample

X_i' = wt. % of component i in the new sample

X_r' = wt. % of 3-pentanol in the new sample

P = wt. of original sample
 Q = wt. of 3-pentanol added
 A_i = thermal response of component i in original sample
 A_r = thermal response of 3-pentanol in original sample
 A_i' = thermal response of component i in new sample
 A_r' = thermal response of 3-pentanol in new sample

(d) The functions f_i 's are determined by using synthetic mixtures in the same way as in the Internal Reference Method.

Substituting Equations (II-8) and (II-9) in Equation (II-7) we have

$$X_i = \frac{P X_r + 100 Q}{P} f_i \left(\frac{A_i'}{A_r'} \right) \quad (\text{II-10})$$

Substituting Equation (II-10) in Equation (II-6), we have

$$X_r = \frac{100 Q f_i (A_i'/A_r')}{P [f_i (A_i/A_r) - f_i (A_i'/A_r')]} \quad (\text{II-11})$$

(e) Once X_r is known, all X_i 's can be calculated by Equation (II-10) or Equation (II-6).

II-2B External Reference Method - Use reference component which is not present in the sample.

- (a) Known weight of reference component is added to known weight of sample.
- (b) This new sample is then analyzed.
- (c) The functions f_i 's are determined by synthetic mixtures containing the reference component.
- (d) Two equations are obtained

$$\frac{X_i'}{X_r'} = f_i \left(\frac{A_i'}{A_r'} \right) \quad (\text{II-12})$$

$$X_i = X_i' \frac{P + Q}{P} \quad (\text{II-13})$$

where P = wt. of original sample

Q = wt. of reference added

X_r' = wt. % of reference in new sample

$$= \frac{100 Q}{P + Q} \%$$

From equations (II-12) and (II-13), we have

$$X_i = \frac{100 Q}{P} f_i \left(\frac{A_i'}{A_r'} \right) \quad (\text{II-14})$$

- (e) Then all X_i 's can be calculated by Equation (II-14).

II-3 Comparison of the Methods

- (a) Methods II-1 and II-2B require one analysis (one injection) for a sample, while Method II-2A require two analyses (two injections) for a sample.

- (b) In both External Reference Methods, the samples have to be diluted with reference component.

This procedure is more prone to error because of more handling of the sample.

- (c) Internal and External Methods of analysis give approximately equal accuracy. A comparison of analyses by both methods is given in Table A-II-4.

Table A-II-4

Comparison of Internal and External Reference Methods

(Liquid Analyses wt. %, Method II-1 vs Method II-2A)

Sample No.	Method	2-Pentene	Water	M.E.K.	n-Propanol	D.E.K.	3-Pentanol
J-3	Int.	0.6213	0.2428	0.0591	0.0367	38.1518	60.8883
	Ext.	0.6222	0.2409	0.0582	0.0361	38.1529	60.8897
J-4	Int.	0.4510	0.2369	0.0399	0.0236	31.7080	67.5406
	Ext.	0.4522	0.2378	0.0402	0.0231	31.7071	67.5396
J-5	Int.	0.4648	0.2287	0.0382	0.0224	27.2555	71.9904
	Ext.	0.4639	0.2295	0.0387	0.0230	27.2561	71.9888
J-6	Int.	0.3538	0.1577	0.0296	0.0168	19.5425	79.8996
	Ext.	0.3535	0.1591	0.0301	0.0172	19.5416	79.8985

- H-17 -

APPENDIX III

EXPERIMENTAL CONDITIONS

Table A-III-1

Experimental Conditions

Run No.	Catalyst Wt. (gm)	Feed Rate (gm/hr)	Reaction Temp. (°C)	Atm. Press. (cm Hg)	Room Temp. (°C)	Gas Sample (l/hr)	Liquid Sample (gm/hr)
1	Glass	8.5626	376.8	70.88	23.5	0.0	8.5591
2	Glass	8.5626	413.5	70.88	23.0	0.0	8.5557
3	Glass	8.5626	473.7	71.00	27.0	0.0	8.5608
4	3.0805	4.2842	349.8	70.27	24.5	0.3810	4.2387
5	3.0805	4.2842	374.0	70.22	23.0	1.6068	4.1741
6	3.0805	4.2842	401.3	69.90	25.0	1.9459	4.0275
7	3.0805	4.2842	426.8	70.22	23.0	2.2737	3.8626
8	3.0805	4.2842	452.2	69.90	24.4	2.5714	3.7298
9	0.9254	4.2842	370.2	70.64	24.4	0.3007	4.2592
10	0.9254	4.2842	370.3	70.64	24.4	0.3048	4.2589
11	0.9254	4.2842	369.8	70.40	24.0	0.2952	4.2597
12	0.9254	4.2842	370.0	70.40	24.0	0.2962	4.2596
13	4.4077	4.2842	370.1	69.80	25.6	0.6072	4.1518
14	4.4077	6.4234	370.0	70.52	26.0	0.7918	6.2310
15	4.4077	8.5626	369.9	69.80	25.7	0.9553	8.3625
16	4.4077	12.8234	370.0	70.52	26.0	1.1760	12.6120
17	4.4077	17.0843	370.0	69.80	26.0	1.3616	16.8788
18	4.4077	25.5995	370.0	70.52	26.0	1.4686	25.4172
19	4.4077	34.1147	369.8	69.80	25.6	1.8278	33.8956
20	2.2045	4.2842	370.0	69.72	27.7	0.5026	4.1504
21	2.2045	8.5626	370.0	69.72	28.0	0.7432	8.4123
22	2.2045	17.0843	369.8	69.72	28.9	0.8566	16.8380
23	2.2045	34.1147	369.8	69.72	29.0	1.0826	33.9512
24	1.4977	12.8234	370.3	70.15	26.0	0.5855	12.7659
25	1.4977	17.0843	370.0	70.15	25.7	0.6165	17.0153
26	1.4977	25.5995	369.8	70.15	26.0	0.7008	25.5233
27	1.4977	34.1147	370.1	70.15	25.1	0.7323	34.0447
28	1.0022	12.8234	370.3	70.05	26.1	0.4332	12.7792
29	1.0022	17.0843	370.0	70.05	25.7	0.4626	17.0277
30	1.0022	25.5995	369.7	70.05	26.0	0.5271	25.5480
31	1.0022	34.1147	369.8	70.05	25.2	0.5488	34.0619
32	1.0020	12.8234	370.1	70.15	26.1	0.4380	12.7365
33	1.0020	25.5995	370.2	70.15	26.0	0.5348	25.5254
34	1.0020	12.8234	370.0	70.05	26.0	0.4297	12.7593
35	1.0020	25.5995	369.7	70.05	26.2	0.5305	25.5328
36	1.0022	12.8234	369.6	70.12	26.4	0.4328	12.7682
37	1.0022	25.5995	370.2	70.12	26.5	0.5285	25.5420
38	1.0022	12.8234	370.0	70.14	26.3	0.4250	12.7582
39	1.0022	25.5995	370.3	70.14	26.3	0.5250	25.5308
40	1.0023	12.8234	370.0	70.02	26.0	0.4329	12.7682
41	1.0023	17.0843	370.4	70.02	26.1	0.4632	17.0195
42	1.0023	25.5995	370.2	70.02	26.0	0.5273	25.5368
43	1.0023	34.1147	369.7	70.02	25.5	0.5487	34.0584
44	1.0023	12.8234	370.3	70.25	24.2	0.4328	12.7785
45	1.0023	12.8234	370.0	70.25	24.0	0.4330	12.7800

Table A-III-2

Catalyst Bed Temperatures

Run No.	Bed Height (cm)	Catalyst Top (°C)	- Bed Temp. Center Bottom (°C)	Temp. Diff. (°C)	Ave. Bed. Temp. (°C)	
1	-	-	376.8	-	-	
2	-	-	413.5	-	-	
3	-	-	473.7	-	-	
4	5.1	351.6	349.8	345.6	6.0	349.0
5	"	-	374.0	-	-	-
6	"	406.4	401.3	391.5	14.9	399.7
7	"	-	426.8	-	-	-
8	"	458.4	452.2	441.3	17.1	450.6
9	1.5	370.6	370.2	369.4	1.2	370.1
10	"	-	370.3	-	-	-
11	"	-	369.8	-	-	-
12	"	370.5	370.0	369.5	1.0	370.0
13	7.3	373.8	370.1	360.2	13.6	368.0
14	"	-	370.0	-	-	-
15	"	373.1	369.9	361.0	12.1	368.0
16	"	-	370.0	-	-	-
17	"	373.0	370.0	362.4	10.6	368.5
18	"	-	370.0	-	-	-
19	"	372.8	369.8	363.0	9.8	368.5
20	3.6	373.0	370.0	369.2	3.8	370.7
21	"	-	370.0	-	-	-
22	"	-	369.8	-	-	-
23	"	372.0	369.8	369.5	2.5	370.4
24	2.5	370.7	370.3	369.6	1.1	370.2
25	"	370.5	370.0	369.5	1.0	370.0
26	"	370.3	369.8	369.5	0.8	369.9
27	"	370.2	370.1	369.6	0.6	370.0
28	1.7	370.6	370.3	369.8	0.8	370.2
29	"	370.4	370.0	370.0	0.4	370.1
30	"	370.0	369.7	369.5	0.5	369.7
31	"	370.0	369.8	369.6	0.4	369.8
32	"	370.5	370.1	369.8	0.7	370.1
33	"	-	370.2	-	-	-
34	"	-	370.0	-	-	-
35	"	370.6	369.7	369.7	0.9	370.0
36	"	370.0	369.6	369.2	0.8	369.6
37	"	-	370.2	-	-	-
38	"	-	370.0	-	-	-
39	"	370.5	370.3	369.7	0.8	370.2
40	"	370.4	370.0	369.4	1.0	369.9
41	"	370.5	370.4	369.6	0.9	370.2
42	"	370.4	370.2	370.0	0.4	370.2
43	"	370.0	369.7	369.5	0.5	369.7

APPENDIX IV
PRODUCTS ANALYSES

Table A-1V-1

Liquid Product Analyses, Wt. %

Run No.	2-Pentene	Water	Methyl Ethyl Ketone	n-Propanol	Diethyl Ketone	3-Pentanol
1	-	-	-	-	-	100.0000
2	-	-	-	-	-	100.0000
3	-	-	-	-	-	100.0000
4	0.0061	-	0.0038	0.0	17.5463	82.0089
5	0.7615	-	0.1106	0.0659	55.9700	43.0920
6	1.7016	-	0.2084	0.1283	76.8317	21.1301
7	2.8343	-	0.3228	0.1408	88.9981	7.7040
8	4.5012	-	0.5591	0.1943	94.5124	0.2330
9	0.5339	0.4629	0.0538	0.0	24.8441	74.1053
10	0.4967	0.5248	0.0603	0.0	24.7707	74.1475
11	0.4995	0.5049	0.0785	0.0	24.4540	74.4631
12	0.4810	0.5223	0.0578	0.0	24.3775	74.5613
13	0.9102	0.3059	0.0919	0.0601	48.5623	50.0696
14	0.7886	0.2834	0.0549	0.0340	42.1565	56.6825
15	0.6452	0.2555	0.0507	0.0310	38.3413	60.6762
16	0.5185	0.2476	0.0393	0.0233	31.9807	67.1905
17	0.4732	0.2450	0.0375	0.0220	27.3689	71.8534
18	0.3455	0.1647	0.0322	0.0184	19.5883	79.8509
19	0.3209	0.1537	0.0214	0.0118	18.1698	81.3223
20	0.7575	0.2569	0.0514	0.0317	40.4186	58.4839
21	0.4542	0.2137	0.0418	0.0249	29.3660	69.8994
22	0.3006	0.1694	0.0259	0.0248	16.4774	83.0243
23	0.2322	0.0830	0.0220	0.0120	10.0147	89.6361
24	0.3944	0.1230	0.0421	0.0	14.7023	84.7382
25	0.3511	0.1041	0.0409	0.0	12.0354	87.4685

Table A-IV-1 (continued)

Liquid Product Analyses, Wt. %

Run No.	2-Pentene	Water	Methyl Ethyl Ketone	n-Propanol	Diethyl Ketone	3-Pentanol
26	0.2683	0.0891	0.0397	0.0	8.8430	90.7598
27	0.2202	0.0764	0.0359	0.0	6.9026	92.7648
28	0.3238	0.1092	0.0405	0.0	11.3265	88.2000
29	0.2716	0.0906	0.0396	0.0	8.7486	90.8496
30	0.2065	0.0789	0.0368	0.0	6.3277	93.3500
31	0.1589	0.0672	0.0350	0.0	4.8170	94.9219
32	0.3210	0.1032	0.0398	0.0	11.2579	88.2780
33	0.2032	0.0777	0.0371	0.0	6.3823	93.2996
34	0.3309	0.0994	0.0410	0.0	11.4241	88.1046
35	0.2116	0.0821	0.0367	0.0	6.4213	93.2484
36	0.3212	0.1108	0.0402	0.0	11.2363	88.2915
37	0.2035	0.0806	0.0369	0.0	6.2798	93.3992
38	0.3142	0.1012	0.0395	0.0	11.1746	88.3705
39	0.2001	0.0733	0.0380	0.0	6.2450	93.4435
40	0.3236	0.1048	0.0400	0.0	11.2560	88.2756
41	0.2701	0.0921	0.0391	0.0	8.7687	90.8301
42	0.2076	0.0804	0.0370	0.0	6.3282	93.3468
43	0.1593	0.0664	0.0348	0.0	4.8235	94.9159
44	0.3282	0.0971	0.0412	0.0	11.4635	88.0700
45	0.3271	0.0941	0.0406	0.0	11.4057	88.1324

Table A-IV-2

Gas Product Analyses, Mole %

Run No.	Hydrogen	Methane	Ethylene	2-Pentene
1	-	-	-	-
2	-	-	-	-
3	-	-	-	-
4	99.6804	0.0465	0.0209	0.2522
5	96.6712	0.1195	0.0521	3.1573
6	96.4051	0.1606	0.0564	3.3378
7	96.1820	0.3497	0.1072	3.3612
8	94.2997	0.8279	0.2680	4.6044
9	99.6778	0.1036	0.0	0.2186
10	99.6890	0.0945	0.0	0.2165
11	99.6819	0.0891	0.0	0.2290
12	99.7080	0.0804	0.0	0.2116
13	99.5401	0.0809	0.0227	0.3564
14	99.6924	0.0894	0.0232	0.1950
15	99.7011	0.0790	0.0194	0.2006
16	99.7473	0.1081	0.0209	0.1238
17	99.7088	0.1241	0.0233	0.1438
18	99.6071	0.2599	0.0279	0.1052
19	99.5778	0.2832	0.0306	0.1084
20	99.7883	0.0782	0.0159	0.1176
21	99.7426	0.0850	0.0180	0.1544
22	99.7115	0.1680	0.0207	0.0997
23	99.3799	0.5318	0.0241	0.0642
24	99.6526	0.1768	0.0	0.1706
25	99.6190	0.3052	0.0	0.0759
26	99.6143	0.2736	0.0	0.1121
27	99.2594	0.6460	0.0	0.0946
28	99.7325	0.1721	0.0	0.0953
29	99.6722	0.2494	0.0	0.0784
30	99.6322	0.3136	0.0	0.0542
31	99.7211	0.2543	0.0	0.0246
32	99.7315	0.1729	0.0	0.0955
33	99.6221	0.3246	0.0	0.0532
34	99.7231	0.1768	0.0	0.1001
35	99.6447	0.3019	0.0	0.0533
36	99.7454	0.1625	0.0	0.0922
37	99.6176	0.3259	0.0	0.0565
38	99.7551	0.1558	0.0	0.0891
39	99.6365	0.3107	0.0	0.0528
40	99.7322	0.1720	0.0	0.0957
41	99.6721	0.2495	0.0	0.0784
42	99.6320	0.3137	0.0	0.0543
43	99.7209	0.2544	0.0	0.0246
44	99.7388	0.1677	0.0	0.0935
45	99.7337	0.1717	0.0	0.0947

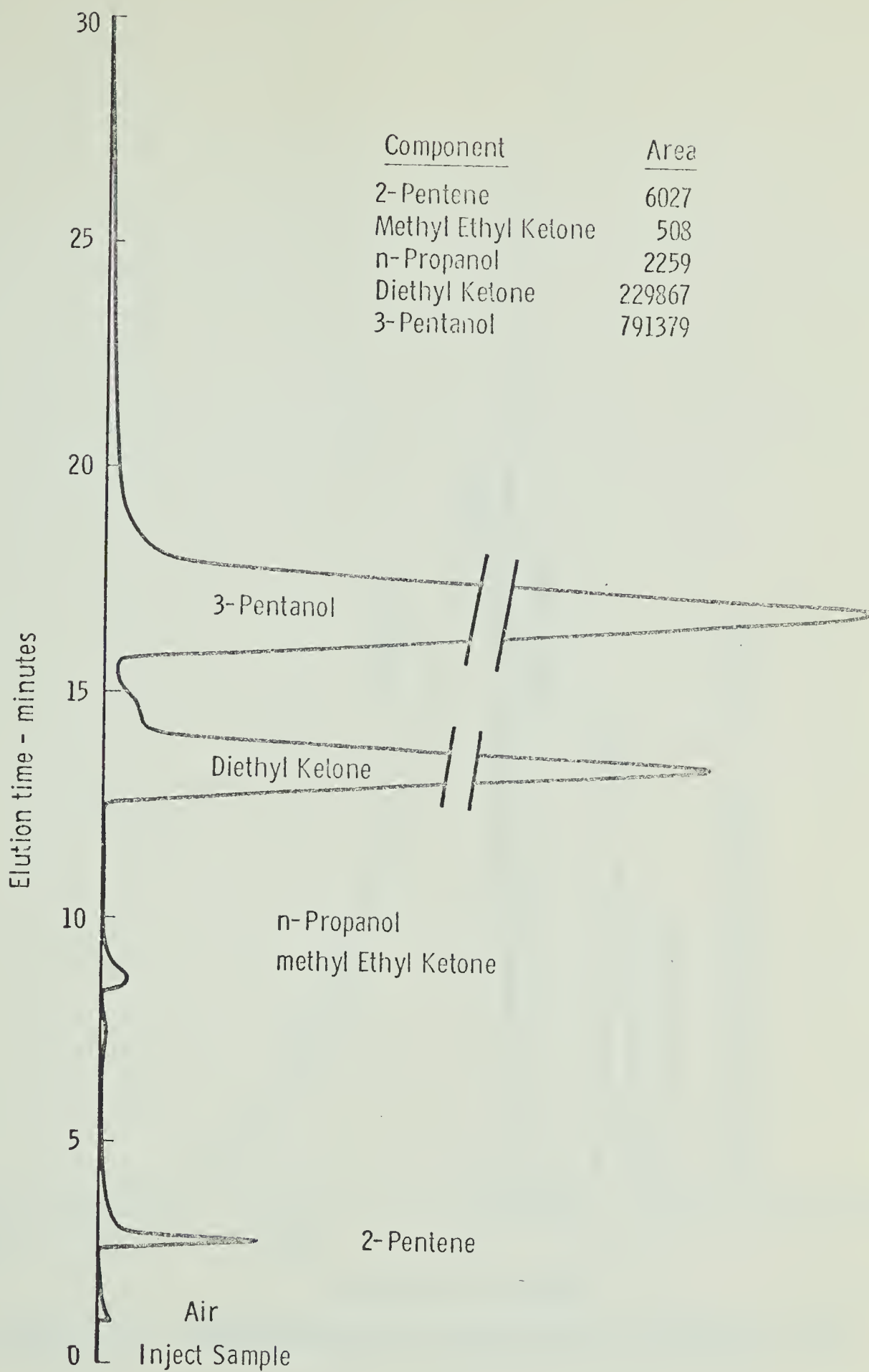


Figure A-IV-1 CHROMATOGRAM FOR LIQUID ANALYSIS
Di-n-decyl PHTHALATE ON CELITE COLUMN

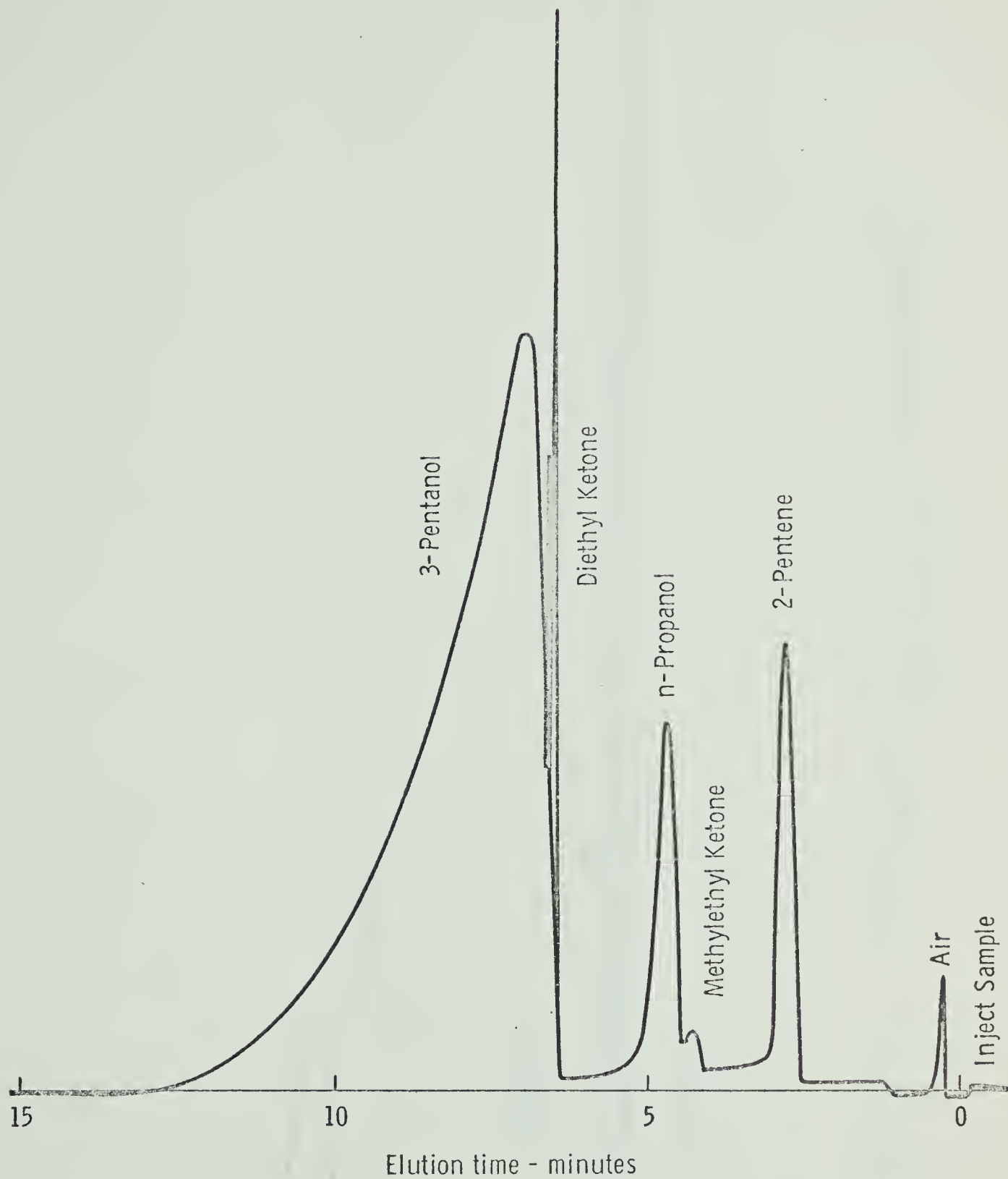


Figure A-IV-2 CHROMATOGRAM FOR LIQUID ANALYSIS PORAPAK COLUMN

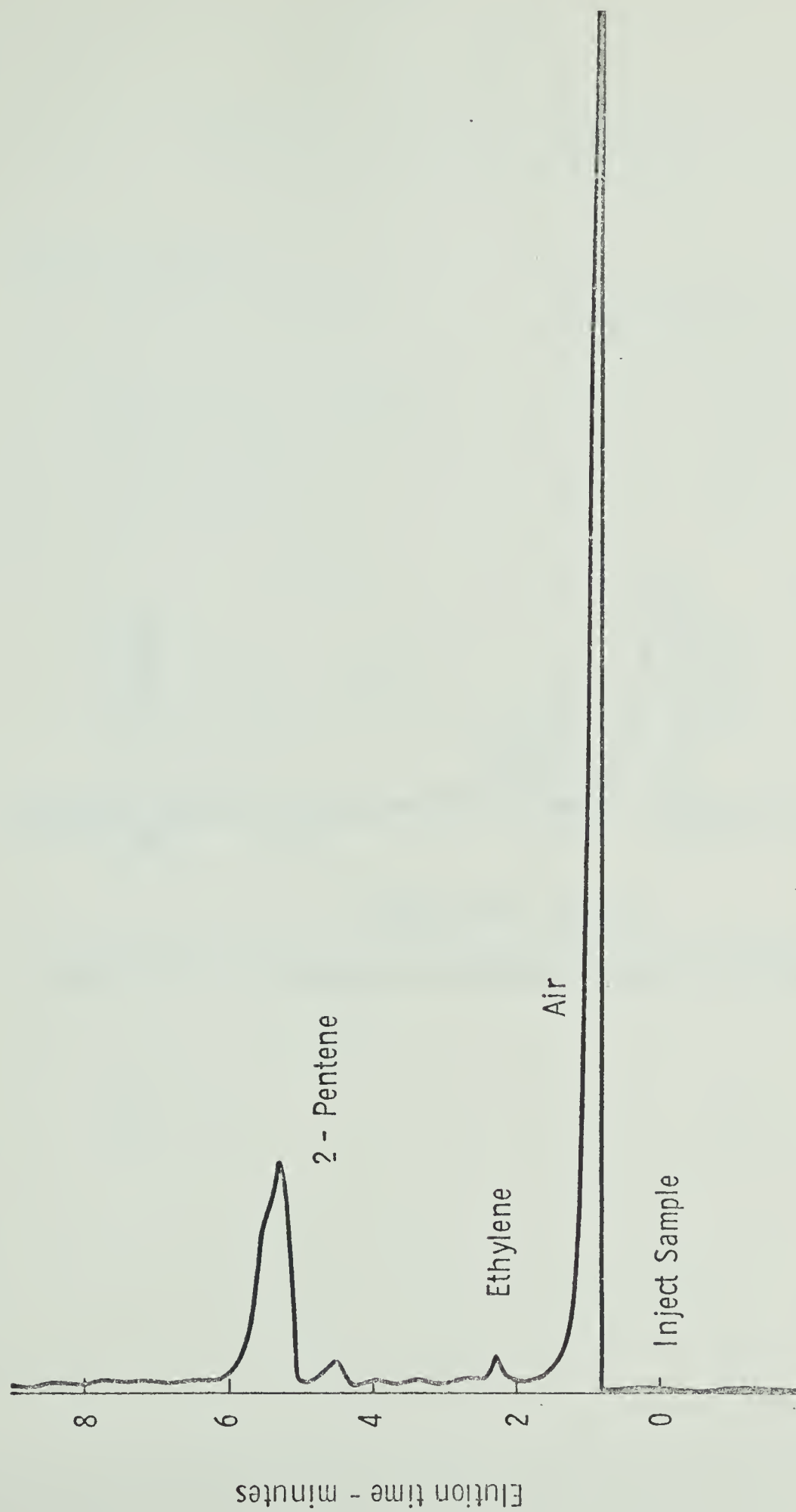


Figure A-IV - 3 CHROMATOGRAM FOR GAS ANALYSIS Di-n-decyl PHTHALATE
ON CELITE COLUMN

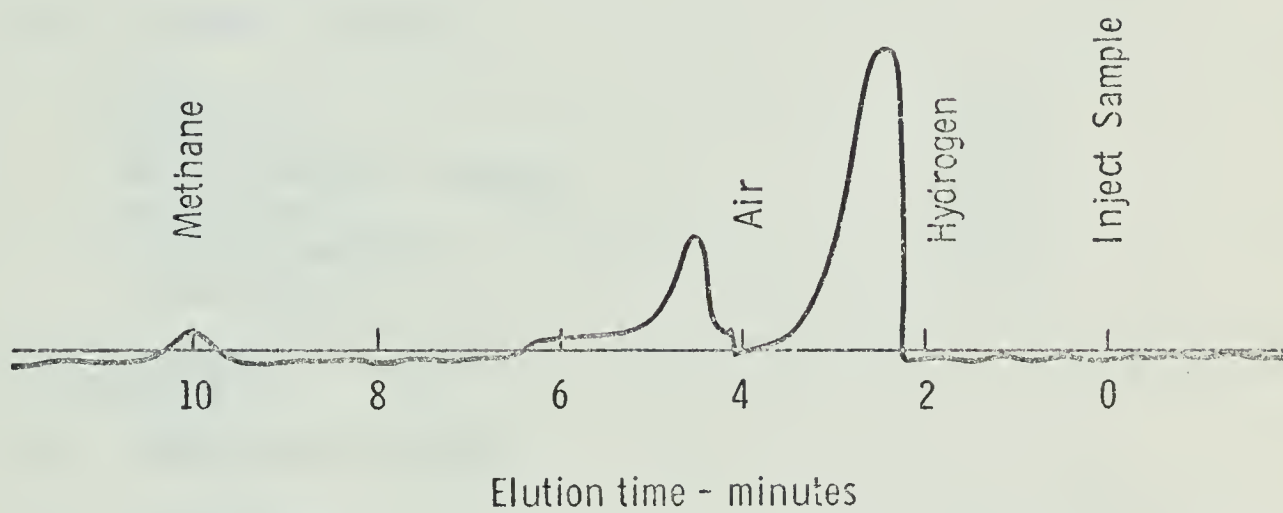


Figure A-IV-4 CHROMATOGRAM FOR GAS ANALYSIS CHARCOAL COLUMN

Table A-IV-3

Retention Times of Components

I. Liquid Sample

A. Phthalate Column	<u>Retention Time (min.)</u>
2-Pentene	2.8
Methyl ethyl ketone	7.0
n-Propanol	8.0
Diethyl ketone	13.4
3-Pentanol	17.0
B. Porapak Column	
Water	1.2
2-Pentene	1.8
Methyl ethyl ketone	4.4
n-Propanol	4.8
Diethyl ketone	6.6
3-Pentanol	7.0

II. Gas Sample

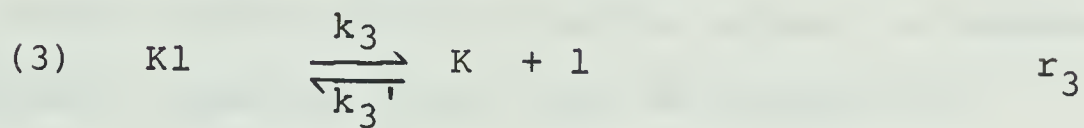
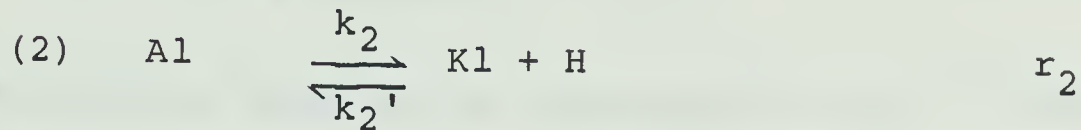
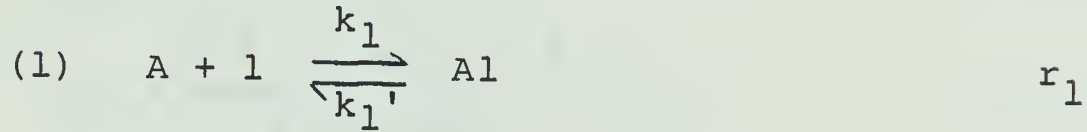
A. Phthalate Column	
Ethylene	2.3
2-Pentene	5.3
B. Charcoal Column	
Hydrogen	2.5
Air	4.5
Methane	10.0

APPENDIX V

DERIVATION OF RATE EQUATIONS

I. Single Site Mechanism

A. Dehydrogenation



where $A = 3\text{-pentanol}$

$K = \text{diethyl ketone}$

$H = H_2$

$l = \text{active site for dehydrogenation}$

$$K_1 = \frac{k_1}{k_{1'}} = \frac{C_{Al}}{p_A C_l} \quad (I-A-1)$$

$$K_2 = \frac{k_2}{k_{2'}} = \frac{C_{Kl} p_H}{C_{Al}} \quad (I-A-2)$$

$$K_3 = \frac{k_3}{k_{3'}} = \frac{p_K C_l}{C_{Kl}} \quad (I-A-3)$$

$$L = C_l + C_{Al} + C_{Kl} \quad (I-A-4)$$

(a) Adsorption Controlling

Assuming step (1) is slow while steps (2) and (3) attain steady state or equilibrium.

$$r_2 = r_3 = 0$$

$$r_K = r_1 = k_1 p_A C_l - k_{1'} C_{Al} \quad (I-A-5)$$

Combining Equations (I-A-1) to (I-A-5) to eliminate C_1 , C_{A1} , C_{K1} and k_1' , we have

$$r_K = \frac{k_1 L (p_A - p_K p_H / K_1 K_2 K_3)}{(1 + p_K p_H / K_2 K_3 + p_K / K_3)} \quad (\text{I-A-6})$$

Since surface reaction is irreversible, $K_2 = \infty$ and L , the total concentration of active sites, is assumed constant, Equation (I-A-6) can be written as

$$r_K = \frac{k p_A}{(1 + K_K p_K)} \quad (\text{I-A-7})$$

(b) Surface Reaction Controlling

Assuming step (2) is slow while steps (1) and (3) attain steady state or equilibrium

$$r_1 = r_3 = 0$$

$$r_K = r_2 = k_2 C_{A1} - k_2' C_{K1} p_H \quad (\text{I-A-8})$$

Combining Equations (I-A-1) to (I-A-4) and Equation (I-A-8) to eliminate C_1 , C_{A1} , C_{K1} and k_2' , we have

$$r_K = \frac{k_2 K_1 L (p_A - p_K p_H / K_1 K_2 K_3)}{(1 + K_1 p_A + p_K / K_3)} \quad (\text{I-A-9})$$

Applying the same assumption as in (a), Equation (I-A-9) can be simplified to give

$$r_K = \frac{k p_A}{(1 + K_A p_A + K_K p_K)} \quad (\text{I-A-10})$$

(c) Desorption Controlling

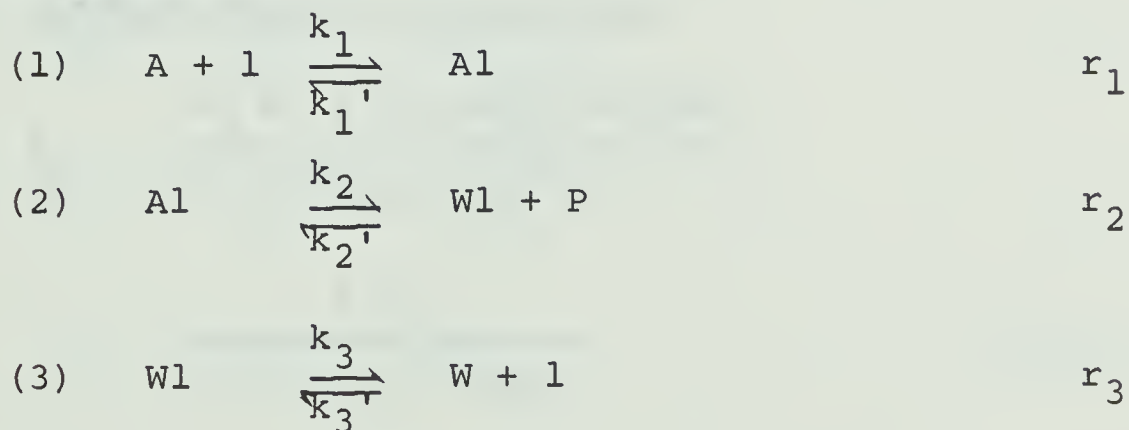
$$r_1 = r_2 = 0$$

$$r_K = r_3 = k_3 C_{K1} - k_3' p_K C_1 \quad (\text{I-A-11})$$

Combining Equations (I-A-1) to (I-A-4) and Equation (I-A-11) to eliminate C_1 , C_{A1} , C_{K1} and k_3' , we have

$$\begin{aligned} r_K &= \frac{k_3 L K_1 K_2 (p_A - p_K p_H / K_1 K_2 K_3)}{p_H (1 + K_1 p_A + K_1 K_2 p_A / p_H)} \\ &= \frac{k p_A}{p_H (1 + K_A p_A + K_{AH} p_A / p_H)} \end{aligned} \quad (\text{I-A-12})$$

B. Dehydration



where A = 3-pentanol

W = Water

P = 2-pentene

l = active site for dehydration

$$K_1 = \frac{k_1}{k_1'} = \frac{C_{A1}}{p_A C_1} \quad (\text{I-B-1})$$

$$K_2 = \frac{k_2}{k_2'} = \frac{C_{W1} p_P}{C_{A1}} \quad (\text{I-B-2})$$

$$K_3 = \frac{k_3}{k_3'} = \frac{p_W C_1}{C_{W1}} \quad (\text{I-B-3})$$

$$L = C_1 + C_{A1} + C_{W1} \quad (\text{I-B-4})$$

The rate equations are derived similarly to the procedure in A.

(a) Adsorption Controlling

$$\begin{aligned} r_p &= \frac{k_1 L (p_A - p_P p_W / K_1 K_2 K_3)}{(1 + p_P p_W / K_2 K_3 + p_W / k_3)} \\ &= \frac{k p_A}{(1 + K_W p_W)} \end{aligned} \quad (\text{I-B-5})$$

(b) Surface Reaction Controlling

$$\begin{aligned} r_p &= \frac{k_2 K_1 L (p_A - p_W p_P / K_1 K_2 K_3)}{(1 + K_1 p_A + p_W / K_3)} \\ &= \frac{k p_A}{(1 + K_A p_A + K_W p_W)} \end{aligned} \quad (\text{I-B-6})$$

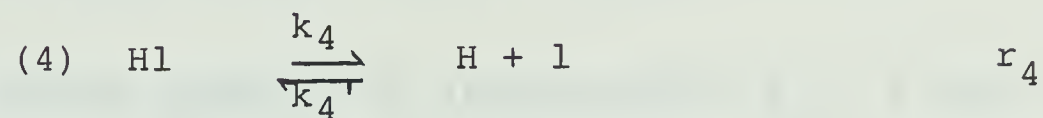
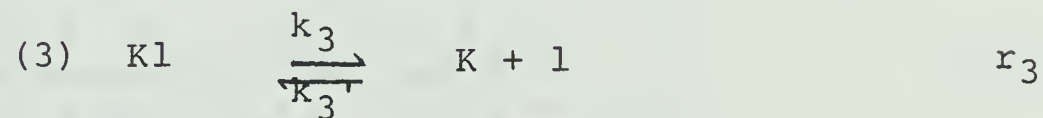
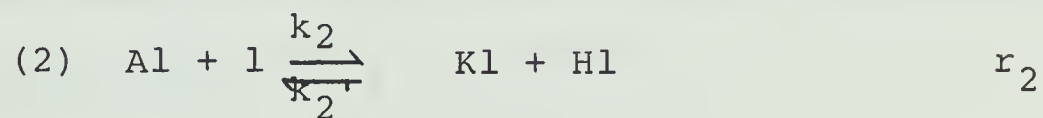
(c) Desorption Controlling

$$r_p = \frac{k_3 L K_1 K_2 (p_A - p_W p_P / K_1 K_2 K_3)}{p_P (1 + K_1 p_A + K_1 K_2 p_A / p_P)}$$

$$= \frac{k p_A}{p_P (1 + K_A p_A + K_{Ap} p_A / p_P)} \quad (\text{I-B-7})$$

II Dual Sites Mechanism

A. Dehydrogenation



$$K_1 = \frac{k_1}{k_1'} = \frac{C_{Al}}{p_A C_l} \quad (\text{II-A-1})$$

$$K_2 = \frac{k_2}{k_2'} = \frac{C_{Kl} C_{Hl}}{C_{Al} C_l} \quad (\text{II-A-2})$$

$$K_3 = \frac{k_3}{k_3'} = \frac{p_K C_l}{C_{Kl}} \quad (\text{II-A-3})$$

$$K_4 = \frac{k_4}{k_4'} = \frac{p_H C_l}{C_{Hl}} \quad (\text{II-A-4})$$

$$L = C_l + C_{Al} + C_{Kl} + C_{Hl} \quad (\text{II-A-5})$$

(a) Adsorption Controlling

$$r_2 = r_3 = r_4 = 0$$

r_1 is slow

$$r_K = k_1 p_A C_1 - k_1' C_{A1} \quad (\text{II-A-6})$$

Combining Equations (II-A-1) to (II-A-6) to eliminate C_1 , C_{A1} , C_{K1} , C_{H1} and k_1' , we have

$$r_K = \frac{k_1 L (p_A - p_K p_H / K_1 K_2 K_3 K_4)}{(1 + p_H p_K / K_2 K_3 K_4 + p_K / K_3 + p_H / K_4)} \quad (\text{II-A-7})$$

Since surface reaction is irreversible, $K_2 = \infty$ and L is assumed constant. Equation (II-A-7) can be simplified to give

$$r_K = \frac{k p_A}{(1 + K_K p_K + K_H p_H)} \quad (\text{II-A-8})$$

(b) Surface Reaction Controlling

r_2 is slow

$$r_1 = r_3 = r_4 = 0$$

$$r_K = r_2 = k_2 C_{A1} C_1 - k_2' C_{K1} C_{H1} \quad (\text{II-A-9})$$

Combining Equations (II-A-1) to (II-A-5) and Equation

(II-A-9) to eliminate C_1 , C_{A1} , C_{K1} , C_{H1} and k_2' , we have

$$r_K = \frac{k_2 K_1 L^2 (p_A - p_K p_H / K_1 K_2 K_3 K_4)}{(1 + K_1 p_A + p_K / K_3 + p_H / K_4)^2} \quad (\text{II-A-10})$$

Since $K_2 = \infty$ and $L = \text{constant}$

$$r_K = \frac{k p_A}{(1 + K_A p_A + K_K p_K + K_H p_H)^2} \quad (\text{II-A-11})$$

(c) Desorption of Ketone Controlling

r_3 is slow

$$r_1 = r_2 = r_4 = 0$$

$$r_K = r_3 = k_3 C_{K1} - k_3' p_K C_1 \quad (\text{II-A-12})$$

Again, combining Equations (II-A-1) to (II-A-5) and Equation (II-A-12), we have

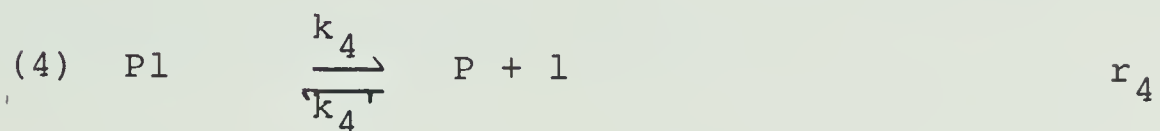
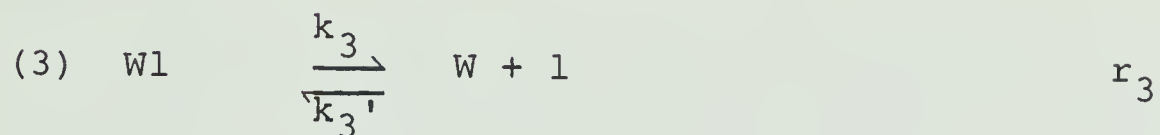
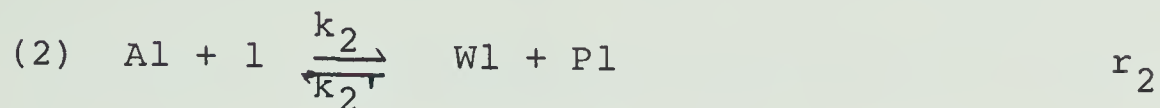
$$r_K = \frac{k_3 K_1 K_2 K_4 L (p_A - p_K p_H / K_1 K_2 K_3 K_4)}{p_H (1 + K_1 p_A + K_1 K_2 K_4 p_A / p_H + p_H / K_4)} \quad (\text{II-A-13})$$

$$r_K = \frac{k p_A}{p_H (1 + K_A p_A + K_{AH} p_A / p_H + K_H p_H)} \quad (\text{II-A-14})$$

B. Dehydration

The rate equations for dehydration are derived in a way

similar to dehydrogenation



(a) Adsorption Controlling

$$r_P = \frac{k p_A}{(1 + K_W p_W + K_P p_P)} \quad (II-B-1)$$

(b) Surface Reaction Controlling

$$r_P = \frac{k p_A}{(1 + K_A p_A + K_W p_W + K_P p_P)^2} \quad (II-B-2)$$

(c) Desorption of Water Controlling

$$r_P = \frac{k p_A}{p_P (1 + K_A p_A + K_{AP} p_A / p_P + K_P p_P)} \quad (II-B-3)$$

APPENDIX VI

PRESSURE DROPS ACROSS CATALYST SURFACE AND AMBIENT GAS STREAM

To test whether the partial pressures in the bulk gas stream can be replaced those at the catalyst surface to correlate the rate data, the pressure drops across the stagnant film are estimated by the method of Hougen et al (48).

In this method, the ratio of pressure drops and partial pressures in the ambient gas stream were correlated with a dimensionless group.

$$\frac{\Delta p_j}{p_j} = f \left(\frac{r_j}{a_m \phi G_M Y_j} \right) = f (X) \quad (\text{VI-1})$$

where Δp_j = pressure drop of component j across the stagnant gas film.

p_j = partial pressure of component j in the bulk gas stream.

r_j = reaction rate of component j, gm-mole per gm of catalyst per hour.

a_m = surface area of catalyst particle, cm^2/gm .

ϕ = shape factor

G_M = molal mass velocity of gas based on the total cross section of bed, gm-mole per cm^2 per hour.

Y_j = mole fraction of component j in bulk gas.

f = function (a graph in Figure 2 in Hougen et al. (48)).

The pressure drops of the components in experimental runs 24 and 31 which had the slowest and fastest flows of gas respectively are estimated by using the following data.

$$\begin{aligned}a_m &= 2.6370 \times 10^5 \text{ cm}^2/\text{gm} \\ \phi &= 0.90 \text{ (for irregular granules)} \\ S &= 0.7854 \text{ cm}^2 \text{ (cross section of catalyst bed)}\end{aligned}$$

The dimensionless groups in equation (VI-1) are calculated by using the data in Table VI-1, and the corresponding pressure ratios are read (from Figure 2 in (48)). The results obtained are shown in Table VI. It is obvious that the pressure drops are negligible.

Table VI-1

Pressure Drops Across Catalyst Surface and Ambient Gas Stream

Run No.	G_M	Component	r_j	Y_j	X	$\frac{\Delta p_j}{p_j}$
24	0.18522	A	0.00896	0.7296	2.794×10^{-7}	3.5×10^{-6}
		K	0.00872	0.1295	1.532×10^{-6}	2.0×10^{-5}
		H	0.00872	0.1295	1.532×10^{-6}	2.0×10^{-5}
		P	0.00024	0.004491	1.216×10^{-6}	1.8×10^{-5}
		W	0.00024	0.004491	1.216×10^{-6}	1.8×10^{-5}
31	0.49275	A	0.02428	0.8974	2.314×10^{-7}	3.0×10^{-6}
		K	0.0175	0.04660	3.211×10^{-6}	4.0×10^{-5}
		H	0.0175	0.04660	3.211×10^{-6}	4.0×10^{-5}
		P	0.00678	0.00190	3.051×10^{-5}	3.8×10^{-4}
		W	0.00678	0.00190	$3/-51 \times 10^{-5}$	3.8×10^{-4}

APPENDIX VII

GAS FEEDING SYSTEM

Gas, such as nitrogen, from a cylinder was fed through a pressure regulator to an up stream cooling coil and then to a small brass critical flow orifice. Both the cooling coil and critical flow orifice were immersed in an ice-water bath to maintain constant temperature. The pressure ratio across the critical flow orifice was set at approximately 15 to 1 with up stream pressure of 200 psig and down stream pressure of about atmospheric pressure. Under these conditions, critical flow was established, giving a constant flow rate of nitrogen. Gas from the critical flow meter was finally fed to the vaporization unit. Different flow rates could be obtained by changing the orifice plates.

In the present work, the smallest orifice of 0.004 inch in diameter still gave a flow rate of nitrogen too high for the reactor.

APPENDIX VIII

NUMERICAL DIFFERENTIATION

COMPILER OPTIONS - NAME= MAIN,OPT=02,LINECNT=59,SOURCE,EBCDIC,NOLIST,NODECK,

C NUMERICAL DIFFERENTIATION

C

```

N 0002      DIMENSION AX(100),AY(10,100),ACC(10,10,10),YY(10,100),X(50),Y(50),
            1C(50),CC(50),AXX(100),XAX(50),YAY(10,50),YAYP(10,50)
N 0003      READ (5,100) M,N,L,NNN
            C M IS NO. OF CURVES
            C N IS NO. OF POINTS PER CURVE
            C L IS NO. OF POINTS PER SEGMENT OF CURVE
            C NNN IS NO. OF POINTS TO BE GENERATED
N 0004      100  FORMAT (4I2)
N 0005      READ (5,101) (AX(J),(AY(I,J),I=1,M),J=1,N)
N 0006      101  FORMAT (4F10.4)
N 0007      READ (5,104) XXX,AXX(1),DX
N 0008      104  FORMAT (3F10.6)
N 0009      WRITE (6,102) M,N,L,NNN
N 0010      102  FORMAT('1',15X,'M=',I3,5X,'N=',I3,5X,'L=',I3,5X,'NNN=',I3//)
N 0011      WRITE (6,600)
N 0012      600  FORMAT ('0',15X,'1/S.V.',16X,'F(P)',16X,'F(K)',16X,'F(A)')
N 0013      WRITE (6,103) (AX(J),(AY(I,J),I=1,M),J=1,N)
N 0014      103  FORMAT ('0',10X,F10.4,10X,F12.9,10X,F12.9,10X,F12.9)
N 0015      WRITE (6,601) XXX,AXX(1),DX
N 0016      601  FORMAT ('0',13X,'XXX=',F10.6,5X,'AXX(1)=',F10.6,5X,'DX=',F10.6)
N 0017      MP1 = M+1
N 0018      DO 10 J=1,N
N 0019      10   AY(MP1,J) = 1.0-AY(M,J)
N 0020      NM2 = N-2
N 0021      DO 20 I=1,MP1
N 0022      DO 20 J=1,NM2
N 0023      LL = J-1
N 0024      DO 40 K=1,L
N 0025      X(K) = AX(K+LL)
N 0026      40   Y(K) = AY(I,K+LL)
N 0027      CALL POLFIT (L,X,Y,C)
N 0028      CALL COPCLY (L,X,C,CC)
N 0029      DO 50 K=1,L
N 0030      50   ACC(I,J,K) = CC(K)
N 0031      20   CONTINUE
N 0032      MB = 5
N 0033      DO 60 I=1,MP1
N 0034      XX = XXX
N 0035      J = 1
N 0036      DO 70 JJ=1,NNN
N 0037      IF (XX.GT.AX(J+1)) GO TO 80
N 0039      1   YY(I,JJ) = ACC(I,J,1)
N 0040      DO 90 K=2,L
N 0041      90   YY(I,JJ) = YY(I,JJ)+ACC(I,J,K)*XX**(K-1)
N 0042      XAX(1) = XX-2.0*DX
N 0043      DO 900 KJ=2,MB
N 0044      900  XAX(KJ) = XAX(KJ-1)+DX
N 0045      DO 901 KJ=1,MB
N 0046      901  YAY(I,KJ) = ACC(I,J,1)
N 0047      DO 902 KJ=1,MB
N 0048      DO 902 K=2,L
N 0049      902  YAY(I,KJ)=YAY(I,KJ)+ACC(I,J,K)*XAX(KJ)**(K-1)
N 0050      CALL DIFFER (JJ,I,MB,DX,YAY,YAYP)
N 0051      GO TO 70
N 0052      80   J = J+1
N 0053      GO TO 1

```



```

N 0054      70      XX = XX+1.0
N 0055      60      CONTINUE
N 0056              DO 92 JJ=2,NNN
N 0057      92      AXX(JJ) = AXX(JJ-1)+1.0
N 0058              WRITE (6,200)
N 0059      200     FORMAT ('1',14X,'1/SV',15X,'RATE(P)',15X,'RATE(K)',15X,'1-FA'///)
N 0060              WRITE (6,201) (AXX(JJ),(YAYP(I,JJ),I=1,2),YY(MP1,JJ),JJ=1,NNN)
N 0061      201     FORMAT (' ',10X,F10.4,10X,F12.9,10X,F12.9,10X,F12.9)
N 0062              STOP
N 0063              END

```

* END OF COMPILATION *****

13 (23 MAY 67)

OS/360 FORTRAN H

COMPILER OPTIONS - NAME= MAIN,OPT=C2,LINECNT=59,SOURCE,EBCDIC,NOLIST,NODECK,

```

N 0002      SUBROUTINE POLFIT (N,X,Y,C)
N 0003      DIMENSION X(50),Y(50),A(50,50),C(50)
N 0004      DO 10 I=1,N
N 0005      10      A(I,1) = Y(I)
N 0006      NN = N-1
N 0007      DO 20 I=1,NN
N 0008      L = N-I
N 0009      DO 20 J=1,L
N 0010      20      A(I+1,J) = (A(I,J+1)-A(I,J))/(X(I+J)-X(J))
N 0011      DO 30 I=1,N
N 0012      30      C(I) = A(I,1)
N 0013      RETURN
N 0014      END

```

* END OF COMPILATION *****

COMPILER OPTIONS - NAME= MAIN,OPT=02,LINECNT=59,SOURCE,EBCDIC,NCLIST,NODECK,

```
N 0002      SUBROUTINE COPOLY (N,X,C,CC)
N 0003      DIMENSION X(50),C(50),A(50,50),CC(50)
N 0004      DO 10 I=1,N
N 0005          10      A(I,I) = 1.0
N 0006      DO 20 J=2,N
N 0007          20      A(1,J) = A(1,J-1)*(-X(J-1))
N 0008      DO 30 J=3,N
N 0009          K = J-1
N 0010      DO 30 I=2,K
N 0011          30      A(I,J) = A(I-1,J-1)+(-X(J-1))*A(I,J-1)
N 0012      DO 40 I=1,N
N 0013          DO 40 J=I,N
N 0014          40      A(I,J) = C(J)*A(I,J)
N 0015      DO 50 I=1,N
N 0016          CC(I) = 0.0
N 0017      DO 50 J=I,N
N 0018          50      CC(I) = CC(I)+A(I,J)
N 0019      RETURN
N 0020      END
```

* END OF COMPILATION *****

13 (23 MAY 67)

OS/360 FORTRAN H

COMPILER OPTIONS - NAME= MAIN,OPT=02,LINECNT=59,SOURCE,EBCDIC,NOLIST,NODECK,

```
N 0002      SUBROUTINE DIFFER (JJ,I,MB,DX,YAY,YAYP)
N 0003      DIMENSION YAY(10,50),YAYP(10,50),CX(10)
N 0004      CX(1) = -2.0
N 0005      DO 10 J=2,MB
N 0006      10  CX(J) = CX(J-1)+1.0
N 0007      SUM = 0.0
N 0008      DO 20 J=1,MB
N 0009      20  SUM = SUM+CX(J)*YAY(I,J)
N 0010      YAYP(I,JJ) = SUM/(10.0*DX)
N 0011      RETURN
N 0012      END
```

* END OF COMPILATION *****

13 (23 MAY 67)

OS/360 FORTRAN H

COMPILER OPTIONS - NAME= MAIN,OPT=02,LINECNT=59,SOURCE,EBCDIC,NOLIST,NODECK,

M= 3 N= 11 L= 3 NNN= 10

1/S.V.	F(P)	F(K)	F(A)
1.0000	0.000840000	0.020299997	0.021599997
2.0000	0.001620000	0.039099999	0.041599996
3.0000	0.002310000	0.056699999	0.059899997
4.0000	0.002900000	0.072999954	0.076999962
5.0000	0.003420000	0.088599980	0.093099952
6.0000	0.003860000	0.102499962	0.107799947
7.0000	0.004229996	0.115300000	0.121299982
8.0000	0.004559997	0.127099991	0.133299947
9.0000	0.004849996	0.137599945	0.144099951
10.0000	0.005109999	0.147099972	0.153699994
11.0000	0.005339999	0.155599952	0.162099957
XXX= 1.000000	AXX(1)= 1.000000	DX= 0.010000	

1/SV

RATE(P)

RATE(K)

1-FA

1.0000	0.000824970	0.019399341	0.978400052
2.0000	0.000734977	0.018199090	0.958400011
3.0000	0.000640005	0.016946796	0.940100014
4.0000	0.000555031	0.015948419	0.923000036
5.0000	0.000480004	0.014749769	0.906899154
6.0000	0.000404976	0.013350252	0.892200053
7.0000	0.000349991	0.012301210	0.878609699
8.0000	0.000309944	0.011148456	0.866700053
9.0000	0.000275038	0.009999275	0.855900049
10.0000	0.000244938	0.008998513	0.846300006

B29906